Aus dem Institut für Klinische Pharmakologie und Toxikologie
der Medizinischen Fakultät Charité – Universitätsmedizin Berlin

DISSERTATION

Experimental and clinical studies in hypertension and kidney disease focusing on glomerular hyperfiltration and tolerability of antihypertensive treatment

Experimentelle und klinische Untersuchungen bei Bluthochdruck- und Nierenerkrankungen mit Fokus auf glomeruläre Hyperfiltration und Verträglichkeit der Therapie

zur Erlangung des akademischen Grades

Doctor rerum medicinalium (Dr. rer. medic.)

vorgelegt der Medizinischen Fakultät
Charité – Universitätsmedizin Berlin

von

Eva Mangelsen

Datum der Promotion: 25.06.2023

Table of Contents

List of Tables

List of Figures

List of Abbreviations

AE	Adverse events
ACEi	Angiotensin converting enzyme inhibitor
ARB	Angiotensin II receptor blocker
BP	Blood pressure
cAMP	Cyclic adenosine monophosphate
CCB	Calcium channel blocker
CI	Confidence interval
CKD	Chronic kidney disease
COX2	Cyclooxygenase 2, Ptgs2, prostaglandin-endoperoxide synthase 2 COX2, murine or human protein; *COX2*, human gene or mRNA *Cox2*, murine gene or mRNA
CREB	cAMP response element-binding protein
DBP	Diastolic blood pressure
EDTA	Ethylenediaminetetraacetic acid
eGFR	Estimated glomerular filtration rate
EP	Prostaglandin E receptor
ESKD	End stage kidney disease
GAPDH	Glyceraldehyde 3-phosphate dehydrogenase
GFR	Glomerular filtration rate
HEK	Human embryonic kidney cells
HMBS	Hydroxymethylbilane synthase
FC	Fold change
FFSS	Fluid flow shear stress
hPC	Human podocytes
LC/ESI-MS/MS	Liquid chromatography electrospray ionization tandem mass spectrometry

MWF	Munich Wistar Frömter rat
PBS	Phosphate buffered saline
PGE_2	Prostaglandin E_2
PKA	Proteinkinase A
PTGER1	Prostaglandin E receptor 1, EP1
PTGER2	Prostaglandin E receptor 2, EP2
PTGER3	Prostaglandin E receptor 3, EP3
PTGER4	Prostaglandin E receptor 4, EP4
qPCR	Quantitative Real-Time PCR (polymerase chain reaction)
RAS	Renin-angiotensin system
RPMI	Roswell Park Memorial Institute
SBP	Systolic blood pressure
SD	Standard deviation
SGLT2	Sodium-glucose cotransporter 2
SHR	Spontaneously Hypertensive Rat
SNGFR	Single nephron glomerular filtration rate
TBP	TATA box-binding protein
US	United States

Abstract

Hypertension is the leading cause of premature death worldwide and results in damage of multiple organs including the kidney. Hypertensive kidney disease involves glomerular hyperfiltration, which is an important mechanism in the development of albuminuria and chronic kidney disease (CKD). During hyperfiltration, podocytes are damaged by increased fluid flow shear stress (FFSS) in Bowman's space, which was previously shown to upregulate prostaglandin E2 (PGE_2) synthesis and cyclooxygenase 2 (COX2). In study 1, the PGE_2 autocrine/paracrine pathway was elucidated in human podocytes (hPC) by experimental *in vitro* studies. Therefore, hPC were treated with PGE_2 with or without separate or combined inhibition of prostaglandin E receptors (EP), EP2, and EP4, followed by analysis of the second messenger cyclic adenosine monophosphate (cAMP), mRNA expression of *COX2*, *PTGER2*, and *PTGER4*, and cellular levels of PGE_2 and its metabolites 15-keto-PGE_2, and 13,14-dihydro-15-keto-PGE_2 by lipidomic analysis using liquid chromatography electrospray ionization tandem mass spectrometry (LC/ESI-MS/MS). To link PGE_2-treatment with glomerular hyperfiltration, quantification of the prostaglandin profile in isolated glomeruli and plasma of an *in vivo* model of hyperfiltration and albuminuria, i.e. the Munich Wistar Frömter rat (MWF) was performed, as well as analysis of *COX2*, *PTGER2*, and *PTGER4* expression after application of FFSS in hPC. In hPC, stimulation with PGE_2 led to an EP2- and EP4-dependent increase of cAMP, *COX2*, and cellular PGE_2. *PTGER4* was reduced after PGE_2 stimulation in hPC. In the corresponding lipidomic analysis at the tissue level, increased PGE_2 and 15-keto-PGE_2 levels were detected in isolated glomeruli obtained from MWF, as compared to the albuminuria-resistant spontaneously hypertensive rat, which substantiated an activation of this pathway during hyperfiltration. Moreover, *COX2* and *PTGER4* were upregulated by FFSS in hPC. Thus, the data of study 1 support an autocrine/paracrine COX2/PGE_2 pathway in hPC related to concerted EP2 and EP4 signaling. Irrespective of the pharmacological mechanism, reducing elevated blood pressures is *per se* renoprotective. Beta-blockers play a fundamental role as combination partners for antihypertensive treatment, especially in patients with cardiac comorbidities, which often accompany CKD. However, previous studies associated depression with beta-blocker use, which may limit their application in clinical practice. Study 2 clarified the question whether beta-blockers cause depression, by means of a systematic review of large-scale data from double-blind,

randomized controlled trials and meta-analyses. Depression did not arise more commonly during beta-blockers than during placebo or active agents. Therefore, concerns about the impact of beta-blockers on psychological well-being should not affect their application in clinical practice including their use in patients with or at risk for CKD.

Zusammenfassung

Die arterielle Hypertonie ist weltweit der Hauptgrund für frühzeitigen Tod und kann viele Organe, einschließlich der Nieren, schädigen. Als mögliche Folgeerscheinung der Hypertonie spielt die glomeruläre Hyperfiltration bei der Entwicklung der Albuminurie und chronischen Nierenerkrankung (CKD) eine wichtige Rolle. Während der Hyperfiltration werden Podozyten durch erhöhten Scherstress des Flüssigkeitsstromes (FFSS) in der Bowman-Kapsel geschädigt, einhergehend mit einer Hochregulation von Prostaglandin E2 (PGE_2) und Cyclooxygenase 2 (COX2). In Studie 1 wurde daher *in vitro* der autokrine/parakrine PGE_2 Signalweg in humanen Podozyten (hPC) untersucht. Dazu wurden hPC mit PGE_2 in An- oder Abwesenheit von Einzel- bzw. Doppelinhibition der Prostaglandin E Rezeptoren (EP) EP2 und EP4 behandelt, gefolgt von Untersuchungen des second messengers cAMP, der mRNA Expression von *COX2*, *PTGER2* und *PTGER4*, sowie Quantifizierung von zellulärem PGE_2 und dessen Metabolite 15-keto-PGE_2 und 13,14-dihydro-15-keto-PGE_2 mittels LC/ESI-MS/MS. Um die PGE_2-Stimulation mit der glomerulären Hyperfiltration zu verknüpfen, wurde das Prostaglandinprofil in isolierten Glomeruli und Plasma eines *in vivo* Hyperfiltrationsmodells mit Albuminurie, der Munich Wistar Frömter Ratte (MWF), sowie die *COX2*, *PTGER2* und *PTGER4* Expression nach FFSS in hPC untersucht. Die PGE_2-Stimulation bewirkte in hPC einen EP2- und EP4-abhängigen Anstieg von cAMP, *COX2* und zellulärem PGE_2. *PTGER4* wurde durch PGE_2-Stimulation vermindert. In der entsprechenden Lipidomanalyse der Gewebe wurden erhöhte PGE_2 und 15-keto-PGE_2 Level in isolierten Glomeruli von MWF im Vergleich zu Albuminurie-resistenten Kontrolltieren detektiert, was die Aktivierung des Signalweges bei Hyperfiltration untermauert. *COX2* und *PTGER4* waren durch FFSS in hPC hochreguliert. Diese Ergebnisse unterstützen somit einen autokrinen/parakrinen COX2/PGE_2 Signalweg in hPC mit gemeinsamen EP2 und EP4 Signalwegen. Die Senkung eines erhöhten Blutdrucks *per se* wird unabhängig vom pharmakologischen Wirkmechanismus als nephroprotektiv angesehen. Betablocker spielen eine wesentliche Rolle als Kombinationspartner bei der antihypertensiven Therapie, besonders für

Patienten mit kardialen Komorbiditäten, die oft mit CKD einhergehen. Eine Therapie mit Betablockern wurde jedoch mit dem Auftreten einer Depression assoziiert, was ihren Einsatz und die Adhärenz in der klinischen Praxis beeinträchtigen könnte. In Studie 2 wurde daher mithilfe eines systematischen Reviews mit großen Datensätzen von doppelblinden randomisierten kontrollierten Studien und Meta-Analysen untersucht, ob Betablocker Depressionen verursachen. Depressionen kamen unter Betablocker Therapie nicht häufiger vor als unter Placebo oder aktiven Kontrollen. Daher sollten Bedenken hinsichtlich eines erhöhten Risikos für Depression ihre Anwendung in der klinischen Praxis nicht vermindern; dies gilt auch für die Therapie bei Patienten mit CKD oder einem erhöhten CKD-Risiko.

Manteltext / Synopsis

Parts of this work were previously published in (1) and (2).

1 Introduction

Hypertension is consistently responsible for the largest number of all-cause deaths worldwide, accounting for >10 million deaths and 218 million disability-adjusted life years in 2017 (3). Referring to office blood pressure (BP), hypertension is defined as systolic BP (SBP) values of at least 140 mmHg and/or diastolic BP (DBP) values of at least 90 mmHg (4). As a modifiable risk factor, hypertension provokes cardiovascular diseases, which are the leading cause of global disease burden (5), and hypertension mediated organ damage affects multiple organs including the kidney (4, 6, 7). Persistent intrarenal hypertension leads to a variety of structural and functional changes, e.g. nephrosclerosis (6, 8). In 2018, hypertension was the most common primary cause of end stage kidney disease (ESKD) after diabetes in the United States (US) (9). Chronic kidney disease (CKD) is prevalent in approximately one-third of the hypertensive population and among CKD patients, hypertension increases all-cause mortality as compared to those without hypertension (10). Globally, kidney diseases ranked as the 10th leading cause of death in 2019 (11), and CKD being prevalent in 9.1% of the world's population ranked as the 12th leading cause of death in 2017 (12). CKD is defined as abnormal kidney structure or function that persists >3 months, and is classified according to cause, glomerular filtration rate (GFR) category, and albuminuria category (13). These clinical markers of kidney disease further increase cardiovascular risk: (Micro-) Albuminuria was independently associated with hypertension (14, 15), and predicted cardiovascular morbidity, as well as cardiovascular and all-cause mortality among hypertensive individuals (16-19), while reduction of albuminuria during antihypertensive treatment decreased cardiovascular events (20, 21). Even in a general population without preexisting cardiovascular disease, trace (10–20 mg/dL) and positive (≥30 mg/dL) proteinuria is associated with a gradual increase in the risk of stroke, myocardial infarction, atrial fibrillation and heart failure, which was more pronounced in hypertensive subjects (22). Moreover, the risk of death, cardiovascular events and hospitalization increased inversely with estimated GFR (eGFR) (23). A rapid decline in eGFR was

associated with higher risk for coronary heart disease and all-cause mortality (24), as well as all-cause and cardiovascular mortality in elderly hypertensive individuals (25). CKD was associated with an 8–10-fold increase of cardiovascular mortality, and is a risk multiplier in patients with hypertension and diabetes (26). Moreover, the absolute risk for death was potentiated by decreasing kidney function (27).Together, these data illustrate that impaired kidney function contributes to a higher cardiovascular risk and mortality.

Hypertension induces changes in glomerular hemodynamics, resulting in increased glomerular pressure, which causes elevated single nephron GFR (SNGFR) and thus higher flow of ultrafiltrate in Bowman's space, i.e. glomerular hyperfiltration (8, 28, 29). In man, nephrosclerosis was associated with both increased SNGFR and a lower number of nephrons (30). Glomerular hyperfiltration is also observed in rodent models with reduced nephron numbers, e.g. due to nephrectomy (28, 29, 31, 32), or genetic mechanisms (33). In this regard, the Munich Wistar Frömter rat (MWF) represents an important CKD model due to an inherited nephron deficit which exhibits hypertension, glomerular hyperfiltration and spontaneous progressive albuminuria (33, 34). Hence, glomerular hyperfiltration is a major risk factor for the progression of CKD (32).

Podocytes, a glomerular cell type encasing the glomerular capillary with a network of interdigitating foot processes, are particularly vulnerable to glomerular hyperfiltration (32, 35) due to their high degree of differentiation (36). Podocyte damage impairs the integrity of the glomerular filtration barrier, which leads to albuminuria, glomerulosclerosis, and alteration in GFR, thus promoting the gradual decline in renal function in CKD (8, 37, 38). Understanding the pathomechanisms of podocyte injury is key to identify potential therapeutic targets to protect against these maladaptive responses to glomerular hyperfiltration. To investigate the impact of hyperfiltration on podocytes, fluid flow shear stress (FFSS) has been established as a surrogate *in vitro*, mimicking the flow of glomerular ultrafiltrate (35, 39-41). Previous studies support a pathophysiological role of an activated prostaglandin E2 (PGE_2) pathway (39), including upregulated COX2 (PTGS2, cyclooxygenase 2) and PTGER2 (prostaglandin E receptor 2, EP2) for the development of albuminuria by increasing the permeability of the glomerular filtration barrier (41). These results suggest, that PGE_2 synthesis by COX2 (42, 43) and signaling *via* prostaglandin E receptors (EP) may contribute to maladaptive responses to hyperfiltration in podocytes. Interestingly, an autocrine/paracrine pathway between PGE_2

and COX2 was delineated previously in various cell types, indicating that PGE_2 leads to upregulation of COX2, which might turn into increased synthesis of intracellular PGE_2, and induction of COX2 thereafter (44-47). In general, four different G-protein coupled prostaglandin E receptors (EP1–4) exist in humans and rodents (reviewed in (48)), of which EP2 and EP4 induce adenylate cyclase activity thereby increasing cyclic adenosine monophosphate (cAMP) levels (reviewed in (49)). However, the expression of EP in human podocytes (hPC) has not yet been determined. Several EP mediated mechanisms can be considered to cause this mutual amplification, suggesting EP4 and the p38 mitogen-activated protein kinase (MAPK) signaling pathway in mouse podocytes (46), and activation of the cAMP/proteinkinase A (PKA) pathway *via* EP2 in other cell types (45, 47, 50). However, regarding FFSS induced damage, the PGE_2-COX2-EP2 axis was suggested as relevant mechanism for murine podocytes (39-41), but this has not been demonstrated in hPC so far. Therefore, study 1 aimed to investigate an autocrine/paracrine PGE_2/COX2 pathway in hPC and to clarify which EP contribute to this crosstalk.

Another crucial point for renoprotection is BP control by antihypertensive treatment as reduction of BP *per se* alleviates progression of kidney damage (51-55). In hypertensive patients with CKD, renin–angiotensin system (RAS-) blockers build the foundation of antihypertensive therapy due to their renoprotective effects (56-59). As such, they are recommended as the backbone of the core-treatment strategy in the 2018 European guidelines for the management of hypertension (4). In this strategy, their use in combination with a calcium channel blocker (CCB) and/or a thiazide/thiazide-like diuretic is recommended for BP control (4). Beta-blockers also belong to the first-line drugs and can be used at any treatment step in specific clinical situations including primarily cardiac indications, e.g. in patients with heart failure, angina, myocardial infarction, and tachycardia, as well as in pregnant women or planning pregnancy (4). However, beta-blockers play also an important role in CKD patients to achieve BP control. This is particularly relevant when considering lower BP targets in CKD patients (13), although the latter are controversial (60). Moreover, treatment with RAS-blockers, i.e. angiotensin converting enzyme inhibitors (ACEi) or angiotensin II receptor blockers (ARB), is often accompanied by adverse events (AE), e.g. hyperkalemia or increase of serum creatinine, which often requires dose reduction or even discontinuation as reviewed in (61, 62). Cardiac comorbidities are widely prevalent in CKD patients, as e.g. shown in 2018 in the

US, where heart failure was present in 39.1% of patients who had CKD stages 4–5 (vs. 6.6% in patients without CKD) (10). Furthermore, a steep decline in eGFR was associated with a higher risk for coronary heart disease (24). Therefore, beta-blockers play an indispensable role for pharmacotherapy in hypertensive CKD patients with and without accompanying cardiac comorbidities. In 2018, among US patients ≥66 years with CKD and heart failure, 77.2% received beta-blockers, whereas only 61.5% received ACEi/ARB/angiotensin receptor neprilysin inhibitor (10). Beta-blockers form the fourth most frequently prescribed drug class in the US (10) and among antihypertensive drugs in Germany (63). In order to achieve efficacy, tolerability is key to attain optimal adherence. Among other AE, psychiatric AE like depression have repeatedly been documented in the context of beta-blocker use, as e.g. reviewed in (64, 65), as well as in postmarketing surveillance systems of the European Medicines Agency (66), and the Food and Drug Administration (67). Other investigators reported an increased use of antidepressants during beta-blocker therapy (68, 69). As safety concerns may derogate adherence, study 2 addressed the question whether beta-blocker use is associated with an increased risk of psychiatric AE in a systematic review and meta-analyses (2).

2 Methods

A detailed and complete description of methods is available in (1, 2). Methods described in the following are those related to my contribution to the publications. Methods 2.1.1–2.1.4 and 2.1.6–2.1.8 were published in “Cells”, and 2.2.1 was published in “Hypertension”. Paragraph 2.1.5 describes a method which was elaborated after publication.

2.1 Study 1

2.1.1 hPC in Cell Culture

Conditionally immortalized hPC were obtained from Moin A. Saleem, University of Bristol, UK, and were cultured according to the original protocol (70, 71) with slight modifications. Briefly, hPC proliferated at 33 °C and 5% CO_2 in Roswell Park Memorial Institute (RPMI)-1640 medium (cat. no. BS.F1215, Bio&SELL, Feucht/Nürnberg, Germany) supplemented with 1% Insulin-Transferrin-Selenium 100X (cat. no. 41400-045, Gibco, Grand Island, NY, USA), 10% fetal bovine serum (FBS, cat. no. F7524, Sigma, Steinheim, Germany) and 1% ZellShield® to inhibit contamination (cat. no. 13-0150, Minerva Biolabs, Berlin, Germany). Medium was replaced 2–3 times per week. At confluency of 70–80%, hPC were relocated to 37–38 °C until full confluence and proliferation arrest, after which cells differentiated during at least 14 days. Differentiated phenotype was confirmed by detection of the podocyte markers synaptopodin, nephrin, and podocin, according to (70, 71). After detachment with Trypsin 0.25%/EDTA 0.02% solution (cat. no. L-2163, Biochrom, Berlin, Germany; EDTA, Ethylenediaminetetraacetic acid), hPC were seeded in 12-well plates at 1×10^5 cells per well and kept in supplemented RPMI-1640 medium to adhere overnight. All experiments were performed in supplement-free RPMI-1640 medium at 37–38 °C using cell passages between 5 and 22. If conducted in duplicate or triplicate, independent experiments were performed on different dates using different cell passages.

2.1.2 PGE_2 Treatment and Blockade of EP Receptors

Stock solutions of PGE_2 (cat. no. 14010, Cayman Chemical, Ann Arbor, MI, USA), the selective EP2 antagonist PF-04418948 (cat. no. PZ0213, Sigma, Steinheim, Germany) (72, 73), and the selective EP4 antagonist ONO-AE3-208 (cat. no. 14522, Cayman

Chemical, Ann Arbor, MI, USA) (74, 75), containing 10 mM were prepared in DMSO (cat. no. D2650, Sigma, Steinheim, Germany) and kept at −20 °C until further use.

Podocytes were stimulated with PGE_2 at concentrations ranging from 10 nM–1 µM, as up to 1 µM are commonly administered to mouse podocytes in *in vitro* experiments (76, 77). In inhibition experiments, PGE_2 100 nM was concomitantly added to 1 µM of EP2 and/or EP4 antagonists for the indicated time-points. The concentration of antagonists was selected according to previous studies, in which equal or even higher concentrations were applied (72, 75, 78-80). If not stated otherwise, experiments consisted of n = 3–8 samples per treatment and were performed at least in duplicate as indicated in detail within figures and figure legends (see below in the Results section).

2.1.3 Analysis of Intracellular cAMP

Intracellular cAMP levels were assessed by an ELISA kit (cat. no. ADI-901-163, Enzo Life Sciences, Farmingdale, NY, USA) after lysis in 300–400 µL 0.1 M HCl containing 0.1% Triton X-100, following the manufacturer's protocol of the non-acetylated format. For optical density measurement at 415 nm within the standard range, samples of PGE_2 stimulation were diluted 1:5, and samples of co-incubation with PGE_2 plus either the EP2 or the EP4 antagonist were diluted 1:2–3 in lysis buffer. In order to normalize intracellular cAMP concentrations, the protein amount of each sample was determined by a colorimetric kit (cat. no. 23227, Pierce™ BCA Protein Assay Kit, Thermo Fisher Scientific, Rockford, IL, USA). Experiments consisted of n = 3–6 samples per treatment and were performed once or in duplicate as indicated within figures and figure legends (see below in the Results section).

2.1.4 Expression Analysis by Quantitative Real-Time PCR

Total RNA of hPC was isolated using the RNeasy® Micro Kit (cat. no. 74004, Qiagen, Hilden, Germany), according to the manufacturer's protocol, followed by a quality check, i.e., determination of the 260/280 nm absorption ratio. Reverse transcription of total RNA was accomplished using the First Strand cDNA Synthesis Kit (cat. no. K1612, Thermo Fisher Scientific, Vilnius, Lithuania).

Quantitative Real-Time PCR (qPCR) was performed in a CFX96 Touch PCR system (Bio-Rad, München, Germany; software version 3.1.1517.0823) or in a 7500 Fast Real-Time PCR System (Applied Biosystems, Darmstadt, Germany; software version 2.0.6) applying

the comparative quantitative cycle method with SYBR-green (cat. no. 4,385,612 and 100029284, Thermo Fisher Scientific, Vilnius, Lithuania) as reported previously (81, 82). Each sample was analyzed in three technical replicates. Gene expression was normalized to the reference gene glyceraldehyde 3-phosphate dehydrogenase *(GAPDH)*, and ΔΔCt was referred to the untreated controls. All results were visualized as log2 of fold change (FC) (2^-ΔΔCt). Primers were ordered from Eurofins Genomics, Ebersberg, Germany or Tib Molbiol, Berlin, Germany and had the sequences listed in Table 1. Whenever possible, intron-spanning primers were selected, and specificity of amplified products detected after reverse transcriptase (RT)-PCR was confirmed by sequencing at Eurofins Genomics, Ebersberg, Germany.

Table 1. Primer sequences used for gene expression analysis in hPC as published in (1).

Gene	Forward primer (5'–3')	Reverse primer (5'–3')
GAPDH	gagtcaacggatttggtcgt	gatctcgctcctggaagatg
COX2	tgatgattgcccgactcccttg	tgaaagctggccctcgcttatg
PTGER1	ttcggcctccaccttctttg	cgcagtaggatgtacacccaag
PTGER2	gacggaccacctcattctcc	tccgacaacagaggactgaac
PTGER3	tctccgctcctgataatgatg	atctttccaaatggtcgctc
PTGER4	ttactcattgccacctccct	agtcaaaggacatcttctgcca

2.1.5 FFSS

After establishment of the FFSS system in the laboratory, first explorative results applying this method were published in (1). These results based on a cell density of 1×10^5–6×10^5 cells, FFSS intensity of solely 2 dynes/cm², and normalization of gene expression data using the housekeeping gene *GAPDH*. After publication, the protocol was optimized regarding cell density, FFSS intensity, and housekeeping genes for qPCR analysis. Uniform cell densities were applied to allow for consistent conditions across independent experiments. Moreover, it was noticed that the designated housekeeping gene *GAPDH*, which was applied in the first analyses, significantly changed its expression upon FFSS, rendering it to an inappropriate reference gene. To overcome this technical problem, expression of multiple well-known housekeeping genes was determined, including actin beta (*ACTB*), which was also used in (39-41), eukaryotic translation elongation factor 2 (*EEF2*), hypoxanthine phosphoribosyltransferase 1 (*HPRT1*), ribosomal RNA 18S,

ribosomal protein L32 (*RPL32*), hydroxymethylbilane synthase (*HMBS*), and TATA box-binding protein (*TBP*). All of these also exhibited significant changes in expression after FFSS, disabling these genes for housekeepers.

In compliance with other investigators (83), the geometric mean of the Ct-values of *TBP*+*HMBS* was selected for normalization, as this normalization factor yielded no significant difference between FFSS and control group. Finally, a refined shear force was applied, according to previously published literature with estimates of 2–3 times higher FFSS in unilaterally nephrectomized rodents, compared to 0.3 dynes/cm² FFSS in healthy control animals (32, 35). To date, there are no robust assumptions about FFSS levels in human glomeruli. Other investigators exposing podocytes to FFSS *in vitro* applied 0.015–0.5 dynes/cm², and 2 dynes/cm² to a murine podocyte cell line, respectively (35, 39), 1.5 dynes/cm² in combination with cyclic strain in primary mouse podocytes (84), and 0.5–2 dynes/cm² in primary hPC co-treated with retinoic acid (85). Based on these data, and particularly assuming 0.6–0.9 dynes/cm² over podocytes in unilaterally nephrectomized mice, a shear force of 1 dyne/cm² was selected as a valuable addition to 2 dynes/cm² for the FFSS setting.

Together, optimized results based on a uniform cell density (3.5×10^5 cells per Culture Slip®), FFSS of both 1 dyne/cm² and 2 dynes/cm², and normalization to the geometric mean of Ct-values of *HMBS* and *TBP*, whose primer sequences are listed in Table 2. The following describes the optimized protocol:

For FFSS, 3.5×10^5 cells were seeded on collagen IV coated Culture Slips® (cat. no. CS-C/IV, Dunn Labortechnik GmbH, Asbach, Germany) and adhered overnight. Culture Slips® are collagen IV coated glass slides framed by a polytetrafluoroethylene border to limit cell distribution to the area of the slip exposed to fluid flow. FFSS experiments were conducted as previously described with minor modifications (39). Briefly, the Streamer® Shear Stress Device (cat. no. STR-400, Dunn Labortechnik GmbH, Asbach, Germany) was set up in a 38 °C incubator with 5% CO_2 and rinsed by 400 mL of PBS followed by RPMI-1640 medium, which were pumped through the apparatus for approximately 10 min each. Prior to each removal of fluid, flow was directed backwards to empty the tubes from the previous liquid. Subsequently, rinsing medium was replaced by 400 mL of fresh pre-warmed medium, and air bubbles and leaks were eliminated during forward flow. Next, flow direction was again reverted until the streamer was half-filled by medium, and the

system was released from the incubator. Culture Slips® with hPC were inserted into the 6 slots of the Streamer®, which had to be occupied completely to allow consistent flow. After transferring the system back into the incubator, FFSS at 1 dyne/cm as well as 2 dynes/cm^2 was applied for 2 h, according to previous research, and assuming 0.6–0.9 dynes/cm² over podocytes in unilaterally nephrectomized mice (32, 35, 39). At the end of each experiment, flow direction was inversed, and cells were released from the Streamer®. Control cells were kept under the same conditions but were not exposed to FFSS.

Table 2. Primer sequences used for refined normalization of gene expression in hPC exposed to FFSS (unpublished).

Gene	Forward primer (5'–3')	Reverse primer (5'–3')
HMBS	AATCATTGCTATGTCCACCAC	TTCCCACCACACTCTTCTC
TBP	TTCCACTCACAGACTCTCAC	GCACACCATTTTCCCAGAAC

2.1.6 Lipidomic Analysis

PGE_2 and its downstream metabolites 15-keto-PGE_2 and 13,14-dihydro-15-keto-PGE_2 were quantified in hPC, as well as in glomeruli and plasma of rats. Cells were exposed to PGE_2 for 2 h as decribed above, with and without a concomitant inhibition of combined EP2 and EP4 antagonists. Glomeruli and plasma of MWF and spontaneously hypertensive rat (SHR) were obtained as described below. All samples were stored at −80 °C until analysis to minimize degradation of analytes. The lipidomic analysis was performed by our collaborator Lipidomix GmbH, who established a refined protocol including phospholipase A2 that also allowed for distinct prostaglandin analysis in small sample amounts, i.e. hPC, as phospholipase A2 releases membranous prostaglandins being then available for quantification. The detailed method of LC/ESI-MS/MS is described in (1).

2.1.7 Experiments in Rat Models

MWF served as a model for CKD with glomerular hyperfiltation and albuminuria, while SHR was used as a control strain because it is resistant to albuminuria development despite early onset of hypertension, as reviewed in (33).

Male rats at 8 weeks of age were received from our MWF/Rkb (RRID:RGD_724569, laboratory code Rkb https://www.nationalacademies.org/ilar/lab-code-database) and SHR/Rkb (RRID:RGD_631696, laboratory code Rkb https://www.nationalacademies.org/ilar/lab-code-database) colonies at Charité – Universitätsmedizin Berlin, Germany, and were housed under standard conditions as described previously (82). All experimental work in rat models was conducted following the guidelines of the Charité – Universitätsmedizin Berlin and the local authority for animal protection (Landesamt für Gesundheit und Soziales, Berlin, Germany) for the use of laboratory animals. The registration numbers for the rat experiments are T 0189/02, G 130/16, and G 0309/19.

Rats were anesthetized by ketamine-xylazine (87 and 13 mg/kg body weight, respectively), and kidneys were collected and decapsulated. Glomeruli were isolated by sieving kidneys through a 125 µm steel sieve (Retsch GmbH, Haan, Germany) rinsed by PBS, and were subsequently separated from the flow through on a 71 µm steel sieve (Retsch GmbH, Haan, Germany), on which glomeruli remained. After rinsing off the sieve with PBS, glomeruli were centrifuged, snap-frozen, and stored at −80 °C until lipidomic analysis. Plasma was collected in EDTA-containing vials by retrobulbary punction or punction of vena cava, centrifuged 2 min at 4 °C, and stored subsequently at −80 °C.

2.1.8 Statistical Analysis

Statistical analysis was performed in GraphPad Prism 8.4.0 (GraphPad Software, San Diego, CA, USA). First, data was checked for normal distribution using the Shapiro–Wilk test. The use of the subsequent statistical test depended on the number of comparisons and was indicated in the figure legends. Normally distributed data were analyzed either by unpaired, two-tailed Student’s t-test or one-way ANOVA with Tukey’s or Dunnett’s multiple comparisons test. Not normally distributed data were compared by Mann–Whitney test or Kruskal–Wallis test with Dunn’s multiple comparisons test. A p-value of <0.05 was considered as statistically significant. Statistical details for a specific experiment can be found within figures and figure legends shown in the Results part.

2.2 Study 2

Study 2 contained a systematic review and meta-analyses of psychiatric AE during beta-blocker therapy, mainly performed by Dr. Thomas G. Riemer (2). Double-blind, randomized controlled trials comparing beta-blocker to placebo, as well as active controls (e.g. RAS-blockers) were analyzed. As the quality of a meta-analysis bases upon the quality of its data sources, the risk of bias was assessed in each underlying study (in total 285 studies). I contributed to this quality assessment and reviewed studies comparing beta-blocker to RAS-blockers (29 studies) as described below (2).

2.2.1 Quality Assessment

The quality of all incorporated studies was rated according to the Cochrane Risk of Bias tool (86), which evaluates overall trial quality, but not AE-related bias. To specifically assess possible sources of bias concerning measurement and reporting of AE, a customized rating instrument designed by Dr. Thomas G. Riemer was employed to disclose the quality of AE measuring and reporting in each study. This tool is shown in Table 3.

Table 3. Self-designed rating sheet for assessment of the quality of AE measuring and reporting, according to Table S5 in (2).

	Item	Response	Next item
Q1	Does the study report AE?	□ Yes □ No	(proceed with Q2) (proceed with Q9)
Q2	Does the study specify how AE were assessed?	□ Yes □ No	(proceed with Q3) (proceed with Q4)
Q3	Were AE assessed actively or passively?*	□ actively □ passively	(proceed with R3)
R3	Record the assessment method(s).		
Q4	Does the study report baseline frequencies for AE?	□ Yes □ No	(proceed with Q5)
Q5	Does the study report symptom severity grades for AE?	□ Yes □ No	(proceed with Q6)
Q6	Does they study report all observed AE?	□ Yes □ No	(proceed with Q9) (proceed with Q7)
Q7	Are there quantitative limitations to AE reporting?[$]	□ Yes □ No	(proceed with R7) (proceed with Q8)
R7	Record the type(s) of quantitative limitation(s). [$]		
Q8	Are there qualitative limitations to AE reporting? [§]	□ Yes □ No	(proceed with R8) (proceed with Q9)
R8	Record the type(s) of qualitative limitation(s).[§]		
Q9	Does the study report the number of patients withdrawn from therapy due to AE?	□ Yes □ No	(proceed with Q10) (end rating)
Q10	Does the study report individual AE leading to the withdrawal of therapy?	□ Yes □ No	(end rating)

*, Active assessment includes specific questions, structured interviews, symptom checklists, and questionnaires; passive assessment includes general questions and spontaneous complaints. $, Quantitative limitations regard any kind of frequency threshold/criterion applied when selecting the AE to be reported, e.g. most common symptoms, symptoms occurring in ≥5%. §, Qualitative limitations consider preselection processes that affect the number reported for individual AE, e.g. drug-related AE, serious AE.

3 Results

3.1 Study 1

3.1.1 PGE_2 Causes an EP2- and EP4- Dependent Increase of cAMP in Differentiated hPC

Time-dependent stimulation of hPC with 100 nM PGE_2 led to an immediate elevation of intracellular cAMP levels observed after 1 min onward and retained at least until 40 min (Figure 1A). In subsequent experiments, cAMP was analyzed after 20 min of PGE_2 treatment, as intracellular cAMP remained comparably high until this incubation time (Figure 1B). Analysis of EP expression on hPC disclosed the presence of *PTGER1*, *PTGER2*, and *PTGER4* mRNA in native differentiated hPC (Figure 1C), which correspond to EP1, EP2, and EP4, respectively. As only EP2 and EP4 promote an increase in intracellular cAMP (reviewed in (49)), the effect of concomitant pharmacological inhibition of EP2 and/or EP4 signaling on PGE_2-stimulated intracellular cAMP levels was analyzed in hPC, using selective antagonists of EP2 (PF-04418948, 1 µM) and/or EP4 (ONO-AE3-208, 1 µM) (Figure 1B). Concomitant to PGE_2 stimulation for 20 min, separate blockade of either EP2 (−92.5%) or EP4 (−63.7%) resulted in a clear, albeit only partial reduction of intracellular cAMP levels compared to stimulated hPC without antagonists. Complete abrogation of the PGE_2 induced intracellular cAMP increase was only achieved by combined EP2 and EP4 antagonism (Figure 1B), suggesting that, in hPC, both EP2 and EP4 may promote PGE_2-dependent signaling.

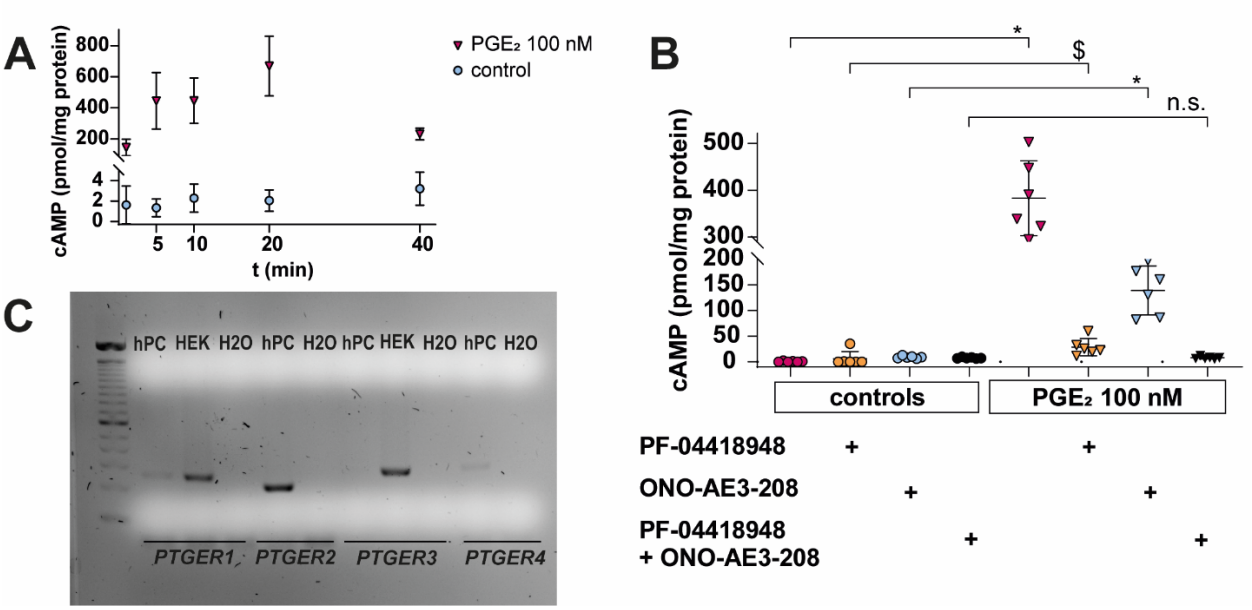

Figure 1. Intracellular cAMP upon PGE_2 stimulation, and concomitant inhibition of EP2 and/or EP4 in hPC and *PTGER* (EP-receptor) expression in unstimulated hPC.

(**A**) Time-dependent increase of intracellular cAMP levels upon PGE_2 stimulation (100 nM, pink triangles), as compared to controls (blue circles). Each data point represents the mean ± SD of one experiment with n = 3–4 samples per time-point. (**B**) Increased intracellular cAMP levels by PGE_2 stimulation were abrogated in part by concomitant treatment with either EP2 or EP4 antagonist, and completely abolished by combination of both antagonists. Representative cAMP levels following stimulation with PGE_2 100 nM for 20 min without concomitant EP2 or EP4 antagonist (100 nM, pink triangles) compared to controls without PGE_2 (pink circles), after co-incubation with either EP2 antagonist (PF-04418948, 1 µM, orange triangles) or EP4 antagonist (ONO-AE3-208, 1 µM, blue triangles) compared to controls without PGE_2 (orange circles for EP2 antagonist, blue circles for EP4 antagonist), and co-incubation of PGE_2 with both antagonists simultaneously (1 µM each, black triangles) compared to controls without PGE_2 (black circles). Each data point represents a single sample and plotted as mean ± SD (horizontal lines) per treatment group consisting of n = 6 samples. Experiments were done in duplicate, with each experiment containing n = 3–6 replicates per experimental group, except for the separate EP4 inhibition, which was only performed once. Statistics: *, $p < 0.01$; $, $p < 0.05$; n.s., not significant, assessed by the Mann–Whitney test. (**C**) *PTGER1* (EP1), *PTGER2* (EP2), and *PTGER4* (EP4) mRNA is present in untreated differentiated hPC. Human embryonic kidney cells HEK293 (HEK) served as a positive control where indicated. Figure 1A and 1B have been previously published in (1) as Figures 1 and 2, Figure 1C is a modified version of Figure S3 in (1).

3.1.2 PGE_2 Increases *COX2* Gene Expression *via* EP2 and EP4 Signaling in Differentiated hPC

PGE_2 stimulation for 2 h induced a dose-dependent upregulation of *COX2* mRNA expression in hPC (Figure 2A). To scrutinize the role of EP2 and EP4 in PGE_2-dependent *COX2* upregulation, either the selective EP2 antagonist PF-04418948 (1 µM) or the

selective EP4 antagonist ONO-AE3-208 (1 µM) were co-incubated with 100 nM PGE_2 individually or in combination (Figure 2B). Upon PGE_2 stimulation, separate antagonism of either EP2 or EP4 revealed an increase in *COX2* mRNA, which was reduced compared to non-antagonized PGE_2-stimulated hPC (Figure 2B). This reduction was statistically significant when EP2 was separately blocked ($p<0.01$) but not after separate EP4 inhibition ($p=0.0504$) as compared to PGE_2-treated hPC without antagonists. Combined EP2 and EP4 blockade completely abolished PGE_2-mediated *COX2* upregulation (Figure 2B), suggesting that PGE_2 signals *via* both EP2 and EP4 to modify *COX2* levels in a positive feedback loop.

3.1.3 Effects of PGE_2 on *PTGER2* and *PTGER4* Gene Expression in Differentiated hPC

Stimulation of hPC with increasing concentrations of PGE_2 for 2 h resulted in inconsistent changes of *PTGER2* mRNA expression: PGE_2 100 nM reduced *PTGER2* expression to a small extent, but 10 nM and 1 µM did not significantly change *PTGER2* expression (Figure 2C). The weak downregulation of *PTGER2* by 100 nM PGE_2 remained unchanged after co-incubation with the selective EP4 antagonist ONO-AE3-208 (1 µM) (Figure 2D). Stimulation of hPC with PGE_2 for 2 h reduced *PTGER4* mRNA expression in a dose-dependent manner (Figure 2E). The downregulation of *PTGER4* by 100 nM PGE_2 remained unchanged after co-incubation with the selective EP2 antagonist PF-04418948 (1 µM) (Figure 2F).

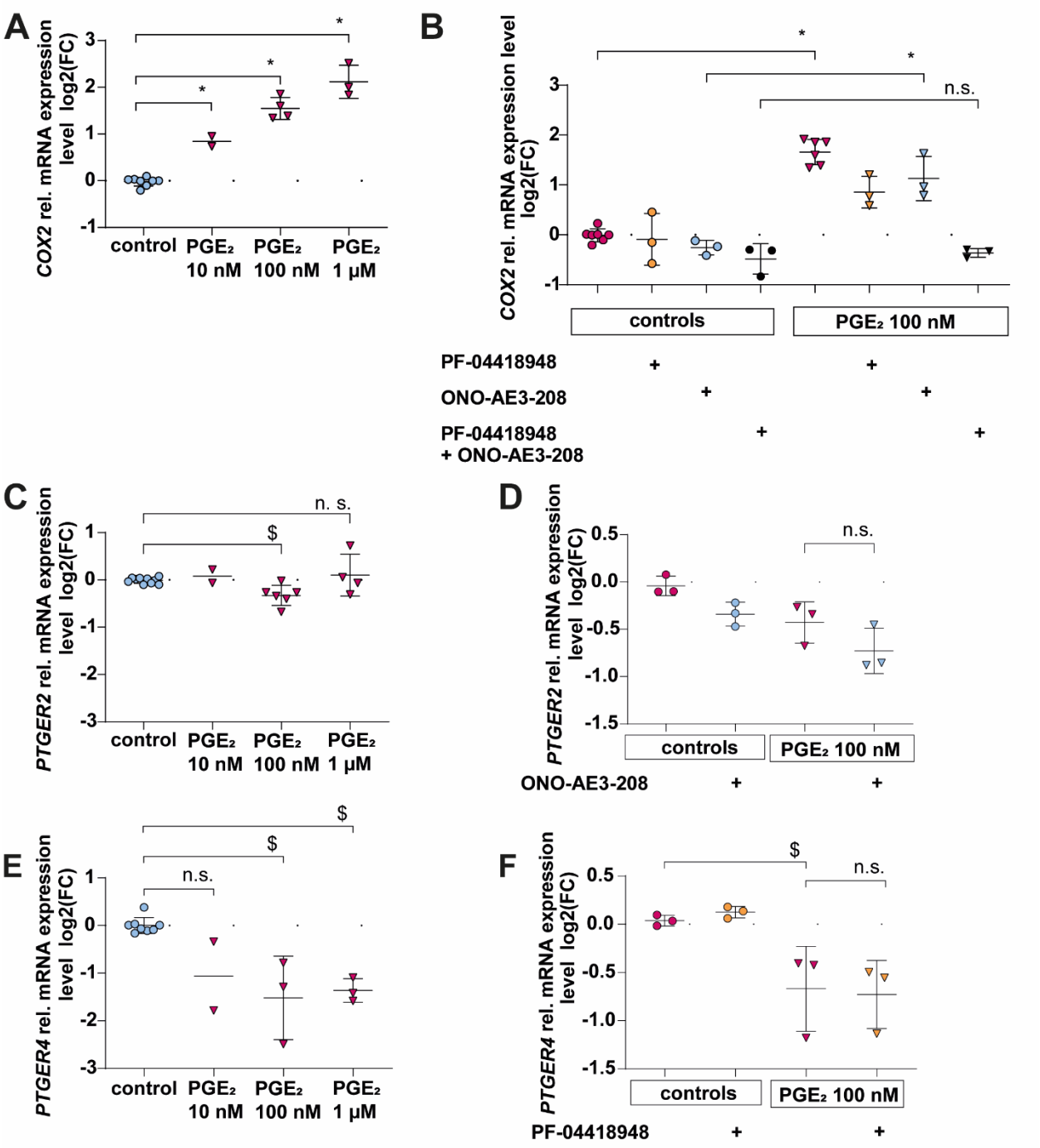

Figure 2. *COX2, PTGER2* and *PTGER4* expression upon PGE_2 stimulation, and concomitant inhibition of EP2 and/or EP4 in hPC.

qPCR results are shown as relative mRNA expression level normalized to *GAPDH,* and referred to untreated control group. Each data point represents the mean of an independent experiment (performed at least in duplicate, each experiment consisted of n ≥3 replicates per treatment), and plotted as combined mean ± SD (horizontal lines). SD was not plotted when only two independent experiments were conducted. (**A**) Dose-dependent induction of *COX2* gene expression by PGE_2 (pink triangles) for 2 h compared to untreated controls (blue circles). (**B**) Induction of *COX2* by PGE_2 stimulation for 2 h was reduced in part by concomitant treatment with either EP2 or EP4 antagonist, and completely abolished by combination of both

antagonists. *COX2* expression after treatment with PGE_2 100 nM for 2 h without concomitant EP2 or EP4 antagonist (100 nM, pink triangles) compared to controls without PGE_2 (pink circles), after co-incubation with either EP2 antagonist (PF-04418948, 1 µM, orange triangles) or EP4 antagonist (ONO-AE3-208, 1 µM, blue triangles) compared to controls without PGE_2 (orange circles for EP2 antagonist, blue circles for EP4 antagonist), and co-incubation of PGE_2 with both antagonists simultaneously (1 µM each, black triangles) compared to controls without PGE_2 (black circles). (**C**) *PTGER2* levels following PGE_2 stimulation as explained in (**A**). (**D**) Downregulation of *PTGER2* upon PGE_2 stimulation was not alleviated by concomitant EP4 antagonist. Colors, symbols and concentrations are explained in (**B**). (**E**) *PTGER4* levels following PGE_2 stimulation as explained in (**A**). (**F**) Downregulation of *PTGER4* upon PGE_2 stimulation was not changed by concomitant EP2 antagonist. Colors, symbols and concentrations are explained in (**B**). Statistics: *, $p < 0.01$; $, $p < 0.05$; n.s., not significant, assessed by (**A, C**) one-way ANOVA with Dunnett's follow-up test; (**B, F**) two-tailed Student's t-test; (**D**) the Mann–Whitney test; and (**E**) a Kruskal–Wallis test with Dunn's multiple comparisons test. Figure 2 has been previously published in (1) as Figures 3 and 4.

3.1.4 Cellular Levels of PGE_2 and its Metabolites in hPC after PGE_2 Stimulation: Effects of Pharmacological EP2 and EP4 Blockade

In order to elucidate whether PGE_2 stimulation and subsequent *COX2* induction result in alterations of cellular PGE_2 and its downstream metabolites 15-keto-PGE_2 and 13,14-dihydro-15-keto-PGE_2, hPC were analyzed by liquid chromatography electrospray ionization tandem mass spectrometry (LC/ESI-MS/MS). After stimulation with PGE_2 100 nM, the cellular PGE_2-level was increased (Figure 3A), while 15-keto-PGE_2 and 13,14-dihydro-15-keto-PGE_2 remained at control levels. Pharmacological inhibition of EP2 and EP4 decreased cellular PGE_2 significantly (Figure 3B). These results suggest an autocrine PGE_2-EP2/EP4-COX2 signaling axis in hPC.

3.1.5 PGE_2 and its Metabolites in Glomeruli and Plasma in the CKD MWF Model

In the rat model of glomerular hyperfiltration, i.e. MWF, lipidomic analysis of PGE_2 and its downstream metabolites 15-keto-PGE_2 and 13,14-dihydro-15-keto-PGE_2 in glomeruli and plasma revealed an increase of glomerular PGE_2 and 15-keto-PGE_2 levels in 8 week old MWF compared to SHR (Figure 3C). No difference was observed for glomerular 13,14-dihydro-15-keto-PGE_2 (Figure 3C), and plasma levels of PGE_2 and 13,14-dihydro-15-keto-PGE_2 (Figure 3D), respectively, whereas the metabolite 15-keto-PGE_2 was below limit of detection in plasma (data not shown).

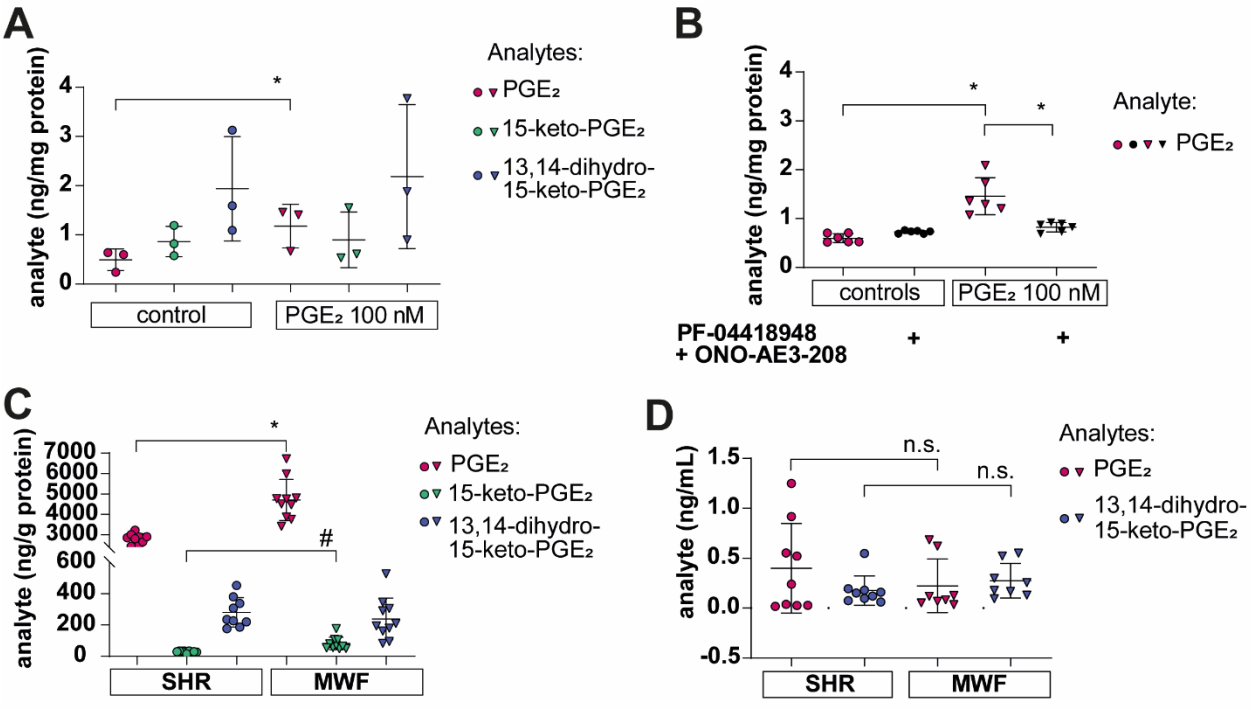

Figure 3. PGE_2 and its metabolites were quantified by LC/ESI-MS/MS in hPC, and in rat glomeruli and plasma.

(**A**) Levels of cellular PGE_2 (pink), 15-keto-PGE_2 (green), and 13,14-dihydro-15-keto-PGE_2 (blue) were determined in hPC after PGE_2 stimulation for 2 h (100 nM, triangles) and in untreated controls (circles). PGE_2 levels were elevated in PGE_2-stimulated cells (pink triangles) vs. controls (pink circles). Each datapoint represents the mean of an independent experiment (performed in triplicate, each experiment consisted of n = 3–6 replicates per treatment) and plotted as combined mean ± SD (horizontal lines). (**B**) Increased cellular PGE_2 levels in hPC induced by PGE_2 stimulation (pink triangles) were abolished by simultaneous co-incubation with combined EP2 and EP4 antagonism (PF-04418948 and ONO-AE3-208, respectively, 1 µM each, black triangles). Each datapoint represents a single sample and plotted as mean ± SD (horizontal lines) per treatment group consisting of n = 6 replicates obtained in a single experiment. (**C – D**) Levels of PGE_2 (pink), 15-keto-PGE_2 (green) and 13,14-dihydro-15-keto-PGE_2 (blue) in MWF (triangles) and SHR (circles) at 8 weeks of age. Each data point represents a single animal and plotted as mean ± SD (horizontal lines) per rat strain consisting of n ≥8 animals, each. (**C**) Glomerular PGE_2 and 15-keto-PGE_2 levels were increased in MWF compared to SHR, whereas glomerular 13,14-dihydro-15-keto-PGE_2 did not differ between both strains. (**D**) In plasma, detectable levels did not differ between both strains. Statistics: *, $p < 0.01$; n.s., not significant, assessed by (**A – C**) a two-tailed Student's t-test, or by (**D**) the Mann–Whitney test. (**C**) #, $p < 0.01$, assessed by the Mann–Whitney test. Figure 3 has been previously published in (1) as Figures 5 b, c and 6 (with modification).

3.1.6 FFSS Increases *COX2* and *PTGER4* Gene Expression in hPC

Due to refinement of the FFSS protocol, novel results are presented in the following.

FFSS was previously shown to increase intracellular PGE_2 levels and COX2 in murine podocytes (39, 41). Correspondingly, FFSS 1 dyne/cm² revealed upregulated *COX2* mRNA expression in hPC, but results were inconsistent after 2 dynes/cm² (Figure 4A). Conversely to previous data in murine podocytes (40, 41), downregulation of *PTGER2* upon FFSS 1 dyne/cm² was observed in hPC, which was not consistent after 2 dynes/cm² (Figure 4B), whereas *PTGER4* expression was upregulated upon both FFSS conditions, as compared to controls (Figure 4C).

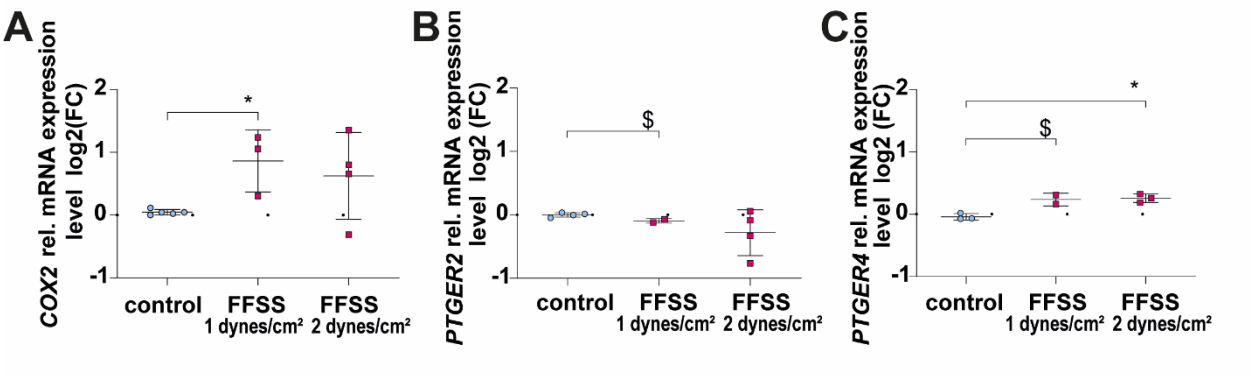

Figure 4. Gene expression of *COX2*, *PTGER2*, and *PTGER4* subjected to FFSS 1 dyne/cm² and 2 dynes/cm² (pink squares) for 2 h in hPC.

qPCR results are shown as relative mRNA expression level normalized to the geometric mean of *HMBS* and *TBP* and referred to control group (blue circles). (**A**) *COX2* was upregulated after FFSS 1 dyne/cm², but this effect was not consistent after 2 dynes/cm². (**B**) *PTGER2* was downregulated to a small extend by FFSS 1 dyne/cm², but this effect was not consistent after 2 dynes/cm². (**C**) *PTGER4* was upregulated after FFSS. Each datapoint represents the mean of an independent experiment (performed at least in duplicate, each experiment consisted of n = 3–6 replicates per treatment) and plotted as combined mean ± SD (horizontal lines). (**A – C**) Statistics: *, $p < 0.01$; $, $p < 0.05$, assessed by a two-tailed Student's t-test.

3.2 Study 2

In total, 285 studies were included in the systematic review, enclosing 53,533 patients exposed to 24 different beta-blockers. Treatment with beta-blocker was compared to placebo in 73 studies, against an active antihypertensive substance in 200 studies and against both active and placebo treatment in 12 studies.

According to the Cochrane Risk of Bias tool (86), the risk of bias was examined to be high, e.g. due to selective reporting, arguable blinding of outcome assessment, and incomplete outcome data. For example, blinding of outcome assessment failed in trials comparing beta-blockers to ACEi, when heart rate was measured, as this parameter would only decrease during beta-blocker treatment. Application of the self-designed rating tool revealed overall a low quality of AE reporting: Only 127 studies reported AE assessment methodology, only 108 studies reported all observed AE, and only 53 studies reported active AE assessment. Among the >30 reported psychiatric AE, depression was most frequently reported, with 1,600 cases out of 26,832 exposed patients, and 47 cases leading to withdrawal out of 13,225 exposed patients. Meta-analytic comparison detected no significant differences in the risk for depression during beta-blocker therapy as compared to placebo (odds ratio, 1.02 [CI, 0.83–1.25]; p = 0.88), which held also true for withdrawal due to depression as reported in 9 studies (odds ratio, 0.97 [CI, 0.51–1.84]; p = 0.91), and in subgroup analyses. Comparison to active drugs also yielded no significant effect on the frequency of depression or withdrawals for depression with beta-blockers. Secondary endpoint analysis indicated possibly higher risk for insomnia, unusual dreams, and sleep disturbance, but risk for anxiety might be alleviated by beta-blocker therapy. Fatigue/tiredness, which was used as a positive control symptom for beta-blocker therapy, occurred more often during beta-blocker therapy than in placebo or active controls and led to more withdrawals than placebo.

4 Discussion

4.1 Study 1

Study 1 demonstrated the presence of an autocrine/paracrine pathway between COX2 and PGE_2 in hPC, which is mediated by EP2 and EP4. The association between PGE_2-elevation and albuminuria due to podocyte damage was further substantiated in a rodent model of glomerular hyperfiltration, i.e. MWF, in which increased glomerular PGE_2 and 15-keto-PGE_2 levels were detected. Understanding prostaglandin signaling in hPC during hyperfiltration may contribute to identifying novel target pathways to prevent maladaptive responses evolving to or aggravating CKD. This is of particular importance, as early detection and treatment of CKD can slow down or prevent ESKD (26).

In human, podocytes comprise 27.7% of glomerular volume, but podocyte number decreases with age or hypertension, leading to compensatory podocyte hypertrophy, which is considered as an early event in glomerulosclerosis (87). The number of functional nephrons seems to be pivotal for glomerular hyperfiltration and further kidney damage. In a population at high risk for renal failure, a lower number of nephrons was observed (88). Furthermore, nephron number declines with age (30), and a nephron deficit was associated with nephrosclerosis and elevated SNGFR (30), as well as hypertension (88). At present, novel treatment options are investigated for the treatment of CKD, including those that directly target podocytes (89), as well as those that presumably lower intraglomerular pressure (90-92), i.e. sodium-glucose cotransporter 2 (SGLT2) inhibitors (93, 94). Yet, treatment with the SGLT2-inhibitor dapagliflozin had no effect on urinary PGE_2 and metabolites (90, 91).

4.1.1 COX2-PGE_2 Axis in Glomerular Hyperfiltration

Previous studies in mouse models of hyperfiltration suggested a pathophysiological impact of autocrine/paracrine COX2/PGE_2 activation on podocyte damage, thus contributing to impairment of the glomerular filtration barrier and the development of albuminuria (39-41). Accordingly, induction of *Cox2* associated with podocyte damage, while inhibition of COX2 restored podocyte cytoskeleton *in vitro* (39), and reduced proteinuria in animal models of CKD (95, 96), as well as in patients (reviewed in (97)). Recently, elevated urinary PGE_2 was suggested as an early biomarker of hyperfiltration preceding overt microalbuminuria (98). In urinary samples from children with solitary

functioning kidney and hyperfiltration due to their lower nephron numbers as compared to control children, albumin and PGE_2 were clearly elevated (98). The authors conclude that PGE_2 is a potential biomarker for early stages of adaptive hyperfiltration (98), which is in agreement with the herein presented hypothesis.

4.1.2 PGE_2 Signaling

To shed light on PGE_2 signaling in hPC, EP1, -2 and -4 expression was detected, as well as increased intracellular cAMP levels upon treatment with PGE_2. In line with stimulation of adenylate cyclase activity *via* both EP2 and EP4 (reviewed in (49)), the PGE_2-stimulated intracellular cAMP increase in hPC was only completely abolished by combined EP2 and EP4 antagonism. Similarly, a dose-dependent upregulation of *COX2* mRNA was detected upon PGE_2 stimulation, which was only completely alleviated by dual blockade of EP2 and EP4. Modulation of *COX2* gene expression by PGE_2 was previously linked to multiple intracellular signaling pathways involving EP2 and EP4 in human cells (99, 100). The cAMP-PKA pathway was described to be involved *in vitro* upon PGE_2 stimulation of mouse podocytes (77) and upon FFSS in osteocytes (101, 102). Yet, this was not seen in murine podocytes after FFSS, potentially due to late assessment of cAMP levels (at the earliest 2 h after applying FFSS) (77). PGE_2 stimulation of EP2 and EP4 was disclosed to induce cAMP response element-binding protein (CREB) in human cells, which was shown to be PKA-dependent for EP2, whereas EP4-coupled phosphatidylinositol 3-kinase signaling could counteract CREB formation (45, 103, 104). Importantly, transcription of *COX2* can be regulated by CREB, as CRE is part of the COX2 promotor (45, 105, 106). Thus, following intracellular cAMP level elevation, subsequent PKA/CREB activation could mediate the increase in *COX2* expression in hPC, but this requires further investigation.

4.1.3 Impact of FFSS

Along with mimicking hyperfiltration by treatment with PGE_2, gene expression of the PGE_2/*COX2*-axis in hPC was quantified after FFSS, i.e. an experimental approach imitating intensified flow of the ultrafiltrate in Bowman's space. FFSS of 2 dynes/cm² was previously shown to increase intracellular PGE_2 levels and COX2, as well as EP2 in murine podocytes, whereas EP4 remained unchanged (39-41). In hPC, FFSS 1 dyne/cm² increased *COX2* and downregulated *PTGER2*, but results were inconsistent after

2 dynes/cm². Conversely to previous findings, upregulated *PTGER4* expression was observed in hPC upon both FFSS conditions, as compared to control. These diverging results may be attributed to species differences and to the shear force applied. In parallel to the FFSS results in hPC, murine podocytes delineated increases of *Ptger4* and *Cox2* after stretch as compared to nonstretched controls (107), and glomerular COX2 was increased in subtotally nephrectomized rats, in which hyperfiltration is postulated due to nephron loss (95, 108). The data added novel evidence to the role of PGE_2/COX2 axis in hPC during FFSS. Some signaling pathways involved in mechanotransduction in mouse podocytes have already been identified (40, 41, 77), but the pathways responsible for FFSS signaling in hPC remain to be elucidated.

Generally, the use of cell lines *in vitro* might not directly represent cellular mechanisms *in vivo*. Isolation of primary podocytes might circumvent a general issue of podocyte cell lines, i.e. dedifferentiation, which is sometimes observed in stiff 2 dimensional cell culture (85, 109-111). Nevertheless, cultured podocytes are still an indispensable resource to dissect some of the primary, cell physiological mechanisms *in vitro* (109), and novel approaches to obtain primary podocytes can complement this knowledge, e.g. in human (85, 111).

4.1.4 Lipidomic Analysis and MWF model

Besides cAMP and *COX2*, PGE_2 stimulation of hPC also increased cellular PGE_2, which was abrogated by combined EP2- and EP4-antagonism. This strengthens the hypothesis of the autocrine/paracrine mechanism, i.e. extracellular PGE_2 induces EP2 and EP4 signaling, thus increasing *COX2* expression, whose induction leads to higher cellular PGE_2 levels in turn, as COX2 represents the rate-limiting step of PGE_2 synthesis (reviewed in (112)).

Of note, our group identified prostaglandin reductase 2 (*Ptgr2*) as a potential candidate gene for the development of albuminuria in the MWF model, which represents a genetic nondiabetic CKD model with glomerular hyperfiltration due to an inherited nephron deficit as reviewed in (33, 34, 113). Male MWF are characterized by increased SNGFR (34, 114), and develop mild arterial hypertension, spontaneous progressive albuminuria between weeks 4 and 8 after birth, podocyte foot process effacement, i.e. a simplification of podocyte's sophisticated ultrastructure (115), and subsequently glomerulosclerosis

(33, 116). Thus, after congenic substitution of a quantitative trait locus on rat chromosome 6 containing *Ptgr2*, with albuminuria-resistant SHR (113, 117), albuminuria decreased in MWF (82). PTGR2 acts in the downstream metabolism of PGE_2 (118), which again links to the hypothesis of an activated PGE_2-pathway during hyperfiltration. Correspondingly, the prostaglandin profile in glomeruli and plasma of MWF was compared to SHR. The detected elevation of both PGE_2 and 15-keto-PGE_2 in isolated glomeruli of MWF support the notion that this pathway is activated in glomerular hyperfiltration. In contrast to glomeruli, the prostaglandin profile in plasma did not differ significantly between MWF and SHR, and could not be assessed completely due to dilution below detection limit. Thus, analysis of glomeruli seems to offer a deeper insight into podocyte prostaglandin profile. However, as glomeruli consist of different cell types, i.e. glomerular endothelial cells, mesangial cells and podocytes, direct conclusions on podocyte pathophysiology cannot be safely drawn.

4.1.5 Summary of Study 1

Collectively, it was shown that an autocrine/paracrine pathway between *COX2* and PGE_2 exists in hPC, and is promoted by both EP2 and EP4. This is of particular interest, as an activation of the PGE_2 axis in MWF was reported, which is in line with previous findings in *in vivo* models of glomerular hyperfiltration (40, 41, 119). Elucidating the pathological mechanisms in podocytes might help to identify novel targets for preventing development or progression of albuminuria and CKD. Prevention, early detection and treatment of CKD is key to alleviate the burden of ESKD (120), and is of urgent need as CKD is currently the 12th leading cause of death worldwide (12), and projected to be among the top 5 by 2040 (121).

4.2 Study 2

4.2.1 Beta-blockers and Renoprotection in Human

Likewise, counteracting hypertension mediated kidney damage by appropriate antihypertensive therapy is crucial to reduce the burden of CKD. It is widely accepted that BP lowering *per se* is renoprotective (4). Irrespective of the applied treatment, a reduction in BP had renoprotective effects in proteinuric (51-53), as well as in diabetic patients (55, 122, 123).

An early study in nondiabetic individuals with impaired renal function suggested that BP reduction lowered intraglomerular pressure and thereby contributed to renoprotection, regardless of interference with RAS, based on similar renal hemodynamic responses by the ACEi enalapril and the beta-blocker atenolol, i.e. an initial fall of GFR, filtration fraction and the slope of GFR within 4 years (54). However, this study was underpowered to identify a difference between treatment regimens (54), and the superiority of RAS-blockers in terms of renoprotection in comparison to other antihypertensive drugs was demonstrated many times (56, 57, 124). In hypertensive patients with CKD, RAS-blockade was more beneficial to mitigate kidney outcomes than e.g. beta-blocker therapy (125). A network meta-analysis comparing RAS-blockers to placebo or active controls depicted decreased risk for kidney failure under RAS-blockade, whereas the active comparators did not show evidence of a significant protective effect on kidney failure (126).

The putative benefit of beta-blockers in delaying CKD progression was discussed controversially. An early study on patients with diabetic nephropathy, atenolol failed to slow renal disease progression, as compared to CCBs and the ACEi lisinopril (127), and corroborated a previous study, where beta-blockers were inferior to enalapril in hypertensive, nondiabetic CKD patients with regard to the cumulative renal survival rate and the slope of the reciprocal serum creatinine concentration (128). A meta-analysis of various populations demonstrated that beta-blockers were less efficacious for the prevention of renal failure and major cardiovascular disease events, relative to other antihypertensive first-line drugs (129).

Some data supported, however, a renoprotective potential of beta-blocker therapy, as they provided evidence for a modification of renal hemodynamics, glomerular filtration, or renal oxygenation under treatment. In patients with uncomplicated hypertension, one-year treatment with the beta-blocker bisoprolol did not change GFR and renal plasma flow, but significantly reduced the filtration fraction as compared to baseline, which was similar to treatment with the ARB losartan (130). Magnetic resonance imaging revealed improved renal tissue oxygenation under beta-blocker therapy, suggesting that decreased renal oxygen consumption potentially prevents the progression of renal dysfunction (131). Of note, CCBs or diuretics had no association, and RAS-blockers were even associated with reduced medullary oxygenation (131). However, in another study,

no significant differences in renal oxygenation and GFR decline were detected between CKD patients treated with the beta-blocker metoprolol vs. the CCB amlodipine and/or RAS-blocker (132).

In general, elevated sympathetic nerve activity causes hypertension and kidney disease, as noradrenaline regulates renin release, renal vascular resistance, as well as sodium and water handling (133, 134). By promoting hypertension and fluid retention, an increased sympathetic tone could potentially stimulate glomerular hyperfiltration. Moreover, renal sympathetic nerve activity is increased in hypertension and thus critical for the perpetuation of hypertension and the development of hypertensive kidney disease (133, 134). Correspondingly, inhibition of sympathetic activity can attenuate hypertensive kidney disease (133, 135). In case of hypertension or deteriorated kidney function, renal sympathetic nerve activity further aggravates cardiovascular and renal disorders by fluid retention, reduction of renal blood flow and GFR, and renin release (133). Of note, beta-blockers were also shown to suppress renin secretion, angiotensin II and aldosterone, and can therefore be considered as weak inhibitors of RAS (136).

A large study in CKD patients comparing different antihypertensive drugs (including beta-blockers) on top of a baseline CCB disclosed comparable efficacy in preventing cardiovascular events and preserving eGFR (137). Equal efficacy was also reported for atenolol and the ACEi captopril in the prevention of renal outcomes (i.e. progression of albuminuria, plasma creatinine concentrations or in the proportion of patients with doubling of baseline creatinine concentration) after long-term treatment in diabetic hypertensive patients (55). Metoprolol significantly reduced microalbuminuria as compared to baseline in mild-to-moderate essential arterial hypertension with normal GFR (51), but was inferior to another beta-blocker, carvedilol, in preventing the progression of microalbuminuria in diabetic hypertensive individuals receiving RAS-blockade (138). Albeit less efficacious than the ACEi ramipril in reducing composite kidney outcomes, metoprolol treatment significantly lowered the risk for ESKD or death, ESKD alone, as well as kidney outcomes in subjects with elevated baseline proteinuria, and attenuated GFR decline in patients with lower baseline GFR, as compared to amlodipine in African Americans with hypertensive renal disease (125). Interestingly, amlodipine belongs to the group of CCBs targeting L-type channels, whose renoprotective effect was recently questioned, as they failed to reduce or even

aggravated baseline proteinuria in hypertensive patients (139, 140). Mathematical modeling supported clinical evidence that L-type CCBs potentiate glomerular hypertension during CKD by dilating glomerular afferent arterioles, resulting in a decline of functional nephrons and hyperfiltration (i.e. elevated SNGFR) (141). In contrast to RAS-blockers or beta-blockers, the use of CCBs was furthermore associated with mortality in patients with CKD in a retrospective cohort study (142). In light of potential renoprotective effects of beta-blockers and possible deleterious effects of L-type CCBs in CKD patients, beta-blockers can be reconsidered as valuable options to complement RAS-blockers for antihypertensive therapy in these patients.

4.2.2 Beta-blockers and Intensified BP Control in CKD Patients: Cardiovascular Outcomes and Mortality

With respect of cardiovascular outcomes and mortality, beta-blockers were shown to be not inferior to other antihypertensive regimens in CKD patients. In subjects without known cardiovascular disease and incident ESKD, beta-blockers, RAS-blockers, and dual combination of both significantly reduced mortality rates as compared to matched controls without antihypertensive treatment (143). In a meta-analysis of randomized controlled trials, SBP reduction decreased risk of major cardiovascular events in patients with and without CKD (cutoff at eGFR <60 mL/min per 1.73 m²), and there were no differential effects between drug regimens, e.g. comparing diuretics/beta-blocker vs. ACEi, or CCB, respectively (144). In African Americans with hypertensive renal disease, there were no significant differences in all-cause mortality or cardiovascular mortality between metoprolol, ramipril, or amlodipine treatment (125). Interestingly, in patients with ESKD receiving hemodialysis, bisoprolol was associated with lower all-cause mortality and a lower risk of major adverse cardiovascular events after 2 years in comparison to carvedilol, mainly attributed to reduced heart failure and ischemic stroke risk (145).

Moreover, large randomized trials and meta-analyses indicated that an intensified BP control (i.e. targeting lower BP levels) in CKD patients reduced cardiovascular and/or all-cause mortality relative to a usual BP control (146-148), but had no protective effects on kidney outcomes (147, 149-152). A meta-analysis demonstrated that every 10 mmHg reduction in SBP resulted in decreased risks of cardiovascular events (e.g. heart failure and stroke) and all-cause mortality in various populations of patients, but there was no significant effect on the risk of renal failure (129). Nevertheless, albeit smaller than in

patients without CKD, individuals with CKD also disclosed risk reduction for major cardiovascular disease events, and regarding their higher absolute risks, marked absolute benefits from BP reduction could be achieved (129). Other analyses including long-term follow-up periods in hypertensive CKD patients provided evidence that intensive BP reduction indeed might attenuate the progression of CKD (153-155), especially in patients with higher baseline proteinuria (52, 147, 149, 154, 156). This is reflected in the current Kidney Disease: Improving Global Outcomes (KDIGO) guideline for BP management in patients with CKD, which recommends a target SBP of <120 mmHg, when tolerated, for most adult patients with CKD not receiving dialysis (13). This lower BP target is, however, more strict than recommended by the 2018 European guidelines for hypertension management that recommend a SBP target of 130–139 mmHg for hypertensive CKD patients (4) and has been criticized (60).

Recent studies indicated that beta-blocker use was associated with reduced mortality in subjects with CKD and heart failure (157-159). Together, beta-blockers play a fundamental role in antihypertensive therapy for patients with cardiac comorbidities, as well as for CKD patients, and can be a valuable contributor to antihypertensive combinations to achieve appropriate BP reductions and concomitantly minimize AE. Real-world data demonstrated that CKD patients receiving antihypertensive combinations with beta-blockers plus diuretics were more likely to have controlled BP compared to other prescribed combinations (160).

4.2.3 Non-Adherence to Antihypertensive Therapy

Safety concerns and side effects of antihypertensive drugs including beta-blockers could negatively influence patients' adherence, thus leading to suboptimal BP control and accelerated kidney damage. In a recent survey, >90% of participating healthcare professionals agreed that patients' concerns about antihypertensive medication influence their adherence (161). A cross-sectional study among hypertensive patients reported a non-adherence rate of 37.7% (162), which is in line with 30–50% of non-adherence reviewed in (163). The prevalence of non-adherence to antihypertensive medication ranged from 24.1% in The Netherlands to 70.3% in Hungary (Germany: 33.2%) in self-reporting Europeans (164), and 25% when detected by urinary LC-MS/MS analysis (165). In treatment-resistant hypertension, non-adherence was detected in 55% of patients (166). Cohort studies indicated that following diagnosis of hypertension, 51.4% of patients

had low adherence to antihypertensive therapy after 6 months (167). Accordingly, a longitudinal study reported that approximately half of the patients stopped their antihypertensive medication within 1 year, although it was supposed to be used indefinitely long (168).

Non-adherence to antihypertensive drugs increased with time, as seen by discontinuation rates being 33%, 41%, 50% of newly-treated hypertensive patients after 6 months, 1 year, and 5 years after initial treatment, respectively (169). Of older adults, 14.3% delineated low adherence of antihypertensive medication at baseline, and over 2 years follow-up, the annual decline in adherence was estimated to be 4.3% (170). Of note, depressive symptoms were associated with a decline in adherence (170), and initial beta-blockers were associated with increased discontinuation (169). Other studies indicated that adherence with beta-blockers decreased over time and was between 30–40% after 6 months, almost 30% after 1 year (171), and <50% after 3 years in various patient populations (172, 173). Depending on whether the patient was discharged on beta-blockers or not following hospitalization for acute myocardial infarction, adherence for beta-blockers was 61% or only 12% after 1 year (174).

4.2.4 Depression and Hypertension

An early study on psychiatric outpatients reported a three-fold higher rate of diagnosed major depression in hypertensive patients than in non-hypertensives (175). Consequently, a meta-analysis summarized that depression is prevalent among 26.8% of hypertensive patients (176).

Potential pathophysiological mechanisms accounting for the high prevalence of depression among hypertensive patients include a dysregulation of the noradrenergic system (177), genetic predisposition (178), and increased activation of the sympathetic nervous system (179). Depressed patients delineated increased heart rates as compared to non-depressed controls (180-182), and plasma levels of noradrenaline were increased in patients with depression and related disorders (180, 183-187). Veith and coworkers suggested an increased activity of the sympathetic nervous system in major depression, as plasma levels of noradrenaline, heart rates and noradrenaline appearance in (extra-) vascular compartments were higher in depressed patients than in controls, whereas noradrenaline clearance from plasma was unchanged (187). A series of cardiovascular

tests indicated that sympathetic reactivity was higher, whereas parasympathetic reactivity was lower in patients with depression than in healthy controls (188).

4.2.5 Beta-blockers and Depression

In a machine learning model, exposure to non-selective beta-blockers was the strongest predictor of major depressive disorders in patients with cardiovascular disease (189). With regard to the discrepancy to the current literature suggesting that beta-blockers do not cause depression, the authors assume that the impact of non-selective beta-blockers could be diluted in those studies, which reflect a broad mixture of various types of beta-blockers (189). A prospective cohort study provided evidence that beta-blockers in general, as well as beta-blockers with serotonergic receptor affinity did not bear an increased risk of depression (190). In contrast, lipophilic beta-blockers, as well as non-selective beta-blockers were associated with a higher risk of depressive symptoms within 3 months after treatment start, possibly due to a strong effect of propranolol belonging to both groups (190). A cross-sectional study in elderly patients reported that beta-blocker use was associated with increased prevalence of depressive symptoms, which was also valid in various subgroups, as compared to other antihypertensive drug classes and non-medicated controls (191). In a secondary analysis, this positive association was more pronounced with lipophilic and non-selective beta-blockers than with hydrophilic and selective beta-blockers, respectively, and there was higher prevalence of depressive symptoms associated with metoprolol (significant), and propranolol and atenolol (trend) (191). Likewise, elderly hypertensive patients using a lipophilic beta-blocker were more likely to have elevated depression scores than those who did not use a lipophilic beta-blocker (192). Nevertheless, atenolol-based antihypertensive treatment strategy was associated with more severe depressive symptoms than a verapamil-based (CCB) strategy (193). Consistent with these findings, other investigators reported increased prescribing of antidepressants following and during beta-blocker therapy (68, 69), and particularly show that the lipophilic beta-blocker propranolol is associated with a higher relative risk of concurrent antidepressant prescription (69). Overall, prescription of antidepressants was more prevalent in subjects receiving lipophilic beta-blockers than hydrophilic beta-blockers, but this difference was mainly related to propranolol (69). A meta-analysis also indicated that propranolol produces a depressed mood (194).

Several potential mechanisms have been described to account for the possible association of beta-blockers and depression. One possible reason for beta-blockers – at least for the lipophilic agents – to cause central nervous system related AE was linked to their distribution in the brain: lipophilic beta-blockers such as propranolol were distributed to a higher degree in the brain than hydrophilic agents, e.g. atenolol (195). Consequently, lipophilic beta-blockers were significantly more likely to provoke central nervous system AE as compared to the hydrophilic beta-blocker atenolol (196, 197). Other investigators speculated that beta-blockers interfere with noradrenergic neurotransmitter function in the brain, and therefore cause depression (68). Furthermore, propranolol and atenolol have been reported to decrease nocturnal production of melatonin, which could account for sleep disturbances (198), and further promote depression.

However, a prescription symmetry analysis provided evidence that there is no causative relation between beta-blockers, particularly propranolol, and depression (199), and a literature search revealed a certain publication cycle on this topic, i.e. studies supporting the hypothesis that beta-blockers cause depression were followed by several studies refuting this hypothesis (200).

4.2.6 Summary of Study 2

As depression is reported concomitantly to the use of beta-blockers (64-67), the suspected causative role of beta-blockers for the development of depression was elucidated in a large systematic review and meta-analyses of double-blind randomized controlled trials (2). Furthermore, study 2 sheds light on the question whether beta-blockers further accelerate the prevalence of depression in hypertensive patients. The risk of bias was evaluated to be high according to (86), and quality of AE reporting was low in most cases. However, validation of results was accomplished with a positive control symptom, i.e. fatigue/tiredness, which is a well-known AE for beta-blockers. Consequently, the risk of fatigue/tiredness was increased during beta-blocker treatment than with placebo, or active agents. Comparison to placebo and active controls further contributed to validation of the results, as well as sensitivity and subgroup analyses, which ensured robustness.

Collectively, the results do not support an association between beta-blocker therapy and depression, which is in line with a previously published meta-analysis with a smaller

population (201). Moreover, in a real-life population-based study from Denmark, continued use of four beta-blockers (i.e. propranolol, atenolol, bisoprolol, and carvedilol) was even associated with decreased rates of depression, whereas the remaining beta-blockers did not increase the risk of depression (202). Therefore, concerns about the impact of beta-blockers on psychological health should not affect their application in clinical practice including their use in patients with or at risk for CKD.

5 Conclusion

The two studies included in this doctoral thesis focused on hypertension and renoprotection. In particular, the autocrine/paracrine PGE_2/COX2 pathway during glomerular hyperfiltration was investigated in study 1 as a potential pathomechanism of hypertensive kidney disease. Study 2 considered safety aspects of antihypertensive drug treatment with beta-blockers, which play an important role for pharmacotherapy in hypertensive CKD patients. The results of study 1 support an autocrine/paracrine COX2/PGE_2 pathway in hPC, which is promoted by concerted EP2 and EP4 signaling. Activation of this pathway during hyperfiltration was shown by upregulated *COX2* and *PTGER4* in hPC after FFSS, and increased PGE_2 and 15-keto-PGE_2 levels in isolated glomeruli from MWF, as compared to a control strain. Study 2 demonstrated that depression did not occur more commonly during beta-blockers than during placebo or active agents, using a systematic review and meta-analyses of double-blind randomized controlled trials. Albeit quality of AE reporting was low in the most underlying studies, results of study 2 were validated using different means, e.g. a positive control symptom.

Hypertension and renoprotection are closely linked with each other, as hypertension and CKD are connected in a self-reinforcing cycle. Together, this thesis contributes to a better comprehension of pathological mechanisms underlying glomerular hyperfiltration and thus CKD, and furthermore helps to improve adherence to beta-blocker therapy by reducing safety concerns about psychological impact.

6 References

1. Mangelsen E, Rothe M, Schulz A, Kourpa A, Panáková D, Kreutz R, Bolbrinker J. Concerted EP2 and EP4 Receptor Signaling Stimulates Autocrine Prostaglandin E(2) Activation in Human Podocytes. Cells. 2020;9(5).

2. Riemer TG, Villagomez Fuentes LE, Algharably EAE, Schäfer MS, Mangelsen E, Fürtig MA, Bittner N, Bär A, Zaidi Touis L, Wachtell K, Majic T, Dinges MJ, Kreutz R. Do β-Blockers Cause Depression?: Systematic Review and Meta-Analysis of Psychiatric Adverse Events During β-Blocker Therapy. Hypertension. 2021;77(5):1539-48.

3. GBD 2017 Risk Factor Collaborators. Global, regional, and national comparative risk assessment of 84 behavioural, environmental and occupational, and metabolic risks or clusters of risks for 195 countries and territories, 1990-2017: a systematic analysis for the Global Burden of Disease Study 2017. Lancet (London, England). 2018;392(10159):1923-94.

4. Williams B, Mancia G, Spiering W, Agabiti Rosei E, Azizi M, Burnier M, Clement DL, Coca A, de Simone G, Dominiczak A, Kahan T, Mahfoud F, Redon J, Ruilope L, Zanchetti A, Kerins M, Kjeldsen SE, Kreutz R, Laurent S, Lip GYH, McManus R, Narkiewicz K, Ruschitzka F, Schmieder RE, Shlyakhto E, Tsioufis C, Aboyans V, Desormais I. 2018 ESC/ESH Guidelines for the management of arterial hypertension. Eur Heart J. 2018;39(33):3021-104.

5. Roth GA, Mensah GA, Johnson CO, Addolorato G, Ammirati E, Baddour LM, Barengo NC, Beaton AZ, Benjamin EJ, Benziger CP, Bonny A, Brauer M, Brodmann M, Cahill TJ, Carapetis J, Catapano AL, Chugh SS, Cooper LT, Coresh J, Criqui M, DeCleene N, Eagle KA, Emmons-Bell S, Feigin VL, Fernández-Solà J, Fowkes G, Gakidou E, Grundy SM, He FJ, Howard G, Hu F, Inker L, Karthikeyan G, Kassebaum N, Koroshetz W, Lavie C, Lloyd-Jones D, Lu HS, Mirijello A, Temesgen AM, Mokdad A, Moran AE, Muntner P, Narula J, Neal B, Ntsekhe M, Moraes de Oliveira G, Otto C, Owolabi M, Pratt M, Rajagopalan S, Reitsma M, Ribeiro ALP, Rigotti N, Rodgers A, Sable C, Shakil S, Sliwa-Hahnle K, Stark B, Sundström J, Timpel P, Tleyjeh IM, Valgimigli M, Vos T, Whelton PK, Yacoub M, Zuhlke L, Murray C, Fuster V. Global Burden of Cardiovascular Diseases and Risk Factors, 1990-2019: Update From the GBD 2019 Study. J Am Coll Cardiol. 2020;76(25):2982-3021.

6. Schwartz GL, Strong CG. Renal parenchymal involvement in essential hypertension. Med Clin North Am. 1987;71(5):843-58.

7. Mensah GA, Croft JB, Giles WH. The heart, kidney, and brain as target organs in hypertension. Cardiol Clin. 2002;20(2):225-47.

8. Brenner BM, Lawler EV, Mackenzie HS. The hyperfiltration theory: a paradigm shift in nephrology. Kidney international. 1996;49(6):1774-7.

9. The United States Renal Data System (USRDS), End Stage Renal Disease, Chapter 1,, [Internet]. [cited 20.10.2021]. Available from: https://adr.usrds.org/2020/end-stage-renal-disease/1-incidence-prevalence-patient-characteristics-and-treatment-modalities.

10. The United States Renal Data System (USRDS), Chronic Kidney Disease, Chapter 1, 3, 4,, [Internet]. [cited 20.10.2021]. Available from: https://adr.usrds.org/2020/chronic-kidney-disease/1-ckd-in-the-general-population.

11. World Health Organization (WHO), The top 10 causes of death [Internet]. 2020 [cited 25.11.2021]. Available from: https://www.who.int/news-room/fact-sheets/detail/the-top-10-causes-of-death.

12. GBD Chronic Kidney Disease Collaboration. Global, regional, and national burden of chronic kidney disease, 1990-2017: a systematic analysis for the Global Burden of Disease Study 2017. Lancet (London, England). 2020;395(10225):709-33.

13. Kidney Disease: Improving Global Outcomes (KDIGO) Blood Pressure Work Group. KDIGO 2021 Clinical Practice Guideline for the Management of Blood Pressure in Chronic Kidney Disease. Kidney international. 2021;99(3s):S1-s87.

14. Hillege HL, Janssen WM, Bak AA, Diercks GF, Grobbee DE, Crijns HJ, Van Gilst WH, De Zeeuw D, De Jong PE. Microalbuminuria is common, also in a nondiabetic, nonhypertensive population, and an independent indicator of cardiovascular risk factors and cardiovascular morbidity. J Intern Med. 2001;249(6):519-26.

15. Yuyun MF, Khaw KT, Luben R, Welch A, Bingham S, Day NE, Wareham NJ. Microalbuminuria, cardiovascular risk factors and cardiovascular morbidity in a British population: the EPIC-Norfolk population-based study. Eur J Cardiovasc Prev Rehabil. 2004;11(3):207-13.

16. Jensen JS, Feldt-Rasmussen B, Borch-Johnsen K, Clausen P, Appleyard M, Jensen G. Microalbuminuria and its relation to cardiovascular disease and risk factors. A population-based study of 1254 hypertensive individuals. J Hum Hypertens. 1997;11(11):727-32.

17. Bigazzi R, Bianchi S, Baldari D, Campese VM. Microalbuminuria predicts cardiovascular events and renal insufficiency in patients with essential hypertension. J Hypertens. 1998;16(9):1325-33.

18. Jager A, Kostense PJ, Ruhé HG, Heine RJ, Nijpels G, Dekker JM, Bouter LM, Stehouwer CD. Microalbuminuria and peripheral arterial disease are independent predictors of cardiovascular and all-cause mortality, especially among hypertensive subjects: five-year follow-up of the Hoorn Study. Arteriosclerosis, thrombosis, and vascular biology. 1999;19(3):617-24.

19. Jensen JS, Feldt-Rasmussen B, Strandgaard S, Schroll M, Borch-Johnsen K. Arterial hypertension, microalbuminuria, and risk of ischemic heart disease. Hypertension. 2000;35(4):898-903.

20. Ibsen H, Olsen MH, Wachtell K, Borch-Johnsen K, Lindholm LH, Mogensen CE, Dahlöf B, Devereux RB, de Faire U, Fyhrquist F, Julius S, Kjeldsen SE, Lederballe-Pedersen O, Nieminen MS, Omvik P, Oparil S, Wan Y. Reduction in albuminuria translates to reduction in cardiovascular events in hypertensive patients: losartan intervention for endpoint reduction in hypertension study. Hypertension. 2005;45(2):198-202.

21. Holtkamp FA, de Zeeuw D, de Graeff PA, Laverman GD, Berl T, Remuzzi G, Packham D, Lewis JB, Parving HH, Lambers Heerspink HJ. Albuminuria and blood pressure, independent targets for cardioprotective therapy in patients with diabetes and nephropathy: a post hoc analysis of the combined RENAAL and IDNT trials. Eur Heart J. 2011;32(12):1493-9.

22. Fukui A, Kaneko H, Okada A, Yano Y, Itoh H, Matsuoka S, Morita K, Kiriyama H, Kamon T, Fujiu K, Michihata N, Jo T, Takeda N, Morita H, Nakamura S, Nishiyama A, Node K, Yokoo T, Nangaku M, Yasunaga H, Komuro I. Semiquantitative assessed proteinuria and risk of heart failure: Analysis of a nationwide epidemiological database. Nephrol Dial Transplant. 2021;gfab248.

23. Go AS, Chertow GM, Fan D, McCulloch CE, Hsu CY. Chronic kidney disease and the risks of death, cardiovascular events, and hospitalization. N Engl J Med. 2004;351(13):1296-305.

24. Matsushita K, Selvin E, Bash LD, Franceschini N, Astor BC, Coresh J. Change in estimated GFR associates with coronary heart disease and mortality. Journal of the American Society of Nephrology : JASN. 2009;20(12):2617-24.

25. Chowdhury EK, Langham RG, Ademi Z, Owen A, Krum H, Wing LM, Nelson MR, Reid CM. Rate of change in renal function and mortality in elderly treated hypertensive patients. Clinical journal of the American Society of Nephrology : CJASN. 2015;10(7):1154-61.

26. Couser WG, Remuzzi G, Mendis S, Tonelli M. The contribution of chronic kidney disease to the global burden of major noncommunicable diseases. Kidney international. 2011;80(12):1258-70.

27. Tonelli M, Wiebe N, Culleton B, House A, Rabbat C, Fok M, McAlister F, Garg AX. Chronic kidney disease and mortality risk: a systematic review. Journal of the American Society of Nephrology : JASN. 2006;17(7):2034-47.

28. Hostetter TH, Olson JL, Rennke HG, Venkatachalam MA, Brenner BM. Hyperfiltration in remnant nephrons: a potentially adverse response to renal ablation. The American journal of physiology. 1981;241(1):F85-93.

29. Celsi G, Savin J, Henter JI, Sohtell M. The contribution of ultrafiltration pressure for glomerular hyperfiltration in young nephrectomized rats. Acta Physiol Scand. 1991;141(4):483-7.

30. Denic A, Mathew J, Lerman LO, Lieske JC, Larson JJ, Alexander MP, Poggio E, Glassock RJ, Rule AD. Single-Nephron Glomerular Filtration Rate in Healthy Adults. N Engl J Med. 2017;376(24):2349-57.

31. Brenner BM. Nephron adaptation to renal injury or ablation. The American journal of physiology. 1985;249(3 Pt 2):F324-37.

32. Srivastava T, Celsi GE, Sharma M, Dai H, McCarthy ET, Ruiz M, Cudmore PA, Alon US, Sharma R, Savin VA. Fluid flow shear stress over podocytes is increased in the solitary kidney. Nephrol Dial Transplant. 2014;29(1):65-72.

33. Schulz A, Kreutz R. Mapping genetic determinants of kidney damage in rat models. Hypertens Res. 2012;35(7):675-94.

34. Fassi A, Sangalli F, Maffi R, Colombi F, Mohamed EI, Brenner BM, Remuzzi G, Remuzzi A. Progressive glomerular injury in the MWF rat is predicted by inborn nephron deficit. Journal of the American Society of Nephrology : JASN. 1998;9(8):1399-406.

35. Friedrich C, Endlich N, Kriz W, Endlich K. Podocytes are sensitive to fluid shear stress in vitro. American journal of physiology Renal physiology. 2006;291(4):F856-65.

36. Pavenstadt H, Kriz W, Kretzler M. Cell biology of the glomerular podocyte. Physiological reviews. 2003;83(1):253-307.

37. Futrakul N, Sridama V, Futrakul P. Microalbuminuria--a biomarker of renal microvascular disease. Ren Fail. 2009;31(2):140-3.

38. Endlich N, Endlich K. The challenge and response of podocytes to glomerular hypertension. Semin Nephrol. 2012;32(4):327-41.

39. Srivastava T, McCarthy ET, Sharma R, Cudmore PA, Sharma M, Johnson ML, Bonewald LF. Prostaglandin E(2) is crucial in the response of podocytes to fluid flow shear stress. Journal of cell communication and signaling. 2010;4(2):79-90.

40. Srivastava T, McCarthy ET, Sharma R, Kats A, Carlton CG, Alon US, Cudmore PA, El-Meanawy A, Sharma M. Fluid flow shear stress upregulates prostanoid receptor EP2 but not EP4 in murine podocytes. Prostaglandins & other lipid mediators. 2013;104-105:49-57.

41. Srivastava T, Alon US, Cudmore PA, Tarakji B, Kats A, Garola RE, Duncan RS, McCarthy ET, Sharma R, Johnson ML, Bonewald LF, El-Meanawy A, Savin VJ, Sharma M. Cyclooxygenase-2, prostaglandin E2, and prostanoid receptor EP2 in fluid flow shear stress-mediated injury in the solitary kidney. American journal of physiology Renal physiology. 2014;307(12):F1323-33.

42. Samuelsson B, Granstrom E, Green K, Hamberg M, Hammarstrom S. Prostaglandins. Annual review of biochemistry. 1975;44:669-95.

43. Smith WL. The eicosanoids and their biochemical mechanisms of action. The Biochemical journal. 1989;259(2):315-24.

44. Cheng B, Kato Y, Zhao S, Luo J, Sprague E, Bonewald LF, Jiang JX. PGE(2) is essential for gap junction-mediated intercellular communication between osteocyte-like MLO-Y4 cells in response to mechanical strain. Endocrinology. 2001;142(8):3464-73.

45. Pino MS, Nawrocki ST, Cognetti F, Abruzzese JL, Xiong HQ, McConkey DJ. Prostaglandin E2 drives cyclooxygenase-2 expression via cyclic AMP response element activation in human pancreatic cancer cells. Cancer biology & therapy. 2005;4(11):1263-9.

46. Faour WH, Gomi K, Kennedy CR. PGE(2) induces COX-2 expression in podocytes via the EP(4) receptor through a PKA-independent mechanism. Cellular signalling. 2008;20(11):2156-64.

47. Díaz-Muñoz Manuel D, Osma-García Inés C, Fresno M, Iñiguez Miguel A. Involvement of PGE2and the cAMP signalling pathway in the up-regulation of COX-2 and mPGES-1 expression in LPS-activated macrophages. Biochemical Journal. 2012;443(2):451-61.

48. Narumiya S, Sugimoto Y, Ushikubi F. Prostanoid receptors: structures, properties, and functions. Physiological reviews. 1999;79(4):1193-226.

49. Negishi M, Sugimoto Y, Ichikawa A. Molecular mechanisms of diverse actions of prostanoid receptors. Biochim Biophys Acta. 1995;1259(1):109-19.

50. Ansari KM, Sung YM, He G, Fischer SM. Prostaglandin receptor EP2 is responsible for cyclooxygenase-2 induction by prostaglandin E2 in mouse skin. Carcinogenesis. 2007;28(10):2063-8.

51. Erley CM, Haefele U, Heyne N, Braun N, Risler T. Microalbuminuria in essential hypertension. Reduction by different antihypertensive drugs. Hypertension. 1993;21(6 Pt 1):810-5.

52. Klahr S, Levey AS, Beck GJ, Caggiula AW, Hunsicker L, Kusek JW, Striker G. The effects of dietary protein restriction and blood-pressure control on the progression of chronic renal disease. Modification of Diet in Renal Disease Study Group. N Engl J Med. 1994;330(13):877-84.

53. Peterson JC, Adler S, Burkart JM, Greene T, Hebert LA, Hunsicker LG, King AJ, Klahr S, Massry SG, Seifter JL. Blood pressure control, proteinuria, and the progression of renal disease. The Modification of Diet in Renal Disease Study. Ann Intern Med. 1995;123(10):754-62.

54. Apperloo AJ, de Zeeuw D, de Jong PE. A short-term antihypertensive treatment-induced fall in glomerular filtration rate predicts long-term stability of renal function. Kidney international. 1997;51(3):793-7.

55. UK Prospective Diabetes Study Group. Efficacy of atenolol and captopril in reducing risk of macrovascular and microvascular complications in type 2 diabetes: UKPDS 39. UK Prospective Diabetes Study Group. Bmj. 1998;317(7160):713-20.

56. Mann JF, Reisch C, Ritz E. Use of angiotensin-converting enzyme inhibitors for the preservation of kidney function. A retrospective study. Nephron. 1990;55 Suppl 1:38-42.

57. Ruggenenti P, Perna A, Gherardi G, Garini G, Zoccali C, Salvadori M, Scolari F, Schena FP, Remuzzi G. Renoprotective properties of ACE-inhibition in non-diabetic nephropathies with non-nephrotic proteinuria. Lancet (London, England). 1999;354(9176):359-64.

58. Jafar TH, Schmid CH, Landa M, Giatras I, Toto R, Remuzzi G, Maschio G, Brenner BM, Kamper A, Zucchelli P, Becker G, Himmelmann A, Bannister K, Landais P, Shahinfar S, de Jong PE, de Zeeuw D, Lau J, Levey AS. Angiotensin-converting enzyme inhibitors and progression of nondiabetic renal disease. A meta-analysis of patient-level data. Ann Intern Med. 2001;135(2):73-87.

59. Haller H, Ito S, Izzo JL, Jr., Januszewicz A, Katayama S, Menne J, Mimran A, Rabelink TJ, Ritz E, Ruilope LM, Rump LC, Viberti G. Olmesartan for the delay or prevention of microalbuminuria in type 2 diabetes. N Engl J Med. 2011;364(10):907-17.

60. Ott C, Schmieder RE. Diagnosis and treatment of arterial hypertension 2021. Kidney international. 2022;101(1):36-46.

61. Palmer BF. Managing hyperkalemia caused by inhibitors of the renin-angiotensin-aldosterone system. N Engl J Med. 2004;351(6):585-92.

62. Loutradis C, Price A, Ferro CJ, Sarafidis P. Renin-angiotensin system blockade in patients with chronic kidney disease: benefits, problems in everyday clinical use, and open questions for advanced renal dysfunction. J Hum Hypertens. 2021;35(6):499-509.

63. Schwabe U, Ludwig W-D, Anlauf M, Weber F. Arzneiverordnungs-Report 2020, Kapitel 15, Antihypertonika Abb. 15.1, p. 384: Springer-Verlag Berlin Heidelberg; 2020.

64. Frishman WH. Beta-adrenergic receptor blockers. Adverse effects and drug interactions. Hypertension. 1988;11(3 Pt 2):Ii21-9.

65. Keller S, Frishman WH. Neuropsychiatric effects of cardiovascular drug therapy. Cardiol Rev. 2003;11(2):73-93.

66. European database of suspected adverse drug reaction reports [Internet]. [cited 20.10.2021]. Available from: https://www.adrreports.eu/en/index.html.

67. FDA Adverse Event Reporting System (FAERS) Public Dashboard [Internet]. [cited 20.10.2021]. Available from: https://www.fda.gov/drugs/questions-and-answers-fdas-adverse-event-reporting-system-faers/fda-adverse-event-reporting-system-faers-public-dashboard.

68. Avorn J, Everitt DE, Weiss S. Increased antidepressant use in patients prescribed beta-blockers. Jama. 1986;255(3):357-60.

69. Thiessen BQ, Wallace SM, Blackburn JL, Wilson TW, Bergman U. Increased prescribing of antidepressants subsequent to beta-blocker therapy. Arch Intern Med. 1990;150(11):2286-90.

70. Saleem MA, O'Hare MJ, Reiser J, Coward RJ, Inward CD, Farren T, Xing CY, Ni L, Mathieson PW, Mundel P. A conditionally immortalized human podocyte cell line demonstrating nephrin and podocin expression. Journal of the American Society of Nephrology : JASN. 2002;13(3):630-8.

71. Ni L, Saleem M, Mathieson PW. Podocyte culture: tricks of the trade. Nephrology (Carlton, Vic). 2012;17(6):525-31.

72. af Forselles KJ, Root J, Clarke T, Davey D, Aughton K, Dack K, Pullen N. In vitro and in vivo characterization of PF-04418948, a novel, potent and selective prostaglandin EP(2) receptor antagonist. British journal of pharmacology. 2011;164(7):1847-56.

73. Ma X, Aoki T, Tsuruyama T, Narumiya S. Definition of Prostaglandin E2-EP2 Signals in the Colon Tumor Microenvironment That Amplify Inflammation and Tumor Growth. Cancer Res. 2015;75(14):2822-32.

74. Kabashima K, Saji T, Murata T, Nagamachi M, Matsuoka T, Segi E, Tsuboi K, Sugimoto Y, Kobayashi T, Miyachi Y, Ichikawa A, Narumiya S. The prostaglandin receptor EP4 suppresses colitis, mucosal damage and CD4 cell activation in the gut. Journal of Clinical Investigation. 2002;109(7):883-93.

75. Thieme K, Majumder S, Brijmohan AS, Batchu SN, Bowskill BB, Alghamdi TA, Advani SL, Kabir MG, Liu Y, Advani A. EP4 inhibition attenuates the development of diabetic and non-diabetic experimental kidney disease. Scientific reports. 2017;7(1):3442.

76. Bek M, Nusing R, Kowark P, Henger A, Mundel P, Pavenstadt H. Characterization of prostanoid receptors in podocytes. Journal of the American Society of Nephrology : JASN. 1999;10(10):2084-93.

77. Srivastava T, Dai H, Heruth DP, Alon US, Garola RE, Zhou J, Duncan RS, El-Meanawy A, McCarthy ET, Sharma R, Johnson ML, Savin VJ, Sharma M. Mechanotransduction signaling in podocytes from fluid flow shear stress. American journal of physiology Renal physiology. 2018;314(1):F22-f34.

78. Dey I, Giembycz MA, Chadee K. Prostaglandin E(2) couples through EP(4) prostanoid receptors to induce IL-8 production in human colonic epithelial cell lines. British journal of pharmacology. 2009;156(3):475-85.

79. Liu C, Zhu P, Wang W, Li W, Shu Q, Chen ZJ, Myatt L, Sun K. Inhibition of lysyl oxidase by prostaglandin E2 via EP2/EP4 receptors in human amnion fibroblasts: Implications for parturition. Molecular and cellular endocrinology. 2016;424:118-27.

80. Lee J, Aoki T, Thumkeo D, Siriwach R, Yao C, Narumiya S. T cell-intrinsic prostaglandin E2-EP2/EP4 signaling is critical in pathogenic TH17 cell-driven inflammation. The Journal of allergy and clinical immunology. 2019;143(2):631-43.

81. Livak KJ, Schmittgen TD. Analysis of relative gene expression data using real-time quantitative PCR and the 2(-Delta Delta C(T)) Method. Methods (San Diego, Calif). 2001;25(4):402-8.

82. Schulz A, Muller NV, van de Lest NA, Eisenreich A, Schmidbauer M, Barysenka A, Purfurst B, Sporbert A, Lorenzen T, Meyer AM, Herlan L, Witten A, Ruhle F, Zhou W, de Heer E, Scharpfenecker M, Panakova D, Stoll M, Kreutz R. Analysis of the genomic architecture of a complex trait locus in hypertensive rat models links Tmem63c to kidney damage. eLife. 2019;8.

83. Vandesompele J, De Preter K, Pattyn F, Poppe B, Van Roy N, De Paepe A, Speleman F. Accurate normalization of real-time quantitative RT-PCR data by geometric averaging of multiple internal control genes. Genome biology. 2002;3(7):Research0034.

84. Feng D, Kumar M, Muntel J, Gurley SB, Birrane G, Stillman IE, Ding L, Wang M, Ahmed S, Schlondorff J, Alper SL, Ferrante T, Marquez SL, Ng CF, Novak R, Ingber DE, Steen H, Pollak MR. Phosphorylation of ACTN4 Leads to Podocyte Vulnerability and Proteinuric Glomerulosclerosis. Journal of the American Society of Nephrology : JASN. 2020;31(7):1479-95.

85. Yang SH, Choi JW, Huh D, Jo HA, Kim S, Lim CS, Lee JC, Kim HC, Kwon HM, Jeong CW, Kwak C, Joo KW, Kim YS, Kim DK. Roles of fluid shear stress and retinoic acid in the differentiation of primary cultured human podocytes. Experimental cell research. 2017;354(1):48-56.

86. Sterne JAC, Savović J, Page MJ, Elbers RG, Blencowe NS, Boutron I, Cates CJ, Cheng HY, Corbett MS, Eldridge SM, Emberson JR, Hernán MA, Hopewell S, Hróbjartsson A, Junqueira DR, Jüni P, Kirkham JJ, Lasserson T, Li T, McAleenan A, Reeves BC, Shepperd S, Shrier I, Stewart LA, Tilling K, White IR, Whiting PF, Higgins JPT. RoB 2: a revised tool for assessing risk of bias in randomised trials. Bmj. 2019;366:l4898.

87. Haruhara K, Sasaki T, de Zoysa N, Okabayashi Y, Kanzaki G, Yamamoto I, Harper IS, Puelles VG, Shimizu A, Cullen-McEwen LA, Tsuboi N, Yokoo T, Bertram JF. Podometrics in Japanese Living Donor Kidneys: Associations with Nephron Number, Age, and Hypertension. Journal of the American Society of Nephrology : JASN. 2021;32(5):1187-99.

88. Hoy WE, Hughson MD, Singh GR, Douglas-Denton R, Bertram JF. Reduced nephron number and glomerulomegaly in Australian Aborigines: a group at high risk for renal disease and hypertension. Kidney international. 2006;70(1):104-10.

89. Walsh L, Reilly JF, Cornwall C, Gaich GA, Gipson DS, Heerspink HJL, Johnson L, Trachtman H, Tuttle KR, Farag YMK, Padmanabhan K, Pan-Zhou XR, Woodworth JR, Czerwiec FS. Safety and Efficacy of GFB-887, a TRPC5 Channel Inhibitor, in Patients With Focal Segmental Glomerulosclerosis, Treatment-Resistant Minimal Change Disease, or Diabetic Nephropathy: TRACTION-2 Trial Design. Kidney Int Rep. 2021;6(10):2575-84.

90. Cherney DZ, Perkins BA, Soleymanlou N, Maione M, Lai V, Lee A, Fagan NM, Woerle HJ, Johansen OE, Broedl UC, von Eynatten M. Renal hemodynamic effect of sodium-glucose cotransporter 2 inhibition in patients with type 1 diabetes mellitus. Circulation. 2014;129(5):587-97.

91. Cherney DZI, Dekkers CCJ, Barbour SJ, Cattran D, Abdul Gafor AH, Greasley PJ, Laverman GD, Lim SK, Di Tanna GL, Reich HN, Vervloet MG, Wong MG, Gansevoort RT, Heerspink HJL. Effects of the SGLT2 inhibitor dapagliflozin on proteinuria in non-diabetic patients with chronic kidney disease (DIAMOND): a randomised, double-blind, crossover trial. Lancet Diabetes Endocrinol. 2020;8(7):582-93.

92. van Bommel EJM, Muskiet MHA, van Baar MJB, Tonneijck L, Smits MM, Emanuel AL, Bozovic A, Danser AHJ, Geurts F, Hoorn EJ, Touw DJ, Larsen EL, Poulsen HE, Kramer MHH, Nieuwdorp M, Joles JA, van Raalte DH. The renal hemodynamic effects of the SGLT2 inhibitor dapagliflozin are caused by post-glomerular vasodilatation rather than pre-glomerular vasoconstriction in metformin-treated patients with type 2 diabetes in the randomized, double-blind RED trial. Kidney international. 2020;97(1):202-12.

93. Heerspink HJL, Stefánsson BV, Correa-Rotter R, Chertow GM, Greene T, Hou FF, Mann JFE, McMurray JJV, Lindberg M, Rossing P, Sjöström CD, Toto RD, Langkilde AM, Wheeler DC. Dapagliflozin in Patients with Chronic Kidney Disease. N Engl J Med. 2020;383(15):1436-46.

94. Chertow G, Vart P, Jongs N, Toto R, Gorriz JL, Hou FF, McMurray J, Correa-Rotter R, Rossing P, Sjöström CD, Stefánsson B, Langkilde AM, Wheeler D, Heerspink H. Effects of Dapagliflozin in Stage 4 Chronic Kidney Disease. Journal of the American Society of Nephrology : JASN. 2021;32(9):2352-61.

95. Fujihara CK, Antunes GR, Mattar AL, Andreoli N, Malheiros DM, Noronha IL, Zatz R. Cyclooxygenase-2 (COX-2) inhibition limits abnormal COX-2 expression and progressive injury in the remnant kidney. Kidney international. 2003;64(6):2172-81.

96. Wang JL, Cheng HF, Shappell S, Harris RC. A selective cyclooxygenase-2 inhibitor decreases proteinuria and retards progressive renal injury in rats. Kidney international. 2000;57(6):2334-42.

97. Vogt L, Laverman GD, Navis G. Time for a comeback of NSAIDs in proteinuric chronic kidney disease? The Netherlands journal of medicine. 2010;68(12):400-7.

98. Srivastava T, Ju W, Milne GL, Rezaiekhaligh MH, Staggs VS, Alon US, Sharma R, Zhou J, El-Meanawy A, McCarthy ET, Savin VJ, Sharma M. Urinary prostaglandin E2 is a biomarker of early adaptive hyperfiltration in solitary functioning kidney. Prostaglandins & other lipid mediators. 2020;146:106403.

99. Fujino H, West KA, Regan JW. Phosphorylation of glycogen synthase kinase-3 and stimulation of T-cell factor signaling following activation of EP2 and EP4 prostanoid receptors by prostaglandin E2. The Journal of biological chemistry. 2002;277(4):2614-9.

100. Hsu HH, Lin YM, Shen CY, Shibu MA, Li SY, Chang SH, Lin CC, Chen RJ, Viswanadha VP, Shih HN, Huang CY. Prostaglandin E2-Induced COX-2 Expressions via EP2 and EP4 Signaling Pathways in Human LoVo Colon Cancer Cells. International journal of molecular sciences. 2017;18(6).

101. Cherian PP, Cheng B, Gu S, Sprague E, Bonewald LF, Jiang JX. Effects of mechanical strain on the function of Gap junctions in osteocytes are mediated through the prostaglandin EP2 receptor. The Journal of biological chemistry. 2003;278(44):43146-56.

102. Kitase Y, Barragan L, Qing H, Kondoh S, Jiang JX, Johnson ML, Bonewald LF. Mechanical induction of PGE2 in osteocytes blocks glucocorticoid-induced apoptosis through both the beta-catenin and PKA pathways. J Bone Miner Res. 2010;25(12):2657-68.

103. Fujino H, Salvi S, Regan JW. Differential regulation of phosphorylation of the cAMP response element-binding protein after activation of EP2 and EP4 prostanoid receptors by prostaglandin E2. Molecular pharmacology. 2005;68(1):251-9.

104. Lu JW, Wang WS, Zhou Q, Gan XW, Myatt L, Sun K. Activation of prostaglandin EP4 receptor attenuates the induction of cyclooxygenase-2 expression by EP2 receptor activation in human amnion fibroblasts: implications for parturition. FASEB journal : official publication of the Federation of American Societies for Experimental Biology. 2019;33(7):8148-60.

105. Kosaka T, Miyata A, Ihara H, Hara S, Sugimoto T, Takeda O, Takahashi E, Tanabe T. Characterization of the human gene (PTGS2) encoding prostaglandin-endoperoxide synthase 2. Eur J Biochem. 1994;221(3):889-97.

106. Gao F, Zafar MI, Juttner S, Hocker M, Wiedenmann B. Expression and Molecular Regulation of the Cox2 Gene in Gastroenteropancreatic Neuroendocrine Tumors and Antiproliferation of Nonsteroidal Anti-Inflammatory Drugs (NSAIDs). Med Sci Monit. 2018;24:8125-40.

107. Martineau LC, McVeigh LI, Jasmin BJ, Kennedy CR. p38 MAP kinase mediates mechanically induced COX-2 and PG EP4 receptor expression in podocytes: implications for the actin cytoskeleton. American journal of physiology Renal physiology. 2004;286(4):F693-701.

108. Wang JL, Cheng HF, Zhang MZ, McKanna JA, Harris RC. Selective increase of cyclooxygenase-2 expression in a model of renal ablation. The American journal of physiology. 1998;275(4):F613-22.

109. Rinschen MM, Schroeter CB, Koehler S, Ising C, Schermer B, Kann M, Benzing T, Brinkkoetter PT. Quantitative deep mapping of the cultured podocyte proteome uncovers shifts in proteostatic mechanisms during differentiation. American journal of physiology Cell physiology. 2016;311(3):C404-17.

110. Hu M, Azeloglu EU, Ron A, Tran-Ba KH, Calizo RC, Tavassoly I, Bhattacharya S, Jayaraman G, Chen Y, Rabinovich V, Iyengar R, Hone JC, He JC, Kaufman LJ. A biomimetic gelatin-based platform elicits a pro-differentiation effect on podocytes through mechanotransduction. Scientific reports. 2017;7:43934.

111. Yoshimura Y, Taguchi A, Tanigawa S, Yatsuda J, Kamba T, Takahashi S, Kurihara H, Mukoyama M, Nishinakamura R. Manipulation of Nephron-Patterning Signals Enables Selective Induction of Podocytes from Human Pluripotent Stem Cells. Journal of the American Society of Nephrology : JASN. 2019;30(2):304-21.

112. Needleman P, Turk J, Jakschik BA, Morrison AR, Lefkowith JB. Arachidonic acid metabolism. Annual review of biochemistry. 1986;55:69-102.

113. Schulz A, Weiss J, Schlesener M, Hansch J, Wehland M, Wendt N, Kossmehl P, Sietmann A, Grimm D, Stoll M, Nyengaard JR, Kreutz R. Development of overt proteinuria in the Munich Wistar Fromter rat is suppressed by replacement of chromosome 6 in a consomic rat strain. Journal of the American Society of Nephrology : JASN. 2007;18(1):113-21.

114. Remuzzi A, Puntorieri S, Mazzoleni A, Remuzzi G. Sex related differences in glomerular ultrafiltration and proteinuria in Munich-Wistar rats. Kidney international. 1988;34(4):481-6.

115. Ijpelaar DH, Schulz A, Koop K, Schlesener M, Bruijn JA, Kerjaschki D, Kreutz R, de Heer E. Glomerular hypertrophy precedes albuminuria and segmental loss of podoplanin in podocytes in Munich-Wistar-Frömter rats. American journal of physiology Renal physiology. 2008;294(4):F758-67.

116. Macconi D, Bonomelli M, Benigni A, Plati T, Sangalli F, Longaretti L, Conti S, Kawachi H, Hill P, Remuzzi G, Remuzzi A. Pathophysiologic implications of reduced podocyte number in a rat model of progressive glomerular injury. The American journal of pathology. 2006;168(1):42-54.

117. van Es N, Schulz A, Ijpelaar D, van der Wal A, Kuhn K, Schütten S, Kossmehl P, Nyengaard JR, de Heer E, Kreutz R. Elimination of severe albuminuria in aging hypertensive rats by exchange of 2 chromosomes in double-consomic rats. Hypertension. 2011;58(2):219-24.

118. Tai HH, Ensor CM, Tong M, Zhou H, Yan F. Prostaglandin catabolizing enzymes. Prostaglandins & other lipid mediators. 2002;68-69:483-93.

119. Ulu N, Schoemaker RG, Henning RH, Buikema H, Teerlink T, Zijlstra FJ, Bakker SJ, van Gilst WH, Navis G. Proteinuria-associated endothelial dysfunction is strain dependent. American journal of nephrology. 2009;30(3):209-17.

120. Tonelli M, Dickinson JA. Early Detection of CKD: Implications for Low-Income, Middle-Income, and High-Income Countries. Journal of the American Society of Nephrology : JASN. 2020;31(9):1931-40.

121. Foreman KJ, Marquez N, Dolgert A, Fukutaki K, Fullman N, McGaughey M, Pletcher MA, Smith AE, Tang K, Yuan CW, Brown JC, Friedman J, He J, Heuton KR, Holmberg M, Patel DJ, Reidy P, Carter A, Cercy K, Chapin A, Douwes-Schultz D, Frank T, Goettsch F, Liu PY, Nandakumar V, Reitsma MB, Reuter V, Sadat N, Sorensen RJD, Srinivasan V, Updike RL, York H, Lopez AD, Lozano R, Lim SS, Mokdad AH, Vollset SE, Murray CJL. Forecasting life expectancy, years of life lost, and all-cause and cause-specific mortality for 250 causes of death: reference and alternative scenarios for 2016-40 for 195 countries and territories. Lancet (London, England). 2018;392(10159):2052-90.

122. Mogensen CE. Long-term antihypertensive treatment inhibiting progression of diabetic nephropathy. Br Med J (Clin Res Ed). 1982;285(6343):685-8.

123. Parving HH, Andersen AR, Smidt UM, Hommel E, Mathiesen ER, Svendsen PA. Effect of antihypertensive treatment on kidney function in diabetic nephropathy. Br Med J (Clin Res Ed). 1987;294(6585):1443-7.

124. Hou FF, Zhang X, Zhang GH, Xie D, Chen PY, Zhang WR, Jiang JP, Liang M, Wang GB, Liu ZR, Geng RW. Efficacy and safety of benazepril for advanced chronic renal insufficiency. N Engl J Med. 2006;354(2):131-40.

125. Wright JT, Jr., Bakris G, Greene T, Agodoa LY, Appel LJ, Charleston J, Cheek D, Douglas-Baltimore JG, Gassman J, Glassock R, Hebert L, Jamerson K, Lewis J, Phillips RA, Toto RD, Middleton JP, Rostand SG. Effect of blood pressure lowering and antihypertensive drug class on progression of hypertensive kidney disease: results from the AASK trial. Jama. 2002;288(19):2421-31.

126. Xie X, Liu Y, Perkovic V, Li X, Ninomiya T, Hou W, Zhao N, Liu L, Lv J, Zhang H, Wang H. Renin-Angiotensin System Inhibitors and Kidney and Cardiovascular Outcomes in Patients With CKD: A Bayesian Network Meta-analysis of Randomized Clinical Trials. Am J Kidney Dis. 2016;67(5):728-41.

127. Bakris GL, Copley JB, Vicknair N, Sadler R, Leurgans S. Calcium channel blockers versus other antihypertensive therapies on progression of NIDDM associated nephropathy. Kidney international. 1996;50(5):1641-50.

128. Hannedouche T, Landais P, Goldfarb B, el Esper N, Fournier A, Godin M, Durand D, Chanard J, Mignon F, Suo JM, Grünfeld JP. Randomised controlled trial of enalapril and beta blockers in non-diabetic chronic renal failure. Bmj. 1994;309(6958):833-7.

129. Ettehad D, Emdin CA, Kiran A, Anderson SG, Callender T, Emberson J, Chalmers J, Rodgers A, Rahimi K. Blood pressure lowering for prevention of cardiovascular disease and death: a systematic review and meta-analysis. Lancet (London, England). 2016;387(10022):957-67.

130. Parrinello G, Paterna S, Torres D, Di Pasquale P, Mezzero M, La Rocca G, Cardillo M, Trapanese C, Caradonna M, Licata G. One-year renal and cardiac effects of bisoprolol versus losartan in recently diagnosed hypertensive patients: a randomized, double-blind study. Clin Drug Investig. 2009;29(9):591-600.

131. Hall ME, Rocco MV, Morgan TM, Hamilton CA, Jordan JH, Edwards MS, Hall JE, Hundley WG. Beta-Blocker Use Is Associated with Higher Renal Tissue Oxygenation in Hypertensive Patients Suspected of Renal Artery Stenosis. Cardiorenal Med. 2016;6(4):261-8.

132. Khatir DS, Pedersen M, Ivarsen P, Christensen KL, Jespersen B, Buus NH. Effects of additional vasodilatory or nonvasodilatory treatment on renal function, vascular resistance and oxygenation in chronic kidney disease: a randomized clinical trial. J Hypertens. 2019;37(1):116-24.

133. Sata Y, Head GA, Denton K, May CN, Schlaich MP. Role of the Sympathetic Nervous System and Its Modulation in Renal Hypertension. Front Med (Lausanne). 2018;5:82.

134. Hering L, Rahman M, Potthoff SA, Rump LC, Stegbauer J. Role of α2-Adrenoceptors in Hypertension: Focus on Renal Sympathetic Neurotransmitter Release, Inflammation, and Sodium Homeostasis. Front Physiol. 2020;11:566871.

135. Hering L, Rahman M, Hoch H, Markó L, Yang G, Reil A, Yakoub M, Gupta V, Potthoff SA, Vonend O, Ralph DL, Gurley SB, McDonough AA, Rump LC, Stegbauer J. α2A-Adrenoceptors Modulate Renal Sympathetic Neurotransmission and Protect against Hypertensive Kidney Disease. Journal of the American Society of Nephrology : JASN. 2020;31(4):783-98.

136. Blumenfeld JD, Sealey JE, Mann SJ, Bragat A, Marion R, Pecker MS, Sotelo J, August P, Pickering TG, Laragh JH. Beta-adrenergic receptor blockade as a therapeutic approach for suppressing the renin-angiotensin-aldosterone system in normotensive and hypertensive subjects. Am J Hypertens. 1999;12(5):451-9.

137. Rakugi H, Ogihara T, Umemoto S, Matsuzaki M, Matsuoka H, Shimada K, Higaki J, Ito S, Kamiya A, Suzuki H, Ohashi Y, Shimamoto K, Saruta T. Combination therapy for hypertension in patients with CKD: a subanalysis of the Combination Therapy of Hypertension to Prevent Cardiovascular Events trial. Hypertens Res. 2013;36(11):947-58.

138. Bakris GL, Fonseca V, Katholi RE, McGill JB, Messerli FH, Phillips RA, Raskin P, Wright JT, Jr., Oakes R, Lukas MA, Anderson KM, Bell DS. Metabolic effects of carvedilol vs metoprolol in patients with type 2 diabetes mellitus and hypertension: a randomized controlled trial. Jama. 2004;292(18):2227-36.

139. Bellinghieri G, Mazzaglia G, Savica V, Santoro D. Effects of manidipine and nifedipine on blood pressure and renal function in patients with chronic renal failure: a multicenter randomized controlled trial. Ren Fail. 2003;25(5):681-9.

140. Bakris GL, Weir MR, Secic M, Campbell B, Weis-McNulty A. Differential effects of calcium antagonist subclasses on markers of nephropathy progression. Kidney international. 2004;65(6):1991-2002.

141. Moore KH, Clemmer JS. Questioning the renoprotective role of L-type calcium channel blockers in chronic kidney disease using physiological modeling. American journal of physiology Renal physiology. 2021;321(4):F548-f57.

142. Haider DG, Sauter T, Lindner G, Masghati S, Peric S, Friedl A, Wolzt M, Hörl WH, Soleiman A, Exadaktylos A, Fuhrmann V. Use of Calcium Channel Blockers is Associated with Mortality in Patients with Chronic Kidney Disease. Kidney & blood pressure research. 2015;40(6):630-7.

143. Ferreira JP, Couchoud C, Gregson J, Tiple A, Glowacki F, London G, Agarwal R, Rossignol P. Angiotensin-converting enzyme inhibitors/angiotensin receptor blockers, β-blockers or both in incident end-stage renal disease patients without cardiovascular disease: a propensity-matched longitudinal cohort study. Nephrol Dial Transplant. 2019;34(7):1216-22.

144. Ninomiya T, Perkovic V, Turnbull F, Neal B, Barzi F, Cass A, Baigent C, Chalmers J, Li N, Woodward M, MacMahon S. Blood pressure lowering and major cardiovascular events in people with and without chronic kidney disease: meta-analysis of randomised controlled trials. Bmj. 2013;347:f5680.

145. Wu PH, Lin YT, Liu JS, Tsai YC, Kuo MC, Chiu YW, Hwang SJ, Carrero JJ. Comparative effectiveness of bisoprolol and carvedilol among patients receiving maintenance hemodialysis. Clin Kidney J. 2021;14(3):983-90.

146. Wright JT, Jr., Williamson JD, Whelton PK, Snyder JK, Sink KM, Rocco MV, Reboussin DM, Rahman M, Oparil S, Lewis CE, Kimmel PL, Johnson KC, Goff DC, Jr., Fine LJ, Cutler JA, Cushman WC, Cheung AK, Ambrosius WT. A Randomized Trial of Intensive versus Standard Blood-Pressure Control. N Engl J Med. 2015;373(22):2103-16.

147. Ku E, Gassman J, Appel LJ, Smogorzewski M, Sarnak MJ, Glidden DV, Bakris G, Gutiérrez OM, Hebert LA, Ix JH, Lea J, Lipkowitz MS, Norris K, Ploth D, Pogue VA, Rostand SG, Siew ED, Sika M, Tisher CC, Toto R, Wright JT, Jr., Wyatt C, Hsu CY. BP Control and Long-Term Risk of ESRD and Mortality. Journal of the American Society of Nephrology : JASN. 2017;28(2):671-7.

148. Malhotra R, Nguyen HA, Benavente O, Mete M, Howard BV, Mant J, Odden MC, Peralta CA, Cheung AK, Nadkarni GN, Coleman RL, Holman RR, Zanchetti A, Peters R, Beckett N, Staessen JA, Ix JH. Association Between More Intensive vs Less Intensive Blood Pressure Lowering and Risk of Mortality in Chronic Kidney Disease Stages 3 to 5: A Systematic Review and Meta-analysis. JAMA Intern Med. 2017;177(10):1498-505.

149. Appel LJ, Wright JT, Jr., Greene T, Agodoa LY, Astor BC, Bakris GL, Cleveland WH, Charleston J, Contreras G, Faulkner ML, Gabbai FB, Gassman JJ, Hebert LA, Jamerson KA, Kopple JD, Kusek JW, Lash JP, Lea JP, Lewis JB, Lipkowitz MS, Massry SG, Miller ER, Norris K, Phillips RA, Pogue VA, Randall OS, Rostand SG, Smogorzewski MJ, Toto RD, Wang X. Intensive blood-pressure control in hypertensive chronic kidney disease. N Engl J Med. 2010;363(10):918-29.

150. Ku E, Glidden DV, Johansen KL, Sarnak M, Tighiouart H, Grimes B, Hsu CY. Association between strict blood pressure control during chronic kidney disease and lower mortality after onset of end-stage renal disease. Kidney international. 2015;87(5):1055-60.

151. Cheung AK, Rahman M, Reboussin DM, Craven TE, Greene T, Kimmel PL, Cushman WC, Hawfield AT, Johnson KC, Lewis CE, Oparil S, Rocco MV, Sink KM, Whelton PK, Wright JT, Jr., Basile J, Beddhu S, Bhatt U, Chang TI, Chertow GM, Chonchol M, Freedman BI, Haley W, Ix JH, Katz LA, Killeen AA, Papademetriou V, Ricardo AC, Servilla K, Wall B, Wolfgram D, Yee J. Effects of Intensive BP Control in CKD. Journal of the American Society of Nephrology : JASN. 2017;28(9):2812-23.

152. Tsai WC, Wu HY, Peng YS, Yang JY, Chen HY, Chiu YL, Hsu SP, Ko MJ, Pai MF, Tu YK, Hung KY, Chien KL. Association of Intensive Blood Pressure Control and Kidney Disease Progression in Nondiabetic Patients With Chronic Kidney Disease: A Systematic Review and Meta-analysis. JAMA Intern Med. 2017;177(6):792-9.

153. Sarnak MJ, Greene T, Wang X, Beck G, Kusek JW, Collins AJ, Levey AS. The effect of a lower target blood pressure on the progression of kidney disease: long-term follow-up of the modification of diet in renal disease study. Ann Intern Med. 2005;142(5):342-51.

154. Lv J, Ehteshami P, Sarnak MJ, Tighiouart H, Jun M, Ninomiya T, Foote C, Rodgers A, Zhang H, Wang H, Strippoli GF, Perkovic V. Effects of intensive blood pressure lowering on the progression of chronic kidney disease: a systematic review and meta-analysis. Cmaj. 2013;185(11):949-57.

155. Xie X, Atkins E, Lv J, Bennett A, Neal B, Ninomiya T, Woodward M, MacMahon S, Turnbull F, Hillis GS, Chalmers J, Mant J, Salam A, Rahimi K, Perkovic V, Rodgers A. Effects of intensive blood pressure lowering on cardiovascular and renal outcomes: updated systematic review and meta-analysis. Lancet (London, England). 2016;387(10017):435-43.

156. Ku E, Sarnak MJ, Toto R, McCulloch CE, Lin F, Smogorzewski M, Hsu CY. Effect of Blood Pressure Control on Long-Term Risk of End-Stage Renal Disease and Death Among Subgroups of Patients With Chronic Kidney Disease. Journal of the American Heart Association. 2019;8(16):e012749.

157. Badve SV, Roberts MA, Hawley CM, Cass A, Garg AX, Krum H, Tonkin A, Perkovic V. Effects of beta-adrenergic antagonists in patients with chronic kidney disease: a systematic review and meta-analysis. J Am Coll Cardiol. 2011;58(11):1152-61.

158. Kotecha D, Gill SK, Flather MD, Holmes J, Packer M, Rosano G, Böhm M, McMurray JJV, Wikstrand J, Anker SD, van Veldhuisen DJ, Manzano L, von Lueder TG, Rigby AS, Andersson B, Kjekshus J, Wedel H, Ruschitzka F, Cleland JGF, Damman K, Redon J, Coats AJS. Impact of Renal Impairment on Beta-Blocker Efficacy in Patients With Heart Failure. J Am Coll Cardiol. 2019;74(23):2893-904.

159. Fu EL, Uijl A, Dekker FW, Lund LH, Savarese G, Carrero JJ. Association Between β-Blocker Use and Mortality/Morbidity in Patients With Heart Failure With Reduced, Midrange, and Preserved Ejection Fraction and Advanced Chronic Kidney Disease. Circ Heart Fail. 2020;13(11):e007180.

160. Magvanjav O, Cooper-DeHoff RM, McDonough CW, Gong Y, Segal MS, Hogan WR, Johnson JA. Antihypertensive therapy prescribing patterns and correlates of blood pressure control among hypertensive patients with chronic kidney disease. J Clin Hypertens (Greenwich). 2019;21(1):91-101.

161. Burnier M, Prejbisz A, Weber T, Azizi M, Cunha V, Versmissen J, Gupta P, Vaclavik J, Januszewicz A, Persu A, Kreutz R. Hypertension healthcare professional beliefs and behaviour regarding patient medication adherence: a survey conducted among European Society of Hypertension Centres of Excellence. Blood Press. 2021;30(5):282-90.

162. Mahmood S, Jalal Z, Hadi MA, Orooj H, Shah KU. Non-Adherence to Prescribed Antihypertensives in Primary, Secondary and Tertiary Healthcare Settings in Islamabad, Pakistan: A Cross-Sectional Study. Patient Prefer Adherence. 2020;14:73-85.

163. Lane D, Lawson A, Burns A, Azizi M, Burnier M, Jones DJL, Kably B, Khunti K, Kreutz R, Patel P, Persu A, Spiering W, Toennes SW, Tomaszewski M, Williams B, Gupta P, Dasgupta I. Nonadherence in Hypertension: How to Develop and Implement Chemical Adherence Testing. Hypertension. 2022;79(1):12-23.

164. Morrison VL, Holmes EA, Parveen S, Plumpton CO, Clyne W, De Geest S, Dobbels F, Vrijens B, Kardas P, Hughes DA. Predictors of self-reported adherence to antihypertensive medicines: a multinational, cross-sectional survey. Value Health. 2015;18(2):206-16.

165. Tomaszewski M, White C, Patel P, Masca N, Damani R, Hepworth J, Samani NJ, Gupta P, Madira W, Stanley A, Williams B. High rates of non-adherence to antihypertensive treatment revealed by high-performance liquid chromatography-tandem mass spectrometry (HP LC-MS/MS) urine analysis. Heart. 2014;100(11):855-61.

166. Lawson AJ, Hameed MA, Brown R, Cappuccio FP, George S, Hinton T, Kapil V, Lenart J, Lobo MD, Martin U, Menon M, Nightingale A, Rylance PB, Webb DJ, Dasgupta I. Nonadherence to antihypertensive medications is related to pill burden in apparent treatment-resistant hypertensive individuals. J Hypertens. 2020;38(6):1165-73.

167. Mazzaglia G, Ambrosioni E, Alacqua M, Filippi A, Sessa E, Immordino V, Borghi C, Brignoli O, Caputi AP, Cricelli C, Mantovani LG. Adherence to antihypertensive medications and cardiovascular morbidity among newly diagnosed hypertensive patients. Circulation. 2009;120(16):1598-605.

168. Vrijens B, Vincze G, Kristanto P, Urquhart J, Burnier M. Adherence to prescribed antihypertensive drug treatments: longitudinal study of electronically compiled dosing histories. Bmj. 2008;336(7653):1114-7.

169. Corrao G, Zambon A, Parodi A, Poluzzi E, Baldi I, Merlino L, Cesana G, Mancia G. Discontinuation of and changes in drug therapy for hypertension among newly-treated patients: a population-based study in Italy. J Hypertens. 2008;26(4):819-24.

170. Krousel-Wood M, Joyce C, Holt E, Muntner P, Webber LS, Morisky DE, Frohlich ED, Re RN. Predictors of decline in medication adherence: results from the cohort study of medication adherence among older adults. Hypertension. 2011;58(5):804-10.

171. Maio V, Marino M, Robeson M, Gagne JJ. Beta-blocker initiation and adherence after hospitalization for acute myocardial infarction. Eur J Cardiovasc Prev Rehabil. 2011;18(3):438-45.

172. Waddell-Smith KE, Li J, Smith W, Crawford J, Skinner JR. β-Blocker Adherence in Familial Long QT Syndrome. Circ Arrhythm Electrophysiol. 2016;9(8).

173. Qin X, Hung J, Teng TK, Briffa T, Sanfilippo FM. Long-Term Adherence to Renin-Angiotensin System Inhibitors and β-Blockers After Heart Failure Hospitalization in Senior Patients. J Cardiovasc Pharmacol Ther. 2020;25(6):531-40.

174. Butler J, Arbogast PG, BeLue R, Daugherty J, Jain MK, Ray WA, Griffin MR. Outpatient adherence to beta-blocker therapy after acute myocardial infarction. J Am Coll Cardiol. 2002;40(9):1589-95.

175. Rabkin JG, Charles E, Kass F. Hypertension and DSM-III depression in psychiatric outpatients. Am J Psychiatry. 1983;140(8):1072-4.

176. Li Z, Li Y, Chen L, Chen P, Hu Y. Prevalence of Depression in Patients With Hypertension: A Systematic Review and Meta-Analysis. Medicine. 2015;94(31):e1317.

177. Siever LJ, Davis KL. Overview: toward a dysregulation hypothesis of depression. Am J Psychiatry. 1985;142(9):1017-31.

178. Lawler KA, Kline K, Seabrook E, Krishnamoorthy J, Anderson SF, Wilcox ZC, Craig F, Adlin R, Thomas S. Family history of hypertension: a psychophysiological analysis. Int J Psychophysiol. 1998;28(2):207-22.

179. Light KC, Koepke JP, Obrist PA, Willis PWt. Psychological stress induces sodium and fluid retention in men at high risk for hypertension. Science (New York, NY). 1983;220(4595):429-31.

180. Lake CR, Pickar D, Ziegler MG, Lipper S, Slater S, Murphy DL. High plasma norepinephrine levels in patients with major affective disorder. Am J Psychiatry. 1982;139(10):1315-8.

181. Stein PK, Carney RM, Freedland KE, Skala JA, Jaffe AS, Kleiger RE, Rottman JN. Severe depression is associated with markedly reduced heart rate variability in patients with stable coronary heart disease. J Psychosom Res. 2000;48(4-5):493-500.

182. Yeragani VK, Rao KA, Smitha MR, Pohl RB, Balon R, Srinivasan K. Diminished chaos of heart rate time series in patients with major depression. Biol Psychiatry. 2002;51(9):733-44.

183. Wyatt RJ, Portnoy B, Kupfer DJ, Snyder F, Engelman K. Resting plasma catecholamine concentrations in patients with depression and anxiety. Arch Gen Psychiatry. 1971;24(1):65-70.

184. Esler M, Turbott J, Schwarz R, Leonard P, Bobik A, Skews H, Jackman G. The peripheral kinetics of norepinephrine in depressive illness. Arch Gen Psychiatry. 1982;39(3):295-300.

185. Roy A, Pickar D, Linnoila M, Potter WZ. Plasma norepinephrine level in affective disorders. Relationship to melancholia. Arch Gen Psychiatry. 1985;42(12):1181-5.

186. de Villiers AS, Russell VA, Carstens ME, Aalbers C, Gagiano CA, Chalton DO, Taljaard JJ. Noradrenergic function and hypothalamic-pituitary-adrenal axis activity in primary unipolar major depressive disorder. Psychiatry Res. 1987;22(2):127-40.

187. Veith RC, Lewis N, Linares OA, Barnes RF, Raskind MA, Villacres EC, Murburg MM, Ashleigh EA, Castillo S, Peskind ER, Pascuali M, Halter JB. Sympathetic nervous system activity in major depression.

Basal and desipramine-induced alterations in plasma norepinephrine kinetics. Arch Gen Psychiatry. 1994;51(5):411-22.

188. Guinjoan SM, Bernabó JL, Cardinali DP. Cardiovascular tests of autonomic function and sympathetic skin responses in patients with major depression. J Neurol Neurosurg Psychiatry. 1995;59(3):299-302.

189. Jin S, Kostka K, Posada JD, Kim Y, Seo SI, Lee DY, Shah NH, Roh S, Lim YH, Chae SG, Jin U, Son SJ, Reich C, Rijnbeek PR, Park RW, You SC. Prediction of Major Depressive Disorder Following Beta-Blocker Therapy in Patients with Cardiovascular Diseases. J Pers Med. 2020;10(4).

190. Luijendijk HJ, van den Berg JF, Hofman A, Tiemeier H, Stricker BH. β-blockers and the risk of incident depression in the elderly. J Clin Psychopharmacol. 2011;31(1):45-50.

191. Agustini B, Mohebbi M, Woods RL, McNeil JJ, Nelson MR, Shah RC, Murray AM, Ernst ME, Reid CM, Tonkin A, Lockery JE, Berk M. The association of antihypertensive use and depressive symptoms in a large older population with hypertension living in Australia and the United States: a cross-sectional study. J Hum Hypertens. 2020;34(11):787-94.

192. Ringoir L, Pedersen SS, Widdershoven JW, Pouwer F, Keyzer JM, Romeijnders AC, Pop VJ. Beta-blockers and depression in elderly hypertension patients in primary care. Fam Med. 2014;46(6):447-53.

193. Wilson DL, Ried LD. Identifying iatrogenic depression using confirmatory factor analysis of the Center for Epidemiologic Studies Depression Scale in patients prescribed a verapamil-sustained-release-led or atenolol-led hypertension treatment strategy. Res Social Adm Pharm. 2012;8(4):309-20.

194. Patten SB. Propranolol and depression: evidence from the antihypertensive trials. Can J Psychiatry. 1990;35(3):257-9.

195. Neil-Dwyer G, Bartlett J, McAinsh J, Cruickshank JM. Beta-adrenoceptor blockers and the blood-brian barrier. Br J Clin Pharmacol. 1981;11(6):549-53.

196. Westerlund A. Central nervous system side-effects with hydrophilic and lipophilic beta-blockers. Eur J Clin Pharmacol. 1985;28 Suppl:73-6.

197. Theodoresen L, Brørs O. The importance of lipid solubility and receptor selectivity of beta-adrenoceptor blocking drugs for the occurrence of symptoms and side-effects in out-patients. J Intern Med. 1989;226(1):17-23.

198. Stoschitzky K, Sakotnik A, Lercher P, Zweiker R, Maier R, Liebmann P, Lindner W. Influence of beta-blockers on melatonin release. Eur J Clin Pharmacol. 1999;55(2):111-5.

199. Hallas J. Evidence of depression provoked by cardiovascular medication: a prescription sequence symmetry analysis. Epidemiology. 1996;7(5):478-84.

200. Luijendijk HJ, Koolman X. The incentive to publish negative studies: how beta-blockers and depression got stuck in the publication cycle. J Clin Epidemiol. 2012;65(5):488-92.

201. Ko DT, Hebert PR, Coffey CS, Sedrakyan A, Curtis JP, Krumholz HM. Beta-blocker therapy and symptoms of depression, fatigue, and sexual dysfunction. Jama. 2002;288(3):351-7.

202. Kessing LV, Rytgaard HC, Ekstrøm CT, Torp-Pedersen C, Berk M, Gerds TA. Antihypertensive Drugs and Risk of Depression: A Nationwide Population-Based Study. Hypertension. 2020;76(4):1263-79.

Eidesstattliche Versicherung

„Ich, Eva Mangelsen, versichere an Eides statt durch meine eigenhändige Unterschrift, dass ich die vorgelegte Dissertation mit dem Thema:

“Experimental and clinical studies in hypertension and kidney disease focusing on glomerular hyperfiltration and tolerability of antihypertensive treatment“ / „Experimentelle und klinische Untersuchungen bei Bluthochdruck- und Nierenerkrankungen mit Fokus auf glomeruläre Hyperfiltration und Verträglichkeit der Therapie“

selbstständig und ohne nicht offengelegte Hilfe Dritter verfasst und keine anderen als die angegebenen Quellen und Hilfsmittel genutzt habe.

Alle Stellen, die wörtlich oder dem Sinne nach auf Publikationen oder Vorträgen anderer Autoren/innen beruhen, sind als solche in korrekter Zitierung kenntlich gemacht. Die Abschnitte zu Methodik (insbesondere praktische Arbeiten, Laborbestimmungen, statistische Aufarbeitung) und Resultaten (insbesondere Abbildungen, Graphiken und Tabellen) werden von mir verantwortet.

Ich versichere ferner, dass ich die in Zusammenarbeit mit anderen Personen generierten Daten, Datenauswertungen und Schlussfolgerungen korrekt gekennzeichnet und meinen eigenen Beitrag sowie die Beiträge anderer Personen korrekt kenntlich gemacht habe (siehe Anteilserklärung). Texte oder Textteile, die gemeinsam mit anderen erstellt oder verwendet wurden, habe ich korrekt kenntlich gemacht.

Meine Anteile an etwaigen Publikationen zu dieser Dissertation entsprechen denen, die in der untenstehenden gemeinsamen Erklärung mit dem Erstbetreuer angegeben sind. Für sämtliche im Rahmen der Dissertation entstandenen Publikationen wurden die Richtlinien des ICMJE (International Committee of Medical Journal Editors; www.icmje.og) zur Autorenschaft eingehalten. Ich erkläre ferner, dass ich mich zur Einhaltung der Satzung der Charité – Universitätsmedizin Berlin zur Sicherung Guter Wissenschaftlicher Praxis verpflichte.

Weiterhin versichere ich, dass ich diese Dissertation weder in gleicher noch in ähnlicher Form bereits an einer anderen Fakultät eingereicht habe.

Die Bedeutung dieser eidesstattlichen Versicherung und die strafrechtlichen Folgen einer unwahren eidesstattlichen Versicherung (§§156, 161 des Strafgesetzbuches) sind mir bekannt und bewusst.“

Berlin, 1. April 2023

Unterschrift Eva Mangelsen

Anteilserklärung an den erfolgten Publikationen

Eva Mangelsen hatte folgenden Anteil an den folgenden Publikationen:

Publikation 1:

Mangelsen E, Rothe M, Schulz A, Kourpa A, Panáková D, Kreutz R, Bolbrinker J. Concerted EP2 and EP4 Receptor Signaling Stimulates Autocrine Prostaglandin E2 Activation in Human Podocytes. Cells. 2020 May 19;9(5):1256.

Beitrag im Einzelnen:

- Federführung bei Planung, Konzeption und Koordination der Experimente (hPC) in Abstimmung mit PD Dr. J. Bolbrinker und Präparationen (Ratte) in Abstimmung mit Dr. A. Schulz
- Beschaffung und Kultivierung von hPC, Durchführung der hPC-Experimente (PGE_2-Stimulationen und Inhibitionen) in Zusammenarbeit mit der Arbeitsgruppe
- Selbständige Etablierung der Methodik für die cAMP-Quantifizierung
- Alleinige Etablierung und Durchführung der FFSS Experimente
- Selbständige Präparation der Ratten, inklusive Glomeruli-Isolation und Mithilfe bei Plasma-Gewinnung
- Probenanalyse (cAMP-ELISA, qPCR) und Primerdesign in Zusammenarbeit mit den technischen Assistentinnen der Arbeitsgruppe
- Koordination der Zusammenarbeit mit Lipidomix GmbH (LC/ESI-MS/MS Auftragslabor)
- Federführende Datenpflege und Datenauswertung (cAMP, qPCR)
- Konzeption und Durchführung aller statistischen Analysen sowie Darstellung aller Ergebnisse in Abstimmung mit PD Dr. J. Bolbrinker
- Durchführung der Literaturrecherche und Auswahl relevanter Literatur
- Federführende Interpretation der Ergebnisse in Abstimmung mit PD Dr. J. Bolbrinker und den Koautor*innen
- Federführung bei der Konzeption des Artikels sowie Entwurf und Fertigung des Manuskripts, d.h. Erstellung der Introduction, Materials and Methods (2.1.–2.4. sowie 2.6.–2.8.), Results, Discussion und Supplement, jeweils in Abstimmung mit PD Dr. J. Bolbrinker
- Maßgebliche Erstellung aller Abbildungen und Abbildungstexte in Abstimmung mit PD Dr. J. Bolbrinker, Erstellung von Tabelle 1
- Einarbeitung der Anmerkungen der Koautor*innen
- Einreichung und Überarbeitung des Manuskripts im Peer-Review Prozess, Antworten auf Reviewer Comments in Zusammenarbeit mit PD Dr. J. Bolbrinker und Professor R. Kreutz, Publikation als Erstautorin, Erstellung des Graphical Abstracts sowie dessen Anpassung für Journal-Cover

Publikation 2:

Riemer TG, Villagomez Fuentes LE, Algharably EAE, Schäfer MS, **Mangelsen E**, Fürtig MA, Bittner N, Bär A, Zaidi Touis L, Wachtell K, Majic T, Dinges MJ, Kreutz R. Do β-Blockers Cause Depression?: Systematic Review and Meta-Analysis of Psychiatric Adverse Events During β-Blocker Therapy. Hypertension. 2021 May 5;77(5):1539-1548.

Beitrag im Einzelnen:

- Quality Assessment (Bias Rating) wie im Methodenteil beschrieben für Studien zum Vergleich von Beta-Blocker vs. RAS-Blocker (aktive Kontrolle), insgesamt 29 Studien
- Vergleich des Quality-Assessments Kollegin, Diskussion der Ergebnisse und Konsensfindung zum Bias-Rating

Unterschrift Eva Mangelsen

Auszug aus der Journal Summary List Publikation 1

Journal Data Filtered By: **Selected JCR Year: 2018** Selected Editions: SCIE,SSCI
Selected Categories: **"CELL BIOLOGY"** Selected Category Scheme: WoS
Gesamtanzahl: 193 Journale

Rank	Full Journal Title	Total Cites	Journal Impact Factor	Eigenfactor Score
1	NATURE REVIEWS MOLECULAR CELL BIOLOGY	45,869	43.351	0.091360
2	CELL	242,829	36.216	0.571850
3	NATURE MEDICINE	79,243	30.641	0.162840
4	CANCER CELL	36,056	23.916	0.091050
5	Cell Metabolism	34,829	22.415	0.099550
6	Cell Stem Cell	24,628	21.464	0.087030
7	CELL RESEARCH	15,131	17.848	0.038680
8	NATURE CELL BIOLOGY	40,615	17.728	0.082430
9	Science Translational Medicine	30,485	17.161	0.121980
10	TRENDS IN CELL BIOLOGY	14,380	16.588	0.034120
11	MOLECULAR CELL	62,812	14.548	0.170680
12	NATURE STRUCTURAL & MOLECULAR BIOLOGY	27,166	12.109	0.069440
13	EMBO JOURNAL	65,212	11.227	0.067930
14	Autophagy	16,161	11.059	0.032630
15	TRENDS IN MOLECULAR MEDICINE	9,946	11.028	0.018900
16	Journal of Extracellular Vesicles	3,675	11.000	0.012110
17	Annual Review of Cell and Developmental Biology	9,734	10.833	0.016750
18	AGEING RESEARCH REVIEWS	6,539	10.390	0.015890
19	CURRENT BIOLOGY	60,772	9.193	0.135820
20	DEVELOPMENTAL CELL	28,572	9.190	0.068550

Rank	Full Journal Title	Total Cites	Journal Impact Factor	Eigenfactor Score
21	Cold Spring Harbor Perspectives in Biology	15,375	9.110	0.041830
22	GENES & DEVELOPMENT	54,563	8.990	0.072340
23	JOURNAL OF CELL BIOLOGY	67,347	8.891	0.075660
24	Cell Systems	2,275	8.640	0.016280
25	PLANT CELL	52,034	8.631	0.057800
26	EMBO REPORTS	13,786	8.383	0.029850
27	CURRENT OPINION IN CELL BIOLOGY	13,417	8.233	0.025790
28	CELL DEATH AND DIFFERENTIATION	19,729	8.086	0.030290
29	Cell Reports	39,510	7.815	0.235540
30	Protein & Cell	3,243	7.575	0.009080
31	AGING CELL	8,993	7.346	0.018810
32	CURRENT OPINION IN STRUCTURAL BIOLOGY	11,066	7.052	0.024160
33	CELLULAR AND MOLECULAR LIFE SCIENCES	24,422	7.014	0.038970
34	MATRIX BIOLOGY	5,699	6.986	0.009540
35	ONCOGENE	63,249	6.634	0.074600
36	Tissue Engineering Part B-Reviews	3,550	6.512	0.004970
37	Science Signaling	11,403	6.481	0.033700
38	Cell Death & Disease	19,001	5.959	0.051780
39	Signal Transduction and Targeted Therapy	371	5.873	0.000990
40	Cells	1,412	5.656	0.003990
41	STEM CELLS	21,467	5.614	0.030220
42	Aging-US	5,185	5.515	0.012440

2

Selected JCR Year: 2018; Selected Categories: "CELL BIOLOGY"

Druckexemplar der Publikation 1

Mangelsen E, Rothe M, Schulz A, Kourpa A, Panáková D, Kreutz R, Bolbrinker J. Concerted EP2 and EP4 Receptor Signaling Stimulates Autocrine Prostaglandin E2 Activation in Human Podocytes. Cells. 2020 May 19;9(5):1256.

cells

MDPI

Article

Concerted EP2 and EP4 Receptor Signaling Stimulates Autocrine Prostaglandin E_2 Activation in Human Podocytes

Eva Mangelsen [1], Michael Rothe [2], Angela Schulz [1], Aikaterini Kourpa [3], Daniela Panáková [3,4], Reinhold Kreutz [1,4] and Juliane Bolbrinker [1,*]

1 Charité – Universitätsmedizin Berlin, Corporate Member of Freie Universität Berlin, Humboldt-Universität zu Berlin, and Berlin Institute of Health, Institute of Clinical Pharmacology and Toxicology, Charitéplatz 1, 10117 Berlin, Germany; eva.mangelsen@charite.de (E.M.); angela-martina.schulz@charite.de (A.S.); reinhold.kreutz@charite.de (R.K.)

2 Lipidomix GmbH, Robert-Rössle-Str. 10, B55, 13125 Berlin, Germany; michael.rothe@lipidomix.de

3 Max Delbrück Center for Molecular Medicine in the Helmholtz Association, Electrochemical Signaling in Development and Disease, Robert-Rössle-Str. 10, 13125 Berlin, Germany; Aikaterini.Kourpa@mdc-berlin.de (A.K.); Daniela.Panakova@mdc-berlin.de (D.P.)

4 DZHK (German Centre for Cardiovascular Research), Partner Site Berlin, Potsdamer Straße 58, 10785 Berlin, Germany

* Correspondence: juliane.bolbrinker@charite.de; Tel.: +49-30-450-525-225

Received: 31 March 2020; Accepted: 14 May 2020; Published: 19 May 2020

check for updates

Abstract: Glomerular hyperfiltration is an important mechanism in the development of albuminuria. During hyperfiltration, podocytes are exposed to increased fluid flow shear stress (FFSS) in Bowman's space. Elevated Prostaglandin E2 (PGE_2) synthesis and upregulated cyclooxygenase 2 (Cox2) are associated with podocyte injury by FFSS. We aimed to elucidate a PGE_2 autocrine/paracrine pathway in human podocytes (hPC). We developed a modified liquid chromatography tandem mass spectrometry (LC/ESI-MS/MS) protocol to quantify cellular PGE_2, 15-keto-PGE_2, and 13,14-dihydro-15-keto-PGE_2 levels. hPC were treated with PGE_2 with or without separate or combined blockade of prostaglandin E receptors (EP), EP2, and EP4. Furthermore, the effect of FFSS on *COX2*, *PTGER2*, and *PTGER4* expression in hPC was quantified. In hPC, stimulation with PGE_2 led to an EP2- and EP4-dependent increase in cyclic adenosine monophosphate (cAMP) and *COX2*, and induced cellular PGE_2. *PTGER4* was downregulated after PGE_2 stimulation in hPC. In the corresponding LC/ESI-MS/MS in vivo analysis at the tissue level, increased PGE_2 and 15-keto-PGE_2 levels were observed in isolated glomeruli obtained from a well-established rat model with glomerular hyperfiltration, the Munich Wistar Frömter rat. *COX2* and *PTGER2* were upregulated by FFSS. Our data thus support an autocrine/paracrine COX2/PGE_2 pathway in hPC linked to concerted EP2 and EP4 signaling.

Keywords: podocyte; hyperfiltration; chronic kidney disease; prostaglandin E2; COX2; EP2; EP4; G protein-coupled receptor (GPCR) signaling; LC/ESI-MS/MS; MWF; SHR

1. Introduction

Podocytes are terminally differentiated epithelial cells that form the third layer of the glomerular filter with their interdigitating foot processes [1]. Their high degree of differentiation permits podocytes to accomplish their highly specialized functions. However, it limits their regenerative capacity, making them particularly vulnerable to pathological conditions such as glomerular hyperfiltration. When nephron number is reduced, compensatory changes of the remaining functional nephrons lead to adaptation of glomerular hemodynamics, resulting in increased glomerular filtration rate (GFR) in

the single nephron and concomitantly in higher ultrafiltrate flow in Bowman's space [2–4] (reviewed in [5]). This causes increased fluid flow shear stress (FFSS) and contributes to podocyte damage [3, 6]. Perturbation of the glomerular filtration barrier contributes to proteinuria, glomerulosclerosis, and alteration in GFR, and thus promotes the gradual decline in renal function as observed in chronic kidney disease (CKD) (reviewed in [7–9]).

Understanding the pathomechanisms underlying podocyte damage due to glomerular hyperfiltration might help to identify therapeutical targets to protect against maladaptive responses of podocytes, which otherwise contribute to renal damage. Previous studies support a pathophysiological role of Cox2 (Ptgs2, cyclooxygenase 2) and prostaglandin E2 (PGE_2) activation for development of albuminuria by increasing the permeability of the glomerular filtration barrier (reviewed in [5]). Furthermore, upregulation of Cox2 and Ptger2 (prostaglandin E receptor 2, EP2) was shown in uninephrectomized mice and murine podocytes exposed to FFSS, i.e., in two different experimental settings to study hyperfiltration [10]. These data suggest that PGE_2 synthesis and signaling may play a role in podocyte responses to hyperfiltration.

Cox2 is long known to mediate increased synthesis of PGE_2 upon diverse stimuli (reviewed in [11,12]). Extracellularly, PGE_2 exerts its effects via four different G-protein coupled prostaglandin E receptors (EP1–4) in human and rodents (reviewed in [13]). EP1, -2 and -4 mRNA expression was reported in mouse podocytes, EP2 and -4 were also detected on protein level [14]. However, the expression of EP in human podocytes (hPC) is unclear. Both EP2 and EP4 stimulate adenylate cyclase activity leading to elevated cyclic adenosine monophosphate (cAMP) levels while EP1 increases intracellular Ca^{2+} (reviewed in [15–17]).

An autocrine/paracrine pathway between PGE_2 and Cox2 was described previously, indicating that PGE_2 leads to upregulation of Cox2 in osteocyte-like cells (murine long bone osteocyte Y4, MLO-Y4) [18]. This, in turn, increases synthesis of intracellular PGE_2, which again induces Cox2. It remains a matter of debate which EP mediates this mutual amplification: In mouse podocytes, EP4 and the p38 mitogen-activated protein kinase (MAPK) signaling pathway were described to be involved in PGE_2-mediated Cox2 upregulation and cAMP increase [19]. In other cell types, activation of EP2 with or without EP4-coupled cAMP/proteinkinase A (PKA) pathway was shown to upregulate Cox2 following PGE_2-treatment [20–22]. EP2 signaling was shown to be the relevant mechanism in response to FFSS in mouse podocytes [14]. Indeed, the PGE_2-Cox2-EP2 axis is suggested to be the relevant target for podocyte damage induced by FFSS [10,23]. So far, the mechanisms involved have not been investigated in hPC in detail. In this study, we therefore aimed to elucidate an autocrine/paracrine PGE_2/COX2 pathway in hPC and to identify which EP contributes to this crosstalk. We determined *COX2*, *PTGER2*, and *PTGER4* expression in hPC after PGE_2 stimulation and FFSS. Our results corroborate recent findings in murine models of hyperfiltration on autocrine/paracrine Cox2 and PGE_2 activation in hPC. Moreover, we find this pathway in hPC to be linked to concerted EP2 and EP4 signaling.

Importantly, distinct analysis of cellular PGE_2 and its metabolites is crucial to elucidate their pathophysiological role in podocyte damage [10,23]. However, precise measurement of intracellular prostaglandins remains challenging. Enzyme-linked immunosorbent assays (ELISA) are widely used but have their limitations, e.g., the lack of standardization across different kits and low specificity, selectivity, and throughput compared to liquid chromatography tandem mass spectrometry (LC-MS/MS) methods [24,25]. As a limitation, LC-MS/MS oftentimes requires large quantities of samples which are difficult to obtain in cell culture experiments [26–32]. We were able to overcome these obstacles and provide an approach to analyze prostaglandins in hPC by liquid chromatography electrospray ionization tandem mass spectrometry (LC/ESI-MS/MS). With our modified LC/ESI-MS/MS protocol, we were able to precisely quantify cellular PGE_2, 15-keto-PGE_2, and 13,14-dihydro-15-keto-PGE_2 levels. After stimulation with PGE_2, the cellular PGE_2-content was elevated, which was completely blocked by pharmacological inhibition EP2 and EP4. In addition, we performed corresponding in vivo analysis at the tissue level by using the LC/ESI-MS/MS methodology and demonstrated increased PGE_2 and

15-keto-PGE_2 levels in isolated glomeruli obtained from a well-established rat model with glomerular hyperfiltration, i.e., the Munich Wistar Frömter rat (MWF).

Our findings on elevated glomerular PGE_2 and 15-keto-PGE_2 levels strengthen the hypothesis that glomerular PGE_2-induction associates with albuminuria due to podocyte damage.

2. Materials and Methods

2.1. Cell Culture

Conditionally immortalized hPC (kindly provided by Moin A. Saleem, University of Bristol, UK) were cultured according to the original protocol [33,34] with slight modifications. The cells proliferate at 33 °C and transform to differentiated hPC when kept at ≥37 °C exhibiting podocyte-specific markers [34]. Briefly, podocytes were grown at 33 °C and 5% CO_2 in Roswell Park Memorial Institute (RPMI)-1640 medium (cat. no. BS.F1215, Bio&SELL, Feucht/Nürnberg, Germany) supplemented with 1% Insulin-Transferrin-Selenium 100X (cat. no. 41400-045, Gibco, Grand Island, NY, USA), 10% fetal bovine serum (FBS, cat. no. F7524, Sigma, Steinheim, Germany) and 1% ZellShield® to prevent contamination (cat. no. 13-0150, Minerva Biolabs, Berlin, Germany). Medium was changed 2–3 times per week. At confluency of 70–80%, podocytes were transferred to 37–38 °C until full confluence and proliferation arrest. Subsequently, cells were kept for a minimum of 14 days at 37–38 °C to obtain full differentiation. Differentiated phenotype was confirmed by analysis of the marker synaptopodin by immunofluorescence (see Supplement Figure S1a,b). Characterization also included overall comparison of the cellular shape ("cobblestone-like" in undifferentiated state and "arborized" in differentiated hPC [33]) by light microscopy, synaptopodin mRNA expression, as well as nephrin and podocin protein detection by immunofluorescence and western blot (see Supplement Figures S1c–e and S2). Prior to experiments, cells were detached with Trypsin 0.25%/EDTA 0.02% solution (cat. no. L-2163, Biochrom, Berlin, Germany), seeded in 12-well plates at 1×10^5 cells per well and kept in RPMI-1640 medium with supplements for adherence overnight. All experimental treatments were carried out in supplement-free RPMI-1640 medium at 37–38 °C with cell passages between 5 and 22.

2.2. PGE_2 Treatment and Inhibition of EP Receptors

PF-04418948 (cat. no. PZ0213, Sigma, Steinheim, Germany) served as EP2 antagonist [35,36] and ONO-AE3-208 (cat. no. 14522, Cayman Chemical, Ann Arbor, MI, USA) was chosen as EP4 antagonist [37,38]. Stock solutions of PGE_2 (cat. no. 14010, Cayman Chemical, Ann Arbor, MI, USA), PF-04418948, and ONO-AE3-208 with 10 mM were prepared in DMSO (cat. no. D2650, Sigma, Steinheim, Germany) and stored at −20 °C until further use.

Podocytes were treated with PGE_2 at 10 nM–1 µM concentrations as PGE_2-concentrations up to 1 µM are commonly used for in vitro experiments in murine podocytes [39,40]. For inhibition experiments, 1 µM or even higher concentrations of the selective EP2 and/or EP4 antagonist were used in previous studies [36,37,41–43]. In a pilot study, treatment with PGE_2 and EP2 antagonist (1 µM each) did not show inhibitory effects (Supplement Figure S4). Thus, antagonists were added concomitantly to PGE_2 100 nM for the indicated time-points.

2.3. Determination of Intracellular cAMP Levels

Intracellular cAMP levels were measured using an ELISA kit (cat. no. ADI-901-163, Enzo Life Sciences, Farmingdale, NY, USA). Cells were lysed in 300–400 µL 0.1 M HCl containing 0.1% Triton X-100 and samples were processed according to the manufacturer's instructions for the non-acetylated format. PGE_2 stimulated samples were diluted 1:5, and samples of PGE_2 stimulation plus co-incubation with either the EP2 or the EP4 antagonist were diluted 1:2–3 in lysis buffer. Optical density was measured at 415 nm and cAMP concentrations were normalized for protein content for each sample. Protein amount was quantified by a colorimetric kit (cat. no. 23227, Pierce™ BCA Protein Assay Kit,

Thermo Fisher Scientific, Rockford, IL, USA). Experiments for cAMP consisted of n = 3–6 samples per experimental group and were performed once or in duplicate as indicated.

2.4. Reverse Transcription and Quantitative Real-Time PCR

Total RNA of hPC was isolated using the RNeasy® Micro Kit (cat. no. 74004, Qiagen, Hilden, Germany) following the manufacturer's protocol. RNA quality was controlled by a 260/280 nm absorption ratio. For cDNA synthesis, total RNA was reverse-transcribed using the First Strand cDNA Synthesis Kit (cat. no. K1612, Thermo Fisher Scientific, Vilnius, Lithuania).

Quantitative Real-Time PCR (qPCR) was conducted in a CFX96 Touch PCR system (Bio-Rad, München, Germany; software version 3.1.1517.0823) or in a 7500 Fast Real-Time PCR System (Applied Biosystems, Darmstadt, Germany; software version 2.0.6) using the comparative quantitative cycle method with SYBR-green (cat. no. 4,385,612 and 100029284, Thermo Fisher Scientific, Vilnius, Lithuania) as reported previously [44,45] Expression analysis of each sample was done in three technical replicates and only samples with an intra-triplicate standard deviation (SD) < 0.2 were used for further calculation. Normalization of expression was done by the reference gene glyceraldehyde 3-phosphate dehydrogenase *(GAPDH)*. ΔΔCt was normalized to the untreated controls in hPC. All results were plotted as log2 of fold change (FC) ($2^{-\Delta\Delta Ct}$). Primer sequences are listed in Table 1. Primers were purchased from Eurofins Genomics, Ebersberg, Germany or Tib Molbiol, Berlin, Germany and specificity of detected reverse transcriptase (RT)-PCR products was confirmed by sequencing at Eurofins Genomics, Ebersberg, Germany. *COX2*-qPCR for hPC consisted of n = 3–8 samples per experimental group and were performed in duplicate or triplicate as indicated.

Table 1. Primer sequences for human (h) genes of interest.

Gene	Forward Primer (5′-3′)	Reverse Primer (5′-3′)
hGAPDH	gagtcaacggatttggtcgt	gatctcgctcctggaagatg
hCOX2	tgatgattgcccgactcccttg	tgaaagctggccctcgcttatg
hPTGER1	ttcggcctccaccttctttg	cgcagtaggatgtacacccaag
hPTGER2	gacggaccacctcattctcc	tccgacaacagaggactgaac
hPTGER3	tctccgctcctgataatgatg	atctttccaaatggtcgctc
hPTGER4	ttactcattgccacctccct	agtcaaaggacatcttctgcca

2.5. LC/ESI-MS/MS for Analysis of Prostaglandins

2.5.1. Sample Preparation

After stimulation or inhibition experiments, supernatants were removed and stored at −80 °C. Cells were washed twice with cold phosphate buffered saline (PBS), PBS was completely aspirated from wells, and the 12-well plates were immediately stored at −80 °C until further processing. Before analysis, cells were scraped from plate and suspended in 500 µL water. A 50 µL aliquot was taken for total protein measurement following the Lowry protocol.

The cell suspensions were spiked with an internal standard consisting of 14,15-Epoxyeicosatrienoic acid-d8, 14,15-Dihydroxyeicosatrienoic acid-d11, 15-Hydroxyeicosatetraenoic acid-d8, 20-Hydroxyeicosatetraenoic acid-d6, Leukotriene B_4-d4, PGE_2-d4 1 ng each (Cayman Chemical, Ann Arbor, MI, USA). In addition, 500 µL methanol and 5 µL 2,6-di-tert-butyl-4-methylphenol (BHT, 10 mg/mL) were added and shaken vigorously.

The total prostaglandins were released using phospholipase A2 from honey bee Apis Mellifera (Sigma-Aldrich, Taufkirchen, Germany) as described previously [46]. After pH adjustment to 6, acetic acid samples were extracted by solid phase extraction (SPE) using Bond Elute Certify II columns (Agilent Technologies, Santa Clara, CA, USA), which were preconditioned with 3 mL methanol, followed by 3 mL of 0.1 mol/L phosphate buffer containing 5% methanol (pH 6). SPE-columns were then washed with 3 mL methanol/H_2O (40/50, v/v). For elution, 2 mL of n-hexane:ethyl acetate 25:75

with 1% acetic acid was used. The extraction was performed with an SPE Vacuum Manifold. The eluate was evaporated on a heating block at 40 °C under a stream of nitrogen to obtain a solid residue which was dissolved in 100 µL methanol/water 60:40 and transferred in an HPLC autosampler vial (HPLC, high performance liquid chromatography).

Experiments for analysis of prostaglandins in hPC consisted of $n = 3$–6 replicates per experimental group and. Experiments were performed once or in triplicate (on different cell passages and on different days) as indicated.

Rat glomeruli obtained by differential sieving of one kidney as described below were divided into 3 parts and stored at −80 °C until further analysis. One aliquot with approximately 1/3 total kidney was prepared as described for cells, but without application of phospholipase A2.

For rat plasma, 200 µL plasma were spiked with internal standard and BHT. In addition, 20 µL glycerol and 500 µL acetonitrile was added and shaken vigorously. pH was adjusted at 6 with 2 mL phosphate buffer (0.1 mol/L). The samples were centrifuged and the clear supernatant was extracted using SPE as described above.

Experiments for analysis of prostaglandins in rat glomeruli or plasma consisted of $n = 8$–10 glomerular isolated or plasma samples of $n = 8$–10 different animals per rat strain.

2.5.2. LC/ESI-MS/MS

The residues were analyzed using an Agilent 1290 HPLC system with binary pump, multisampler and column thermostat with a Zorbax Eclipse plus C-18, 2.1 × 150 mm, 1.8 µm column using a solvent system of aqueous acetic acid (0.05%) and acetonitrile. The elution gradient was started with 5% organic phase, which was increased within 0.5 min to 32%, 16 min to 36.5%, 20 min to 38%, 28 min to 98% and held there for 5 min. The flow rate was set at 0.3 mL/min, the injection volume was 20 µL. The HPLC was coupled with an Agilent 6495 Triplequad mass spectrometer (Agilent Technologies, Santa Clara, CA, USA) with electrospray ionisation source. The source parameters were Drying gas: 115 °C/16 L/min, Sheath gas: 390 °C/12 L/min, Capillary voltage: 4300 V, Nozzle voltage: 1950 V, and Nebulizer pressure: 35 psi.

Analysis was performed with Multiple Reaction Monitoring in negative mode. For details, see Table S1. Unless stated otherwise, all solvents and chemicals were purchased from VWR International GmbH, Darmstadt, Germany.

2.6. FFSS

For FFSS, 1×10^5–6×10^5 cells where seeded on collagen IV coated Culture Slips® (cat. no. CS-C/IV, Dunn Labortechnik GmbH, Asbach, Germany), which are glass slides coated with collagen type IV and rimmed with a 1.0 mm wide polytetrafluoroethylene border to limit cell culture growth to the portion of the slip exposed to fluid flow. FFSS experiments were performed as previously described with slight modifications [23]. The Streamer® Shear Stress Device (cat. no. STR-400, Dunn Labortechnik GmbH, Asbach, Germany) was installed in a 38 °C incubator with 5% CO_2 and prepared as follows: 400 mL of PBS followed by RPMI-1640 medium were pumped through the device for approximately 10 min each. Prior to each change of content, flow direction was reversed to empty the tubes from the previous liquid. After washing, medium was replaced by 400 mL of new medium. The system was checked for leaks and air bubbles were eliminated. After preparation of the streamer, flow direction was again reversed until the streamer was half-filled by medium. Tubes were released from the pump, the system was taken out of the incubator, Culture Slips® with hPC were inserted in the Streamer®, and the system was placed back into the incubator. All 6 slots of the Streamer® were filled to allow consistent flow. Based on previous research, we applied FFSS at 2 dynes/cm^2 for 2 h [23]. At the end of each experiment, flow rate was reversed and cells were released from the device. Control cells were put in the same incubator with the same medium but were not exposed to FFSS.

2.7. Animals

The MWF rat served as a model for CKD with albuminuria, while the spontaneously hypertensive rat (SHR) served as a control strain. SHR rats develop hypertension early in life but are resistant to albuminuria development as reviewed in [47].

Male rats at 8 weeks of age were deployed from our MWF/Rkb (RRID:RGD_724569, laboratory code Rkb https://www.nationalacademies.org/ilar/lab-code-database) and SHR/Rkb (RRID:RGD_631696, laboratory code Rkb https://www.nationalacademies.org/ilar/lab-code-database) colonies at Charité—Universitätsmedizin Berlin, Germany. Rats were kept under standard conditions as described previously [44]. All experimental work in rat models was performed in accordance with the guidelines of the Charité—Universitätsmedizin Berlin and the local authority for animal protection (Landesamt für Gesundheit und Soziales, Berlin, Germany) for the use of laboratory animals. The registration numbers for the rat experiments are G 130/16 (approved 2 August 2016) and T 0189/02 (approved 31 August 2018). Anesthesia was achieved by ketamine-xylazine (87 and 13 mg/kg body weight, respectively). Kidneys were obtained, decapsulated, and sieved using a 125 µm steel sieve (Retsch GmbH, Haan, Germany) rinsed by PBS. The filtrate was then placed on a 71 µm steel sieve (Retsch GmbH, Haan, Germany) and washed with PBS. Glomeruli were kept on the sieve and were separated from the flow-through. Glomeruli were rinsed off the sieve with PBS, centrifuged, snap-frozen, and stored at −80 °C until further processing. Plasma was obtained by retrobulbary punction or punction of vena cava and collected in ethylenediaminetetraacetic acid (EDTA)-containing vials, centrifuged at 2 min at 4 °C, and stored subsequently at −80 °C.

2.8. Statistics

Statistical analysis was conducted using GraphPad Prism 8.4.0 (GraphPad Software, San Diego, CA, USA). Normal distribution was tested with the Shapiro–Wilk test. Normally distributed data were compared either by unpaired, two-tailed Student's *t*-test or one-way ANOVA with Tukey's or Dunnett's multiple comparisons test as indicated. Multiple comparisons tests after one-way ANOVA were used to compare every mean to every other mean (Tukey' follow up test) or to a control mean (Dunnett's follow up test). Results not normally distributed were analyzed by Mann–Whitney test or Kruskal–Wallis test with Dunn's multiple comparisons test as indicated. Significance level was set at $p < 0.05$. Statistical details for specific experiment can be found within figures and figure legends.

3. Results

3.1. PGE_2 Leads to EP2- and EP4- Dependent Increased cAMP Levels in Differentiated hPC

Stimulation of hPC with 100 nM PGE_2 led to an immediate time-dependent increase in intracellular cAMP levels detected after 1 min onward and retained at least until 40 min of PGE_2 stimulation (Figure 1). As intracellular cAMP levels remained comparably high until 20 min of PGE_2 stimulation, this incubation time was chosen for subsequent cAMP measurements.

Analysis of EP expression on hPC revealed the presence of *PTGER1*, *PTGER2*, and *PTGER4* mRNA in differentiated hPC (Figure S3), which encode for EP1, EP2, and EP4, respectively. As only EP2 and EP4 are reported to mediate an increase in intracellular cAMP (reviewed in [15–17]), we next investigated the effect of pharmacological inhibition of EP2 and EP4 signaling on PGE_2-stimulated intracellular cAMP levels in hPC. Therefore, either the selective antagonist of EP2 (PF-04418948, 1 µM) or EP4 (ONO-AE3-208, 1 µM) were co-incubated with 100 nM PGE_2 individually and in combination (Figure 2). Upon PGE_2 stimulation, antagonism of either EP2 (−92.5%) or EP4 (−63.7%) alone resulted in a marked albeit only partial decrease of intracellular cAMP levels compared to stimulated hPC without antagonists. In contrast, the PGE_2 stimulated intracellular cAMP increase was completely abrogated by combined EP2 and EP4 antagonism (Figure 2), suggesting that, in hPC, both EP2 and EP4 may mediate PGE_2-dependent signaling.

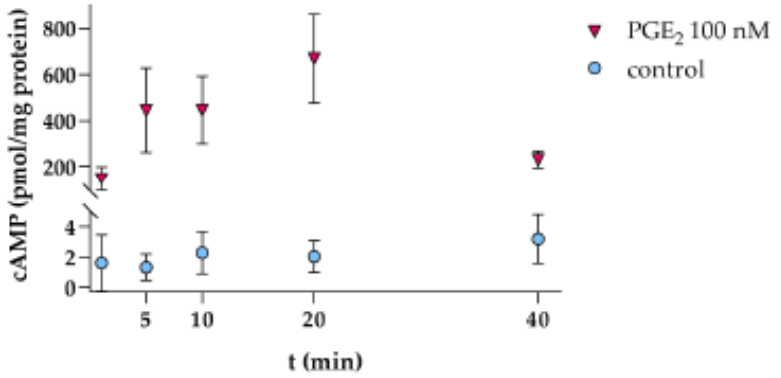

Figure 1. Intracellular cAMP levels in hPC are increased by PGE_2 stimulation (100 nM, pink triangles) in a time-dependent manner. For several controls (blue circles), cAMP levels fell below the lowest concentration of the recommended standard curve (0.78 pmol/mL) and were therefore set to zero. Each data point represents the mean ± SD of one experiment with n = 3–4 samples per time-point.

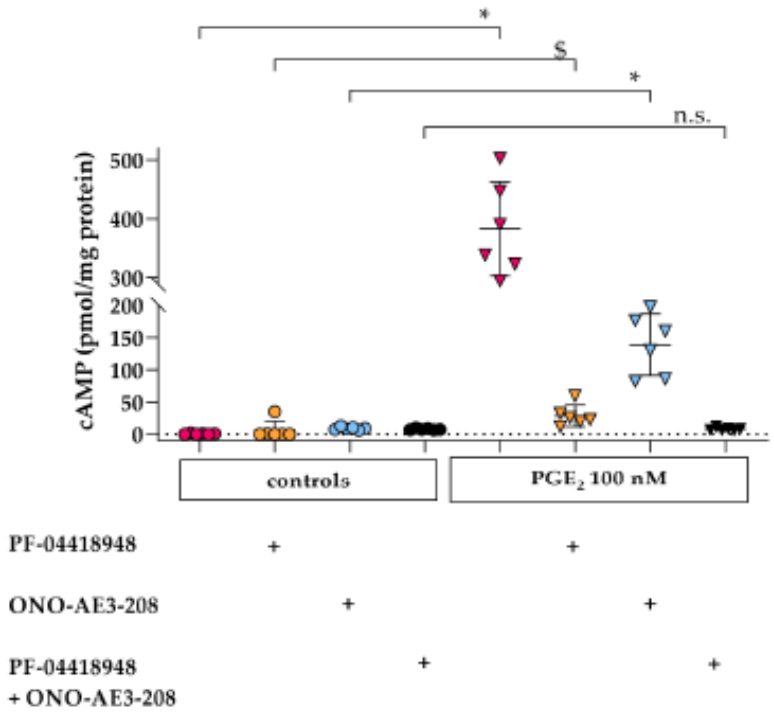

Figure 2. Intracellular cAMP is increased by PGE_2 stimulation via EP2 and EP4 in hPC. Representative cAMP levels following PGE_2 stimulation for 20 min without concomitant EP2 or EP4 antagonist (100 nM, pink triangles) compared to controls without PGE_2 (pink circles), after co-incubation with either EP2 antagonist (PF-04418948, 1 µM, orange triangles) or EP4 antagonist (ONO-AE3-208, 1 µM, blue triangles) compared to controls without PGE_2 (orange circles for EP2 antagonist, blue circles for EP4 antagonist), and co-incubation of PGE_2 with both antagonists simultaneously (1 µM each, black triangles) compared to controls without PGE_2 (black circles). Each data point represents a single sample and plotted as mean ± SD (horizontal lines) per treatment group consisting of n = 6 samples. For several controls, cAMP levels fell below the lowest concentration of the recommended standard curve (0.78 pmol/mL) and were therefore set to zero. Experiments were done in duplicate on different cell passages and on different dates, each consisting of n = 3–6 replicates per treatment, except for the separate EP4 inhibition, which was only performed once. Statistics: *, $p < 0.01$; $, $p < 0.05$; n.s., not significant, assessed by a Mann–Whitney test. + denotes addition of the respective EP antagonists.

3.2. PGE_2 Induces *COX2* Gene Expression via EP2 and EP4 Signaling in Differentiated hPC

Stimulation of hPC with PGE_2 for 2 h revealed a dose-dependent upregulation of *COX2* mRNA expression (Figure 3a). In order to elucidate the role of EP2 and EP4 in PGE_2-mediated *COX2* upregulation, either the selective EP2 antagonist PF-04418948 (1 µM) or the selective EP4 antagonist ONO-AE3-208 (1 µM) were co-incubated with 100 nM PGE_2 individually or in combination (Figure 3b). Upon PGE_2 stimulation, antagonism of either EP2 or EP4 alone resulted in an increase in *COX2* mRNA although lower compared to PGE_2-stimulated hPC without antagonists (Figure 3b). Combined EP2 and EP4 antagonism completely inhibited PGE_2-mediated *COX2* upregulation (Figure 3b), suggesting that PGE_2 signals via both EP2 and EP4 to regulate *COX2* levels in a positive feedback loop.

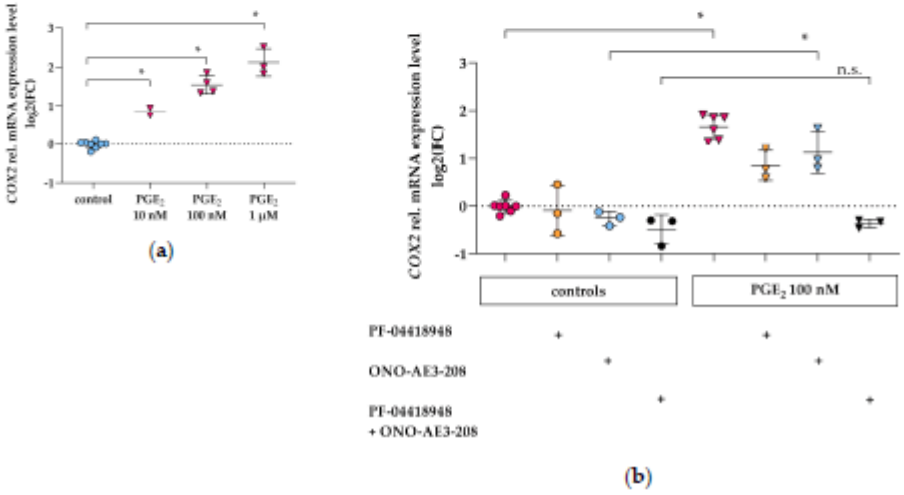

Figure 3. *COX2* gene expression is increased by PGE_2 via EP2 and EP4 in hPC. qPCR results are presented as relative mRNA expression level normalized to *GAPDH* and referred to control group. (**a**) *COX2* levels following PGE_2 stimulation (pink triangles) for 2 h were upregulated in a dose-dependent manner compared to untreated control (blue circles). Each data point represents the mean of an independent experiment (performed at least in duplicate on different cell passages and on different dates, each consisting of n = 3–8 replicates per treatment) and plotted as combined mean ± SD (horizontal lines). SD was not plotted when only two independent experiments were performed. Statistics: *, $p < 0.01$, assessed by one-way ANOVA with Dunnett's follow-up test; (**b**) *COX2* levels following PGE_2 stimulation for 2 h without concomitant EP2 or EP4 antagonist (100 nM, pink triangles) compared to controls without PGE_2 (pink circles), after co-incubation with either EP2 antagonist (PF-04418948, 1 µM, orange triangles) or EP4 antagonist (ONO-AE3-208, 1 µM, blue triangles) compared to controls without PGE_2 (orange circles for EP2 antagonist, blue circles for EP4 antagonist), and co-incubation of PGE_2 with both antagonists simultaneously (1 µM each, black triangles) compared to controls without PGE_2 (black circles) obtained in three independent experiments. Each data point represents the mean of an independent experiment (performed at least in triplicate on different cell passages and on different dates, each consisting of n = 3–6 replicates per treatment) and plotted as combined mean ± SD (horizontal lines). + indicates addition of the respective EP antagonists. Statistics: *, $p < 0.01$; n.s., not significant, assessed by two-tailed Student's t-test.

3.3. PGE_2 Reduces *PTGER2* and *PTGER4* Gene Expression Which Is Not Modified by EP2 or EP4 Antagonists in Differentiated hPC

Stimulation of hPC with rising concentrations of PGE_2 for 2 h revealed inconsistent changes of *PTGER2* mRNA expression: 10 nM and 1 µM did not significantly change *PTGER2* expression, whereas PGE_2 100 nM slightly reduced *PTGER2* expression (Figure 4a). The weak downregulation by *PTGER2* of 100 nM PGE_2 was not abrogated by co-incubation with the selective EP4 antagonist ONO-AE3-208 (1 µM) (Figure 4b).

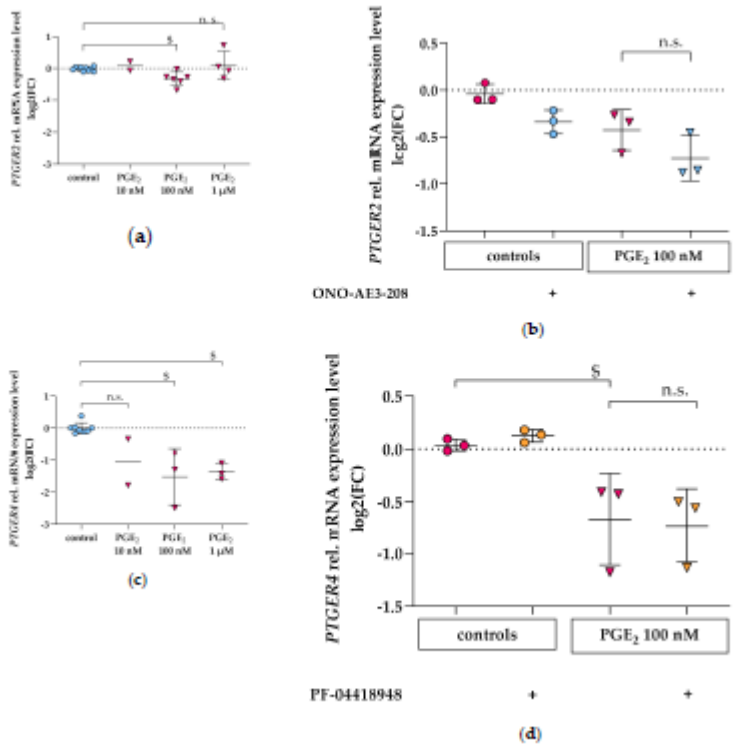

Figure 4. *PTGER2 and PTGER4* gene expression in hPC after PGE_2 stimulation and following co-incubation with EP antagonists. qPCR results are presented as relative mRNA expression level normalized to *GAPDH* and referred to control group. (**a**) *PTGER2* levels following PGE_2 stimulation with 10 nM, 100 nM, and 1 µM (pink triangles) for 2 h compared to untreated control (blue circles). Each data point represents the mean of an independent experiment (performed at least in duplicate on different cell passages and on different dates, each consisting of n = 3–8 replicates per treatment) and plotted as combined mean ± SD (horizontal lines). SD was not plotted when only two independent experiments were performed. Statistics: $, $p < 0.05$, assessed by one-way ANOVA with Dunnett's follow-up test; (**b**) *PTGER2* levels following PGE_2 stimulation for 2 h without concomitant EP4 antagonist (100 nM, pink triangles) compared to controls without PGE_2 (pink circles), and after co-incubation with EP4 antagonist (ONO-AE3-208, 1 µM, blue triangles) compared to controls without PGE_2 (blue circles) obtained in three independent experiments. Each data point represents the mean of an independent experiment (performed in triplicate on different cell passages and on different dates, each consisting of n = 3–6 replicates per treatment) and plotted as combined mean ± SD (horizontal lines). + denotes addition of ONO-AE3-208. Statistics: n.s., not significant, assessed by a Mann–Whitney test; (**c**) *PTGER4* levels following PGE_2 stimulation with 10 nM, 100 nM, and 1 µM (pink triangles) for 2 h compared to untreated control (blue circles). Each data point represents the mean of an independent experiment (performed at least in duplicate on different cell passages and on different dates, each consisting of n = 3–8 replicates per treatment) and plotted as combined mean ± SD (horizontal lines). SD was not plotted when only two independent experiments were performed. Statistics: $, $p < 0.05$, assessed by a Kruskal–Wallis test with Dunn's multiple comparisons test; (**d**) *PTGER4* levels following PGE_2 stimulation for 2 h without concomitant EP2 antagonist (100 nM, pink triangles) compared to controls without PGE_2 (pink circles), after co-incubation with EP2 antagonist (PF-04418948, 1 µM, orange triangles) compared to controls without PGE_2 (orange circles) obtained in three independent experiments. Each data point represents the mean of an independent experiment (performed in triplicate on different cell passages and on different dates, each consisting of n = 5–6 replicates per treatment) and plotted as combined mean ± SD (horizontal lines). + denotes addition of PF-04418948. Statistics: $, $p < 0.05$; n.s., not significant, assessed by a two-tailed Student's *t*-test.

Stimulation of hPC with PGE_2 for 2 h revealed a dose-dependent reduction of *PTGER4* mRNA expression (Figure 4c). In order to elucidate the role of EP2 in PGE_2-mediated *PTGER4* downregulation, the selective EP2 antagonist PF-04418948 (1 µM) was co-incubated with 100 nM PGE_2 (Figure 4d). The PGE_2-induced decrease in *PTGER4* mRNA was not abolished by co-incubation with the EP2 antagonist (Figure 4d).

3.4. Cellular PGE_2 and Metabolite Profile in hPC after PGE_2 Stimulation: Effects of EP2 and EP4 Blockade

To investigate whether PGE_2 stimulation and subsequent *COX2* induction lead to changes in cellular levels of PGE_2 and its downstream metabolites 15-keto-PGE_2 and 13,14-dihydro-15-keto-PGE_2 (Figure 5a), hPC were analyzed by LC/ESI-MS/MS. After stimulation with PGE_2, the cellular PGE_2-content was elevated (Figure 5b), while 15-keto-PGE_2 and 13,14-dihydro-15-keto-PGE_2 remained at control levels. Pharmacological inhibition of EP2 and EP4 reduced cellular PGE_2 significantly (Figure 5c). Our findings point towards an autocrine PGE_2-EP2/EP4-COX2 signaling axis in hPC.

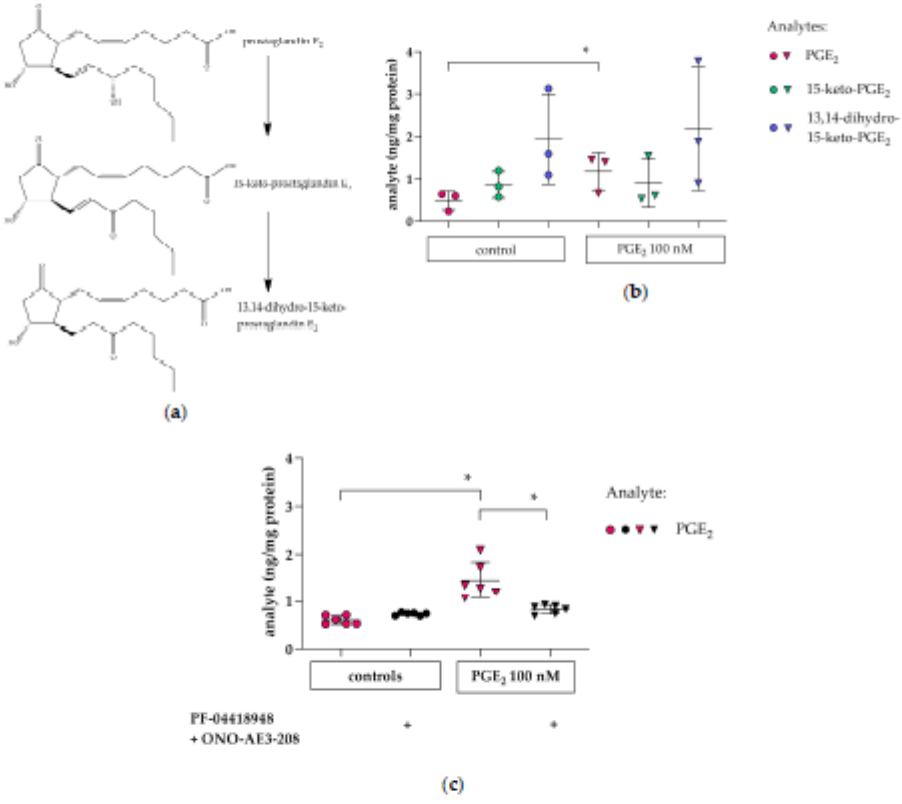

Figure 5. PGE_2 and its metabolites were measured by LC/ESI-MS/MS in hPC. (**a**) structure of PGE_2 and its metabolites; (**b**) levels of cellular PGE_2 (pink), 15-keto-PGE_2 (green), and 13,14-dihydro-15-keto-PGE_2 (blue) were measured after PGE_2 stimulation for 2 h (100 nM, triangles) and in untreated controls (circles). PGE_2 levels were increased in PGE_2-stimulated cells (pink triangles) vs. controls (pink circles). Each datapoint represents the mean of an independent experiment (performed in triplicate on different cell passages and on different dates, each consisting of $n = 3$–6 replicates per treatment) and plotted as combined mean ± SD (horizontal lines). Statistics: *, $p < 0.01$, assessed by a two-tailed Student's *t*-test in each experiment; (**c**) elevated cellular PGE_2 levels caused by PGE_2 stimulation (pink triangles) were abrogated by simultaneous co-incubation with combined EP2 and EP4 antagonism (PF-04418948 and ONO-AE3-208, respectively, 1 µM each). + indicates addition of combined EP antagonists. Each datapoint represents a single sample and plotted as mean ± SD (horizontal lines) per treatment group consisting of $n = 6$ replicates obtained in a single experiment. Statistics: *, $p < 0.01$, assessed by a two-tailed Student's *t*-test.

3.5. Glomerular PGE_2 and Metabolite Profile in Glomeruli and Plasma in the CKD MWF Model

Analysis of PGE_2 and its subsequent metabolites 15-keto-PGE_2 and 13,14-dihydro-15-keto-PGE_2 in glomeruli and plasma of MWF and SHR at eight weeks of age revealed an increase of glomerular PGE_2 and 15-keto-PGE_2 levels in MWF compared to SHR. No difference was observed for 13,14-dihydro-15-keto-PGE_2 (Figure 6a). In plasma, levels of PGE_2 and 13,14-dihydro-15-keto-PGE_2 did not differ between MWF and SHR (Figure 6b). The metabolite 15-keto-PGE_2 in plasma was below level of detection (data not shown).

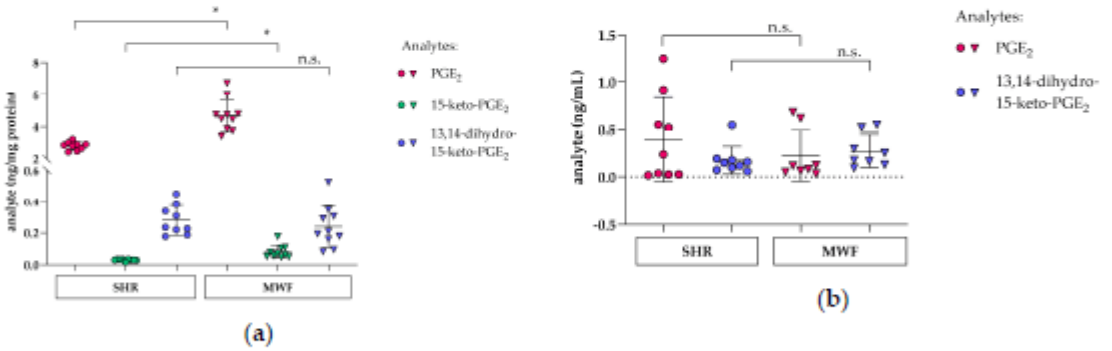

Figure 6. Levels of PGE_2 (pink), 15-keto-PGE_2 (green) and 13,14-dihydro-15-keto-PGE_2 (blue) were measured in glomeruli of MWF (triangles) and SHR (circles) at 8 weeks of age. (**a**) glomerular PGE_2 and 15-keto-PGE_2 levels were increased in MWF (pink and green triangles, respectively) compared to SHR (pink and green circles, respectively), whereas glomerular 13,14-dihydro-15-keto-PGE_2 (blue circles and triangles) did not differ between both strains. Each data point represents a single animal and plotted as mean ± SD (horizontal lines) per rat strain consisting of n = 9–10 animals each. Statistics: *, $p < 0.01$; *n.s.*, not significant assessed by a two-tailed Student's *t*-test; (**b**) levels of PGE_2 (pink) and 13,14-dihydro-15-keto-PGE_2 (blue) in plasma did not differ between MWF (triangles) and SHR (circles). Each data point represents a single animal and plotted as mean ± SD (horizontal lines) per rat strain consisting of n = 8–9 animals, each. Statistics: *n.s.*, not significant assessed by the Mann–Whitney test.

3.6. FFSS Increases *COX2* and *PTGER2* Gene Expression in hPC

FFSS was previously shown to elevate intracellular PGE_2 levels and Cox2 in murine podocytes [10,23]. We therefore investigated *COX2* mRNA expression after FFSS in hPC. FFSS led to increased *COX2* mRNA expression in hPC as shown in Figure 7.

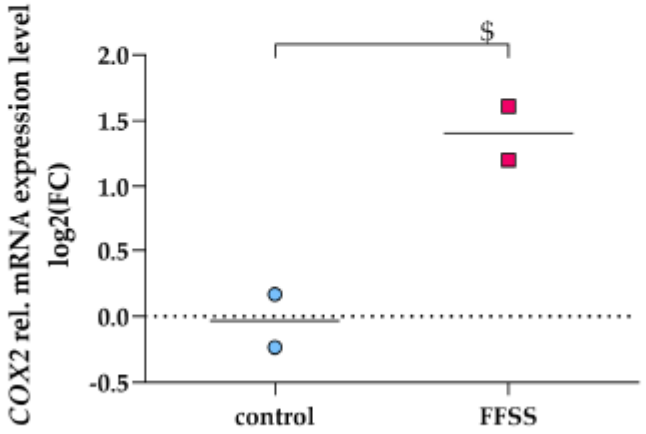

Figure 7. FFSS upregulated *COX2* gene expression in hPC (pink squares). qPCR results are presented as relative mRNA expression level normalized to *GAPDH* and referred to control group (blue circles). *COX2* upregulation was quantified after 2 h of FFSS with 2 dynes/cm^2. Statistics: $, $p < 0.05$, assessed

by a two-tailed Student's *t*-test. Each datapoint represents the mean of an independent experiment (performed in duplicate on different cell passages and on different dates, each consisting of $n = 5–6$ replicates per treatment) and plotted as combined mean (horizontal lines).

Furthermore, EP2 protein was reported to be upregulated upon FFSS in murine podocytes [10]. In hPC, FFSS slightly upregulated *PTGER2* (Figure 8a), whereas *PTGER4* expression did not change compared to control (Figure 8b).

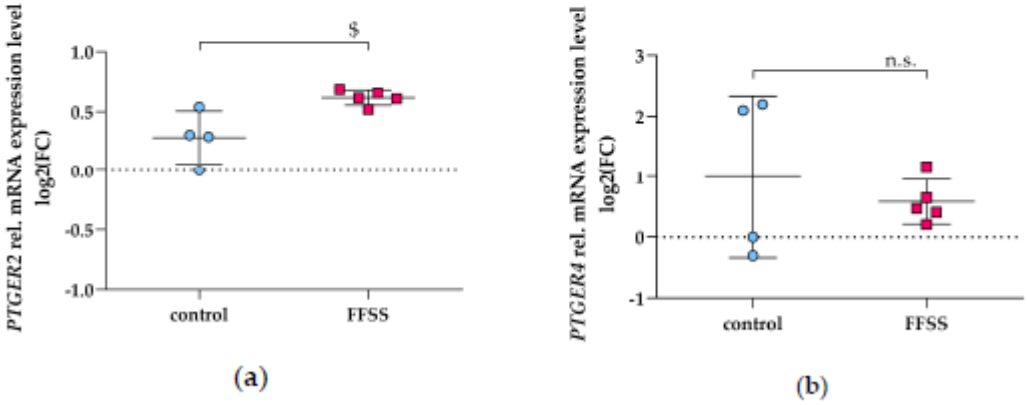

Figure 8. *PTGER2* and *PTGER4* gene expression in hPC subjected to FFSS (pink squares). qPCR results are presented as relative mRNA expression level normalized to *GAPDH* and referred to control group (blue circles). mRNA expression of *PTGER2* (**a**) and *PTGER4* (**b**) was quantified after 2 h of FFSS with 2 dynes/cm^2. Statistics: $, $p < 0.05$, assessed by a two-tailed Student's *t*-test. Each datapoint represents a single sample and plotted as mean ± SD (horizontal lines) per treatment group consisting of $n = 4–5$ replicates obtained in a single experiment.

4. Discussion

Recent studies in murine models of hyperfiltration support a pathophysiological role of autocrine/paracrine COX2/PGE_2 activation on podocyte damage, thus contributing to disturbances of the glomerular filtration barrier including the development of albuminuria [10,14,23] (reviewed in [2,5]). These findings suggest that induction of COX2 associates with podocyte damage, while selective or non-selective inhibition of COX2 reduces proteinuria in animal models as well as in patients (reviewed in [48]). So far, the mechanisms involved have not been investigated in detail.

In mouse podocytes, EP1, -2 and -4 expression was reported and EP2 and -4 were also detected on protein level [14]. In this study, we corroborate these findings in hPC, which also express EP1, -2 and -4. EP4 is known as a constitutively expressed protein reflected by abundant protein levels in untreated murine podocytes compared to EP2 [10]. Our results on apparently lower *PTGER4* mRNA expression compared to *PTGER2* in hPC should be interpreted with caution as they need to be confirmed on the protein level in future investigations. Stimulation of hPC with PGE_2 led to an immediate intracellular cAMP increase starting at 1 min after PGE_2 stimulation until at least 40 min of stimulation (Figure 1). Of note, the detected intracellular cAMP levels are net levels resulting from cAMP generation by adenylate cyclase and its concomitant degradation by phosphodiesterases. Phosphodiesterase activity was only blocked at the end of the stimulation experiments by adding HCl. Previous studies in immortalized murine podocytes revealed a similar time-course of cAMP increase occurring within the first 30 min after EP2 and/or EP4 stimulation [39,49,50]. In our experimental setting in hPC, this PGE_2-stimulated intracellular cAMP increase was only completely abrogated by combined EP2 and EP4 antagonism pointing towards a comparable role of both receptors for cAMP induction in hPC (Figure 2). Multiple intracellular signaling pathways have been described for either

EP2 and EP4 (reviewed in [51]). PGE_2 stimulation of EP2 and EP4 activated the transcription factors T-cell factor (Tcf) and lymphocyte enhancer factor (Lef) signaling via PKA- and phosphatidylinositol 3-kinase/proteinkinase B (PI3K/Akt)-dependent phosphorylation of glycogen synthase kinase 3 (GSK3), thus promoting translocation of the transcription cofactor β-catenin into the nucleus where interaction with Tcf and Lef modulated gene expression, e.g., of COX2 [52,53]. However, participation of EP2 in PI3K/Akt signaling remains a matter of debate, as some investigators suggest that only EP4 but not EP2 are linked with PI3K/Akt [54]. Mechanotransduction in murine podocytes was previously suggested to be mediated by Akt-GSK3β-β-catenin, extracellular-signal regulated kinases (ERK)1/2, and p38MAPK, but not cAMP-PKA signaling upon FFSS [40]. The lack of cAMP elevation upon FFSS in that study might be explained, though by the experimental design as intracellular cAMP was measured at the earliest 2 h after applying FFSS. In contrast, the cAMP-PKA pathway was shown to be involved upon PGE_2 stimulation of murine podocytes [40], which better matches our setting of PGE_2 stimulation of hPC. Moreover, the cAMP-PKA pathway has been shown in intracellular signaling upon FFSS in osteocytes [55,56].

We detected upregulation of *COX2* by PGE_2 in a dose-dependent fashion with both EP2 and EP4 being involved in hPC (Figure 3). PGE_2 stimulation of EP2 and EP4 was reported to increase cAMP response element-binding protein (CREB), which was demonstrated to be PKA-dependent for EP2, whereas EP4-coupled PI3K signaling was suggested to counteract CREB formation [57–60]. Of note, transcription of *COX2* can be modulated by CREB, as CRE is part of the COX2 promotor [61,62]. Therefore, subsequent PKA/CREB activation could play a role for the observed increase in *COX2* expression following intracellular cAMP level elevation in hPC. To further investigate this aspect, experiments with PKA-inhibitors, e.g., H-89, will be performed as well as analysis of CREB phosphorylation status, and activation of the transcription factors Tcf and Lef. Functional analysis of COX2 protein activity might also be helpful. However, previous data in various cell types including murine podocytes already revealed that COX2 protein is indeed increased after 2 h stimulation with PGE_2 [19,58]. Taken together, our results on concerted EP2 and EP4 signaling being involved in upregulation of intracellular cAMP and *COX2* levels represent a novel finding. To validate our results on the role of EP2 and EP4 on the intracellular cAMP increase and upregulation of *COX2*, effects of hPC stimulation with an EP2 and/or EP4 agonist without PGE_2 should be investigated in future experiments.

Accompanied by these findings, PGE_2 stimulation also increased cellular PGE_2, i.e., PGE_2, which is released from membranes and appears intracellularly (Figure 5b). This effect is abrogated by combined EP2- and EP4-antagonism (Figure 5c). Intracellularly generated PGE_2 is degraded by 15-prostaglandin dehydrogenase (HPGD) to 15-keto-PGE_2, which is then terminally inactivated, albeit with different efficiency, by prostaglandin reductase (PTGR) 1, -2 and -3 to 13,14-dihydro-15-keto-PGE_2 [63,64] (reviewed in [65]). Intracellular PGE_2 was reported to exit the cell by simple diffusion or by an efflux transport mediated by prostaglandin transporter (PGT), i.e., solute carrier organic anion transporter family, member 2A1 (OATP2A1), or ATP-binding cassette, subfamily C, member 4 (MRP4) [66–68].

Elevated PGE_2 levels were previously associated with podocyte damage, suggesting that it might be a biomarker of progressive CKD [10,69]. LC-MS/MS based methods are beneficial to precisely study cellular prostaglandin metabolism with a maximum of selectivity and specificity. However, cell culture experiments are mainly restricted to small sample amounts that might hamper analysis by LC-MS/MS [26–32]. Here, we present a refined protocol for prostaglandin analysis in cells by LC/ESI/MS-MS. This might help to further elucidate cellular prostaglandin metabolism under pathophysiological conditions particularly in vitro but also in vivo. The observed increases in cellular PGE_2 content upon PGE_2 stimulation in hPC might be due to several mechanisms. One possibility is that extracellular PGE_2 enters the podocyte by simple diffusion or by uptake transport mediated by OATP2A1, which was previously reported to facilitate bidirectional transport of PGE_2 over membranes [66–68]. A second reason could be autocrine/paracrine mechanisms, i.e., extracellular PGE_2 activates EP2 and EP4 signaling, thus increasing COX2 transcription and translation. As COX2 delineates the rate-limiting step of PGE_2 synthesis (reviewed in [70]), its induction leads to higher

cellular PGE_2 levels. Our results support the latter option, as combined inhibition of EP2 and EP4 signaling diminished the increase in cellular PGE_2 levels.

In our corresponding in vivo study, we employed the MWF model, which represents a suitable model with glomerular hyperfiltration and thus FFSS [47]. The MWF model was previously extensively characterized (reviewed [47]). Thus, the MWF model is a non-diabetic inbred, genetic model with an inherited nephron deficit of 30–50% depending on the comparator rat strain [71,72]. Consequently, male MWF rats are characterized by increased single nephron glomerular filtration rate but with normal mean glomerular capillary pressure [72,73]. In addition, MWF rats develop mild arterial hypertension and spontaneous progressive albuminuria [47]. Thus, male MWF rats develop spontaneous albuminuria at an early age between weeks 4 and 8 after birth and subsequently progressive proteinuria and glomerulosclerosis [74]. The latter was also demonstrated in the MWF strain from our own colony and thus in the animals used in the current study [47]. Early onset albuminuria in young MWF animals occurs at six weeks of age and is preceded by glomerular hypertrophy, accompanied by focal and segmental loss of podoplanin and followed by podocyte foot process effacement at 8 weeks of age, i.e., at onset of albuminuria [75]. For these reasons, we selected animals at this age for our analysis in the current study. As a comparator strain, we use the previously characterized spontaneously hypertensive rats (SHR) that are resistant to albuminuria development [71,76]. Taken together, we showed the feasibility of the LC/ESI-MS/MS methodology to characterize the PGE_2 pathway at the glomerular tissue level by using the MWF strain. The observed increases in both PGE_2 and 15-keto-PGE_2 in isolated glomeruli of MWF support the activation of this pathway in glomerular hyperfiltration. However, these results should be viewed against the background that the cellular origin of this finding was not determined, and thus the contribution of other cell types, e.g., glomerular endothelial cells or mesangial cells remains unclear. Up to now, direct isolation of podocytes from glomeruli was reported for transgenic mice [77–80]. In the rat, there seem to be more technical difficulties as transgenic implementation of fluorescent dyes was not yet accomplished. Antibody staining for podocyte markers and subsequent analysis by FACS is possible [81], but whether isolated primary rat podocytes can be subjected to transcriptomic, proteomic, or lipidomic analysis remains to be investigated. Urinary PGE_2 was suggested as a biomarker for adaptive hyperfiltration in human solitary kidney [69]. The analysis of the urinary PGE_2 and metabolite profile in our CKD MWF model is currently not established due to experimental challenges to establish robust LS/ESI-MS/MS analysis in rat urine. In contrast, the profile in plasma did not differ significantly between MWF and SHR (Figure 6b). In plasma, dilution of prostaglandins might be a major problem as 15-keto-PGE_2 levels were below the limit of detection. Therefore, plasma levels provide rather a rough estimate, while analysis of glomeruli offers a closer insight into podocyte prostaglandin metabolism.

Besides mimicking hyperfiltration by exogenous supplementation with PGE_2, we also applied FFSS on hPC. This model aimed to imitate intensified flow of the ultrafiltrate in Bowman's space, thus causing podocyte injury. Similar to PGE_2 treatment, FFSS leads to upregulation of *COX2* (Figure 7). Our data corroborate the work by Srivastava and coworkers, who suggested Akt/GSK3β-βcatenin and the MAPK pathway to be involved in mechanotransduction on mouse podocytes [10,40]. We thus aim to investigate these signaling pathways in hPC upon FFSS in our future work. We corroborate recent findings that EP2 is upregulated by FFSS while EP4 expression is not changed [10] (Figure 8).

5. Conclusions

An autocrine/paracrine pathway between COX2 and PGE_2 exists also in hPC and is mediated by both EP2 and EP4. Distinct analysis of cellular PGE_2 and its metabolites was enabled by a modified protocol using LS/ESI-MS/MS. Elevated PGE_2 and 15-keto-PGE_2 levels were detected in glomeruli of MWF, a model for CKD, thereby strengthening the hypothesis that glomerular PGE_2 accumulation is associated with albuminuria due to podocyte damage. Understanding prostaglandin signaling in hPC may contribute to identifying novel target pathways to protect against maladaptive responses to hyperfiltration in podocytes.

Supplementary Materials: The following are available online at http://www.mdpi.com/2073-4409/9/5/1256/s1, Figure S1: Differentiation of hPC was confirmed by immunofluorescence of synaptopodin, podocin, and nephrin, Figure S2: Characterization of differentiated and undifferentiated hPC. Figure S3: Expression of EP receptors in hPC, Figure S4: EP2 antagonist does not inhibit PGE_2 mediated *COX2* upregulation when applied with the same concentration as PGE_2. Table 1: Multiple Reaction Monitoring in negative mode for LC/ESI-MS/MS

Author Contributions: Conceptualization, J.B., D.P., and R.K.; methodology, A.S., E.M., and M.R.; validation, J.B. and E.M.; formal analysis, J.B. and E.M.; investigation, E.M., A.K., and M.R.; resources, R.K.; data curation, J.B.; writing—original draft preparation, E.M.; writing—review and editing, J.B. and R.K.; visualization, E.M.; supervision, J.B., D.P., and R.K.; project administration, J.B. and R.K.; funding acquisition, D.P. and R.K. All authors have read and agreed to the published version of the manuscript.

Funding: This research was funded by the Deutsche Forschungsgemeinschaft (DFG, German Research Foundation)—project number 394046635—SFB 1365. The FFSS device was funded by the Sonnenfeld-Stiftung, Berlin, Germany.

Acknowledgments: We thankfully acknowledge the contributions of Karen Böhme, Bettina Bublath, Petra Karsten, and Claudia Plum for excellent laboratory or animal assistance. We furthermore thank Jörg Rösner and the Charité Neuroscience Research Center for support with confocal microscopy and Moin A. Saleem, University of Bristol, UK for providing hPC.

Conflicts of Interest: The authors declare no conflict of interest.

References

1. Pavenstadt, H.; Kriz, W.; Kretzler, M. Cell biology of the glomerular podocyte. *Physiol. Rev.* **2003**, *83*, 253–307. [CrossRef] [PubMed]
2. Srivastava, T.; Hariharan, S.; Alon, U.S.; McCarthy, E.T.; Sharma, R.; El-Meanawy, A.; Savin, V.J.; Sharma, M. Hyperfiltration-mediated Injury in the Remaining Kidney of a Transplant Donor. *Transplantation* **2018**, *102*, 1624–1635. [CrossRef] [PubMed]
3. Srivastava, T.; Celsi, G.E.; Sharma, M.; Dai, H.; McCarthy, E.T.; Ruiz, M.; Cudmore, P.A.; Alon, U.S.; Sharma, R.; Savin, V.A. Fluid flow shear stress over podocytes is increased in the solitary kidney. *Nephrol Dial. Transpl.* **2014**, *29*, 65–72. [CrossRef] [PubMed]
4. Brenner, B.M. Nephron adaptation to renal injury or ablation. *Am. J. Physiol.* **1985**, *249*, F324–F337. [CrossRef]
5. Sharma, M.; Sharma, R.; McCarthy, E.T.; Savin, V.J.; Srivastava, T. Hyperfiltration-associated biomechanical forces in glomerular injury and response: Potential role for eicosanoids. *Prostaglandins Lipid Mediat.* **2017**, *132*, 59–68. [CrossRef]
6. Friedrich, C.; Endlich, N.; Kriz, W.; Endlich, K. Podocytes are sensitive to fluid shear stress in vitro. *Am. J. Physiol. Ren. Physiol.* **2006**, *291*, F856–865. [CrossRef]
7. Endlich, N.; Endlich, K. The challenge and response of podocytes to glomerular hypertension. *Semin. Nephrol* **2012**, *32*, 327–341. [CrossRef]
8. Brenner, B.M.; Lawler, E.V.; Mackenzie, H.S. The hyperfiltration theory: A paradigm shift in nephrology. *Kidney Int.* **1996**, *49*, 1774–1777. [CrossRef]
9. Futrakul, N.; Sridama, V.; Futrakul, P. Microalbuminuria–A biomarker of renal microvascular disease. *Ren Fail.* **2009**, *31*, 140–143. [CrossRef]
10. Srivastava, T.; Alon, U.S.; Cudmore, P.A.; Tarakji, B.; Kats, A.; Garola, R.E.; Duncan, R.S.; McCarthy, E.T.; Sharma, R.; Johnson, M.L.; et al. Cyclooxygenase-2, prostaglandin E2, and prostanoid receptor EP2 in fluid flow shear stress-mediated injury in the solitary kidney. *Am. J. Physiol. Ren. Physiol.* **2014**, *307*, F1323–1333. [CrossRef]
11. Smith, W.L. The eicosanoids and their biochemical mechanisms of action. *Biochem. J.* **1989**, *259*, 315–324. [CrossRef] [PubMed]
12. Samuelsson, B.; Granstrom, E.; Green, K.; Hamberg, M.; Hammarstrom, S. Prostaglandins. *Annu. Rev. Biochem.* **1975**, *44*, 669–695. [CrossRef] [PubMed]
13. Narumiya, S.; Sugimoto, Y.; Ushikubi, F. Prostanoid receptors: structures, properties, and functions. *Physiol. Rev.* **1999**, *79*, 1193–1226. [CrossRef] [PubMed]
14. Srivastava, T.; McCarthy, E.T.; Sharma, R.; Kats, A.; Carlton, C.G.; Alon, U.S.; Cudmore, P.A.; El-Meanawy, A.; Sharma, M. Fluid flow shear stress upregulates prostanoid receptor EP2 but not EP4 in murine podocytes. *Prostaglandins Lipid Mediat.* **2013**, *104–105*, 49–57. [CrossRef]

15. Funk, C.D. Prostaglandins and leukotrienes: advances in eicosanoid biology. *Science (N. Y.)* **2001**, *294*, 1871–1875. [CrossRef]
16. Sugimoto, Y.; Narumiya, S.; Ichikawa, A. Distribution and function of prostanoid receptors: studies from knockout mice. *Prog Lipid Res.* **2000**, *39*, 289–314. [CrossRef]
17. Negishi, M.; Sugimoto, Y.; Ichikawa, A. Molecular mechanisms of diverse actions of prostanoid receptors. *Biochim. Biophys Acta* **1995**, *1259*, 109–119. [CrossRef]
18. Cheng, B.; Kato, Y.; Zhao, S.; Luo, J.; Sprague, E.; Bonewald, L.F.; Jiang, J.X. PGE(2) is essential for gap junction-mediated intercellular communication between osteocyte-like MLO-Y4 cells in response to mechanical strain. *Endocrinology* **2001**, *142*, 3464–3473. [CrossRef]
19. Faour, W.H.; Gomi, K.; Kennedy, C.R. PGE(2) induces COX-2 expression in podocytes via the EP(4) receptor through a PKA-independent mechanism. *Cell. Signal.* **2008**, *20*, 2156–2164. [CrossRef]
20. Pino, M.S.; Nawrocki, S.T.; Cognetti, F.; Abruzzese, J.L.; Xiong, H.Q.; McConkey, D.J. Prostaglandin E2 drives cyclooxygenase-2 expression via cyclic AMP response element activation in human pancreatic cancer cells. *Cancer Biol. Ther.* **2005**, *4*, 1263–1269. [CrossRef]
21. Ansari, K.M.; Sung, Y.M.; He, G.; Fischer, S.M. Prostaglandin receptor EP2 is responsible for cyclooxygenase-2 induction by prostaglandin E2 in mouse skin. *Carcinogenesis* **2007**, *28*, 2063–2068. [CrossRef] [PubMed]
22. Díaz-Muñoz, M.D.; Osma-García, I.C.; Fresno, M.; Iñiguez, M.A. Involvement of PGE2and the cAMP signalling pathway in the up-regulation of COX-2 and mPGES-1 expression in LPS-activated macrophages. *Biochem. J.* **2012**, *443*, 451–461. [CrossRef] [PubMed]
23. Srivastava, T.; McCarthy, E.T.; Sharma, R.; Cudmore, P.A.; Sharma, M.; Johnson, M.L.; Bonewald, L.F. Prostaglandin E(2) is crucial in the response of podocytes to fluid flow shear stress. *J. Cell Commun. Signal.* **2010**, *4*, 79–90. [CrossRef] [PubMed]
24. Faupel-Badger, J.M.; Fuhrman, B.J.; Xu, X.; Falk, R.T.; Keefer, L.K.; Veenstra, T.D.; Hoover, R.N.; Ziegler, R.G. Comparison of liquid chromatography-tandem mass spectrometry, RIA, and ELISA methods for measurement of urinary estrogens. *Cancer Epidemiol. Biomark. Prev.* **2010**, *19*, 292–300. [CrossRef] [PubMed]
25. Gandhi, A.S.; Budac, D.; Khayrullina, T.; Staal, R.; Chandrasena, G. Quantitative analysis of lipids: a higher-throughput LC-MS/MS-based method and its comparison to ELISA. *Future Sci. OA* **2017**, *3*, Fso157. [CrossRef] [PubMed]
26. Mesaros, C.; Lee, S.H.; Blair, I.A. Analysis of epoxyeicosatrienoic acids by chiral liquid chromatography/electron capture atmospheric pressure chemical ionization mass spectrometry using [13C]-analog internal standards. *Rapid Commun. Mass Spectrom.* **2010**, *24*, 3237–3247. [CrossRef]
27. Nithipatikom, K.; Laabs, N.D.; Isbell, M.A.; Campbell, W.B. Liquid chromatographic-mass spectrometric determination of cyclooxygenase metabolites of arachidonic acid in cultured cells. *J. Chromatogr. B Anal. Technol. Biomed. Life Sci.* **2003**, *785*, 135–145. [CrossRef]
28. Kempen, E.C.; Yang, P.; Felix, E.; Madden, T.; Newman, R.A. Simultaneous quantification of arachidonic acid metabolites in cultured tumor cells using high-performance liquid chromatography/electrospray ionization tandem mass spectrometry. *Anal. Biochem.* **2001**, *297*, 183–190. [CrossRef]
29. Rund, K.M.; Ostermann, A.I.; Kutzner, L.; Galano, J.M.; Oger, C.; Vigor, C.; Wecklein, S.; Seiwert, N.; Durand, T.; Schebb, N.H. Development of an LC-ESI(-)-MS/MS method for the simultaneous quantification of 35 isoprostanes and isofurans derived from the major n3- and n6-PUFAs. *Anal. Chim. Acta* **2018**, *1037*, 63–74. [CrossRef]
30. Deems, R.; Buczynski, M.W.; Bowers-Gentry, R.; Harkewicz, R.; Dennis, E.A. Detection and quantitation of eicosanoids via high performance liquid chromatography-electrospray ionization-mass spectrometry. *Methods Enzym.* **2007**, *432*, 59–82. [CrossRef]
31. Bollinger, J.G.; Thompson, W.; Lai, Y.; Oslund, R.C.; Hallstrand, T.S.; Sadilek, M.; Turecek, F.; Gelb, M.H. Improved sensitivity mass spectrometric detection of eicosanoids by charge reversal derivatization. *Anal. Chem.* **2010**, *82*, 6790–6796. [CrossRef] [PubMed]
32. Le Faouder, P.; Baillif, V.; Spreadbury, I.; Motta, J.P.; Rousset, P.; Chene, G.; Guigne, C.; Terce, F.; Vanner, S.; Vergnolle, N.; et al. LC-MS/MS method for rapid and concomitant quantification of pro-inflammatory and pro-resolving polyunsaturated fatty acid metabolites. *J. Chromatogr. B Anal. Technol. Biomed. Life Sci.* **2013**, *932*, 123–133. [CrossRef]

33. Saleem, M.A.; O'Hare, M.J.; Reiser, J.; Coward, R.J.; Inward, C.D.; Farren, T.; Xing, C.Y.; Ni, L.; Mathieson, P.W.; Mundel, P. A conditionally immortalized human podocyte cell line demonstrating nephrin and podocin expression. *J. Am. Soc. Nephrol.* **2002**, *13*, 630–638. [PubMed]
34. Ni, L.; Saleem, M.; Mathieson, P.W. Podocyte culture: Tricks of the trade. *Nephrology (Carlton Vic.)* **2012**, *12*, 525–531. [CrossRef] [PubMed]
35. Ma, X.; Aoki, T.; Tsuruyama, T.; Narumiya, S. Definition of Prostaglandin E2-EP2 Signals in the Colon Tumor Microenvironment That Amplify Inflammation and Tumor Growth. *Cancer Res.* **2015**, *75*, 2822–2832. [CrossRef] [PubMed]
36. af Forselles, K.J.; Root, J.; Clarke, T.; Davey, D.; Aughton, K.; Dack, K.; Pullen, N. In vitro and in vivo characterization of PF-04418948, a novel, potent and selective prostaglandin EP(2) receptor antagonist. *Br. J. Pharmacol.* **2011**, *164*, 1847–1856. [CrossRef]
37. Thieme, K.; Majumder, S.; Brijmohan, A.S.; Batchu, S.N.; Bowskill, B.B.; Alghamdi, T.A.; Advani, S.L.; Kabir, M.G.; Liu, Y.; Advani, A. EP4 inhibition attenuates the development of diabetic and non-diabetic experimental kidney disease. *Sci. Rep.* **2017**, *7*, 3442. [CrossRef]
38. Kabashima, K.; Saji, T.; Murata, T.; Nagamachi, M.; Matsuoka, T.; Segi, E.; Tsuboi, K.; Sugimoto, Y.; Kobayashi, T.; Miyachi, Y.; et al. The prostaglandin receptor EP4 suppresses colitis, mucosal damage and CD4 cell activation in the gut. *J. Clin. Investig.* **2002**, *109*, 883–893. [CrossRef]
39. Bek, M.; Nusing, R.; Kowark, P.; Henger, A.; Mundel, P.; Pavenstadt, H. Characterization of prostanoid receptors in podocytes. *J. Am. Soc. Nephrol.* **1999**, *10*, 2084–2093.
40. Srivastava, T.; Dai, H.; Heruth, D.P.; Alon, U.S.; Garola, R.E.; Zhou, J.; Duncan, R.S.; El-Meanawy, A.; McCarthy, E.T.; Sharma, R.; et al. Mechanotransduction signaling in podocytes from fluid flow shear stress. *Am. J. Physiol. Ren. Physiol.* **2018**, *314*, F22–F34. [CrossRef]
41. Dey, I.; Giembycz, M.A.; Chadee, K. Prostaglandin E(2) couples through EP(4) prostanoid receptors to induce IL-8 production in human colonic epithelial cell lines. *Br. J. Pharmacol.* **2009**, *156*, 475–485. [CrossRef] [PubMed]
42. Lee, J.; Aoki, T.; Thumkeo, D.; Siriwach, R.; Yao, C.; Narumiya, S. T cell-intrinsic prostaglandin E2-EP2/EP4 signaling is critical in pathogenic TH17 cell-driven inflammation. *J. Allergy Clin. Immunol.* **2019**, *143*, 631–643. [CrossRef] [PubMed]
43. Liu, C.; Zhu, P.; Wang, W.; Li, W.; Shu, Q.; Chen, Z.J.; Myatt, L.; Sun, K. Inhibition of lysyl oxidase by prostaglandin E2 via EP2/EP4 receptors in human amnion fibroblasts: Implications for parturition. *Mol. Cell. Endocrinol.* **2016**, *424*, 118–127. [CrossRef] [PubMed]
44. Schulz, A.; Muller, N.V.; van de Lest, N.A.; Eisenreich, A.; Schmidbauer, M.; Barysenka, A.; Purfurst, B.; Sporbert, A.; Lorenzen, T.; Meyer, A.M.; et al. Analysis of the genomic architecture of a complex trait locus in hypertensive rat models links Tmem63c to kidney damage. *eLife* **2019**, *8*. [CrossRef]
45. Livak, K.J.; Schmittgen, T.D. Analysis of relative gene expression data using real-time quantitative PCR and the 2(-Delta Delta C(T)) Method. *Methods* **2001**, *25*, 402–408. [CrossRef] [PubMed]
46. Jiang, H.; McGiff, J.C.; Quilley, J.; Sacerdoti, D.; Reddy, L.M.; Falck, J.R.; Zhang, F.; Lerea, K.M.; Wong, P.Y. Identification of 5,6-trans-epoxyeicosatrienoic acid in the phospholipids of red blood cells. *J. Biol. Chem.* **2004**, *279*, 36412–36418. [CrossRef]
47. Schulz, A.; Kreutz, R. Mapping genetic determinants of kidney damage in rat models. *Hypertens. Res.* **2012**, *35*, 675–694. [CrossRef]
48. Vogt, L.; Laverman, G.D.; Navis, G. Time for a comeback of NSAIDs in proteinuric chronic kidney disease? *Neth. J. Med.* **2010**, *68*, 400–407.
49. Liu, J.; Zhang, Y.D.; Chen, X.L.; Zhu, X.L.; Chen, X.; Wu, J.H.; Guo, N.F. The protective effect of the EP2 receptor on TGF-beta1 induced podocyte injury via the PI3K/Akt signaling pathway. *PLoS ONE* **2018**, *13*, e0197158. [CrossRef]
50. Lemieux, L.I.; Rahal, S.S.; Kennedy, C.R. PGE2 reduces arachidonic acid release in murine podocytes: evidence for an autocrine feedback loop. *Am. J. Physiol. Cell Physiol.* **2003**, *284*, C302–309. [CrossRef]
51. Regan, J.W. EP2 and EP4 prostanoid receptor signaling. *Life Sci.* **2003**, *74*, 143–153. [CrossRef] [PubMed]
52. Fujino, H.; West, K.A.; Regan, J.W. Phosphorylation of glycogen synthase kinase-3 and stimulation of T-cell factor signaling following activation of EP2 and EP4 prostanoid receptors by prostaglandin E2. *J. Biol. Chem.* **2002**, *277*, 2614–2619. [CrossRef] [PubMed]

53. Hsu, H.H.; Lin, Y.M.; Shen, C.Y.; Shibu, M.A.; Li, S.Y.; Chang, S.H.; Lin, C.C.; Chen, R.J.; Viswanadha, V.P.; Shih, H.N.; et al. Prostaglandin E2-Induced COX-2 Expressions via EP2 and EP4 Signaling Pathways in Human LoVo Colon Cancer Cells. *Int. J. Mol. Sci.* **2017**, *18*, 1132. [CrossRef] [PubMed]
54. Fujino, H.; Xu, W.; Regan, J.W. Prostaglandin E2 induced functional expression of early growth response factor-1 by EP4, but not EP2, prostanoid receptors via the phosphatidylinositol 3-kinase and extracellular signal-regulated kinases. *J. Biol. Chem.* **2003**, *278*, 12151–12156. [CrossRef]
55. Kitase, Y.; Barragan, L.; Qing, H.; Kondoh, S.; Jiang, J.X.; Johnson, M.L.; Bonewald, L.F. Mechanical induction of PGE2 in osteocytes blocks glucocorticoid-induced apoptosis through both the beta-catenin and PKA pathways. *J. Bone Min. Res.* **2010**, *25*, 2657–2668. [CrossRef]
56. Cherian, P.P.; Cheng, B.; Gu, S.; Sprague, E.; Bonewald, L.F.; Jiang, J.X. Effects of mechanical strain on the function of Gap junctions in osteocytes are mediated through the prostaglandin EP2 receptor. *J. Biol. Chem.* **2003**, *278*, 43146–43156. [CrossRef]
57. Fujino, H.; Salvi, S.; Regan, J.W. Differential regulation of phosphorylation of the cAMP response element-binding protein after activation of EP2 and EP4 prostanoid receptors by prostaglandin E2. *Mol. Pharmacol.* **2005**, *68*, 251–259. [CrossRef]
58. Lu, J.W.; Wang, W.S.; Zhou, Q.; Gan, X.W.; Myatt, L.; Sun, K. Activation of prostaglandin EP4 receptor attenuates the induction of cyclooxygenase-2 expression by EP2 receptor activation in human amnion fibroblasts: implications for parturition. *Faseb J. Off. Publ. Fed. Am. Soc. Exp. Biol.* **2019**, *33*, 8148–8160. [CrossRef]
59. Majumder, M.; Xin, X.; Liu, L.; Tutunea-Fatan, E.; Rodriguez-Torres, M.; Vincent, K.; Postovit, L.M.; Hess, D.; Lala, P.K. COX-2 Induces Breast Cancer Stem Cells via EP4/PI3K/AKT/NOTCH/WNT Axis. *Stem Cells* **2016**, *34*, 2290–2305. [CrossRef]
60. Vo, B.T.; Morton, D., Jr.; Komaragiri, S.; Millena, A.C.; Leath, C.; Khan, S.A. TGF-beta effects on prostate cancer cell migration and invasion are mediated by PGE2 through activation of PI3K/AKT/mTOR pathway. *Endocrinology* **2013**, *154*, 1768–1779. [CrossRef]
61. Gao, F.; Zafar, M.I.; Juttner, S.; Hocker, M.; Wiedenmann, B. Expression and Molecular Regulation of the Cox2 Gene in Gastroenteropancreatic Neuroendocrine Tumors and Antiproliferation of Nonsteroidal Anti-Inflammatory Drugs (NSAIDs). *Med. Sci. Monit.* **2018**, *24*, 8125–8140. [CrossRef] [PubMed]
62. Mesa, J.; Alsina, C.; Oppermann, U.; Pares, X.; Farres, J.; Porte, S. Human prostaglandin reductase 1 (PGR1): Substrate specificity, inhibitor analysis and site-directed mutagenesis. *Chem. Biol. Interact.* **2015**, *234*, 105–113. [CrossRef] [PubMed]
63. Yu, Y.H.; Chang, Y.C.; Su, T.H.; Nong, J.Y.; Li, C.C.; Chuang, L.M. Prostaglandin reductase-3 negatively modulates adipogenesis through regulation of PPARgamma activity. *J. Lipid Res.* **2013**, *54*, 2391–2399. [CrossRef] [PubMed]
64. Tai, H.H.; Ensor, C.M.; Tong, M.; Zhou, H.; Yan, F. Prostaglandin catabolizing enzymes. *Prostaglandins Lipid Mediat.* **2002**, *68–69*, 483–493. [CrossRef]
65. Reid, G.; Wielinga, P.; Zelcer, N.; van der Heijden, I.; Kuil, A.; de Haas, M.; Wijnholds, J.; Borst, P. The human multidrug resistance protein MRP4 functions as a prostaglandin efflux transporter and is inhibited by nonsteroidal antiinflammatory drugs. *Proc. Natl. Acad. Sci. USA* **2003**, *100*, 9244–9249. [CrossRef]
66. Chan, B.S.; Satriano, J.A.; Pucci, M.; Schuster, V.L. Mechanism of prostaglandin E2 transport across the plasma membrane of HeLa cells and Xenopus oocytes expressing the prostaglandin transporter ''PGT''. *J. Biol. Chem.* **1998**, *273*, 6689–6697. [CrossRef]
67. Shirasaka, Y.; Shichiri, M.; Kasai, T.; Ohno, Y.; Nakanishi, T.; Hayashi, K.; Nishiura, A.; Tamai, I. A role of prostaglandin transporter in regulating PGE(2) release from human bronchial epithelial BEAS-2B cells in response to LPS. *J. Endocrinol.* **2013**, *217*, 265–274. [CrossRef]
68. Kosaka, T.; Miyata, A.; Ihara, H.; Hara, S.; Sugimoto, T.; Takeda, O.; Takahashi, E.; Tanabe, T. Characterization of the human gene (PTGS2) encoding prostaglandin-endoperoxide synthase 2. *Eur. J. Biochem.* **1994**, *221*, 889–897. [CrossRef]
69. Srivastava, T.; Ju, W.; Milne, G.L.; Rezaiekhaligh, M.H.; Staggs, V.S.; Alon, U.S.; Sharma, R.; Zhou, J.; El-Meanawy, A.; McCarthy, E.T.; et al. Urinary prostaglandin E2 is a biomarker of early adaptive hyperfiltration in solitary functioning kidney. *Prostaglandins Lipid Mediat.* **2020**, *146*, 106403. [CrossRef]
70. Needleman, P.; Turk, J.; Jakschik, B.A.; Morrison, A.R.; Lefkowith, J.B. Arachidonic acid metabolism. *Annu. Rev. Biochem.* **1986**, *55*, 69–102. [CrossRef]

71. Schulz, A.; Weiss, J.; Schlesener, M.; Hansch, J.; Wehland, M.; Wendt, N.; Kossmehl, P.; Sietmann, A.; Grimm, D.; Stoll, M.; et al. Development of overt proteinuria in the Munich Wistar Fromter rat is suppressed by replacement of chromosome 6 in a consomic rat strain. *J. Am. Soc. Nephrol.* **2007**, *18*, 113–121. [CrossRef] [PubMed]
72. Fassi, A.; Sangalli, F.; Maffi, R.; Colombi, F.; Mohamed, E.I.; Brenner, B.M.; Remuzzi, G.; Remuzzi, A. Progressive glomerular injury in the MWF rat is predicted by inborn nephron deficit. *J. Am. Soc. Nephrol.* **1998**, *9*, 1399–1406. [PubMed]
73. Remuzzi, A.; Puntorieri, S.; Mazzoleni, A.; Remuzzi, G. Sex related differences in glomerular ultrafiltration and proteinuria in Munich-Wistar rats. *Kidney Int.* **1988**, *34*, 481–486. [CrossRef] [PubMed]
74. Macconi, D.; Bonomelli, M.; Benigni, A.; Plati, T.; Sangalli, F.; Longaretti, L.; Conti, S.; Kawachi, H.; Hill, P.; Remuzzi, G.; et al. Pathophysiologic implications of reduced podocyte number in a rat model of progressive glomerular injury. *Am. J. Pathol.* **2006**, *168*, 42–54. [CrossRef] [PubMed]
75. Ijpelaar, D.H.; Schulz, A.; Koop, K.; Schlesener, M.; Bruijn, J.A.; Kerjaschki, D.; Kreutz, R.; de Heer, E. Glomerular hypertrophy precedes albuminuria and segmental loss of podoplanin in podocytes in Munich-Wistar-Frömter rats. *Am. J. Physiol. Ren. Physiol.* **2008**, *294*, F758–F767. [CrossRef]
76. van Es, N.; Schulz, A.; Ijpelaar, D.; van der Wal, A.; Kuhn, K.; Schutten, S.; Kossmehl, P.; Nyengaard, J.R.; de Heer, E.; Kreutz, R. Elimination of severe albuminuria in aging hypertensive rats by exchange of 2 chromosomes in double-consomic rats. *Hypertension* **2011**, *58*, 219–224. [CrossRef]
77. Boerries, M.; Grahammer, F.; Eiselein, S.; Buck, M.; Meyer, C.; Goedel, M.; Bechtel, W.; Zschiedrich, S.; Pfeifer, D.; Laloe, D.; et al. Molecular fingerprinting of the podocyte reveals novel gene and protein regulatory networks. *Kidney Int.* **2013**, *83*, 1052–1064. [CrossRef]
78. Schell, C.; Baumhakl, L.; Salou, S.; Conzelmann, A.C.; Meyer, C.; Helmstadter, M.; Wrede, C.; Grahammer, F.; Eimer, S.; Kerjaschki, D.; et al. N-wasp is required for stabilization of podocyte foot processes. *J. Am. Soc. Nephrol.* **2013**, *24*, 713–721. [CrossRef]
79. Staffel, J.; Valletta, D.; Federlein, A.; Ehm, K.; Volkmann, R.; Fuchsl, A.M.; Witzgall, R.; Kuhn, M.; Schweda, F. Natriuretic Peptide Receptor Guanylyl Cyclase-A in Podocytes is Renoprotective but Dispensable for Physiologic Renal Function. *J. Am. Soc. Nephrol.* **2017**, *28*, 260–277. [CrossRef]
80. Koehler, S.; Kuczkowski, A.; Kuehne, L.; Jungst, C.; Hoehne, M.; Grahammer, F.; Eddy, S.; Kretzler, M.; Beck, B.B.; Hohfeld, J.; et al. Proteome Analysis of Isolated Podocytes Reveals Stress Responses in Glomerular Sclerosis. *J. Am. Soc. Nephrol.* **2020**, *31*, 544–559. [CrossRef]
81. Sharma, R.; Waller, A.P.; Agrawal, S.; Wolfgang, K.J.; Luu, H.; Shahzad, K.; Isermann, B.; Smoyer, W.E.; Nieman, M.T.; Kerlin, B.A. Thrombin-Induced Podocyte Injury Is Protease-Activated Receptor Dependent. *J. Am. Soc. Nephrol.* **2017**, *28*, 2618–2630. [CrossRef] [PubMed]

© 2020 by the authors. Licensee MDPI, Basel, Switzerland. This article is an open access article distributed under the terms and conditions of the Creative Commons Attribution (CC BY) license (http://creativecommons.org/licenses/by/4.0/).

cells

MDPI

Supplemental Material

S 1. Immunofluorescence of Synaptopodin, Podocin, and Nephrin

Differentiated phenotype of hPC was confirmed by analysis of the marker synaptopodin by immunofluorescence. Briefly, cells were seeded on 8-chamber-glass slides at 12 x 10^3 cells per well (NUNC Lab-Tek II Chamber Slide, cat. no. 154534) and kept in RPMI-1640 medium with supplements for adherence overnight. Medium was then discarded and cells were washed twice with PBS. Fixation of cells was achieved with 80% acetone/PBS at 4 °C for 10 min. Afterwards, cells were washed three times with cold PBS. Blocking solution consisting of PBS+5%FBS was applied for 20 min at room temperature. Primary antibody mouse anti-synaptopodin (cat. no. 65194, Progen Biotechnik GmbH, Germany) diluted 1:25 was added and incubation lasted 1 h at room temperature. After three washing steps, the secondary antibody donkey anti-mouse IgG Alexa Fluor Plus 594 (cat. no. A32744, Thermo Fisher Scientific, Germany) diluted 1:200 was added and incubated for 1 h at room temperature in darkness. Cells were washed twice with PBS and nuclei were stained with 4',6-diamidino-2-phenylindole (DAPI, cat. no. P36931, Invitrogen, Germany) for 24 h at room temperature in darkness. Immunofluorescence was detected at 405 nm (DAPI) and 594 nm (donkey anti mouse for synaptopodin) on a Leica confocal SPE microscope (Figure S1 (a) and (b)).

Additionally, immunofluorescence for the podocyte markers podocin and nephrin was performed in 24-well plates. For nephrin, the protocol of synaptopodin staining was followed using rabbit anti-nephrin (cat. no. PA5-72826, Invitrogen, Germany) diluted 1:50 as primary antibody and goat anti-rabbit Alexa Fluor Plus 488 (cat. no. A32732, Invitrogen, Germany) 1:200 as secondary antibody. Nuclei staining was performed using DAPI 1:3000 (cat. no. D1306, Thermo Fisher, Germany) with incubation for 10 min at room temperature in darkness. Cells were finally washed twice with PBS and covered with Fluoromount (cat. no. 00-4958-02, Invitrogen, Germany). For podocin, fixation of cells was achieved by 4% paraformaldehyde+1 mM $MgCl_2$+0.5% Triton X100 using 800 µL per well and an incubation time of 10 min at room temperature. After three washing steps with PBS, blocking solution consisting of PBS+5% FBS+0.1% Triton X100 was added to each well and incubated for 20 min at room temperature. Primary antibody rabbit anti-podocin (cat. no. P0372, Sigma-Aldrich, Germany) diluted 1:50 was added and incubation lasted 1 h at room temperature. Afterwards, the same protocol was followed as for podocin staining. Immunofluorescence was detected at 405 nm (DAPI) and 488 nm (goat anti-rabbit for podocin and nephrin) on an EVOS fluorescence microscope (Thermo Fisher, Germany) (Figure S1 (c)-(e)).

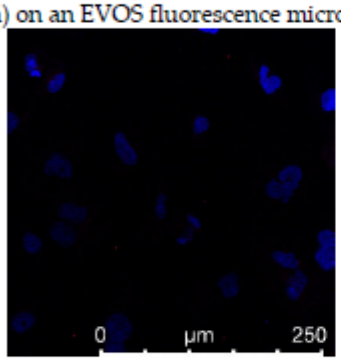

(a)

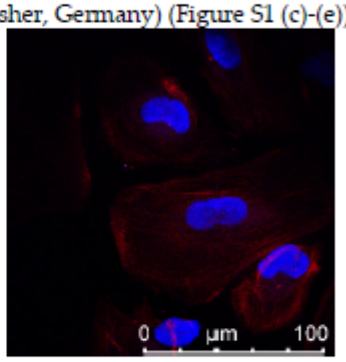

(b)

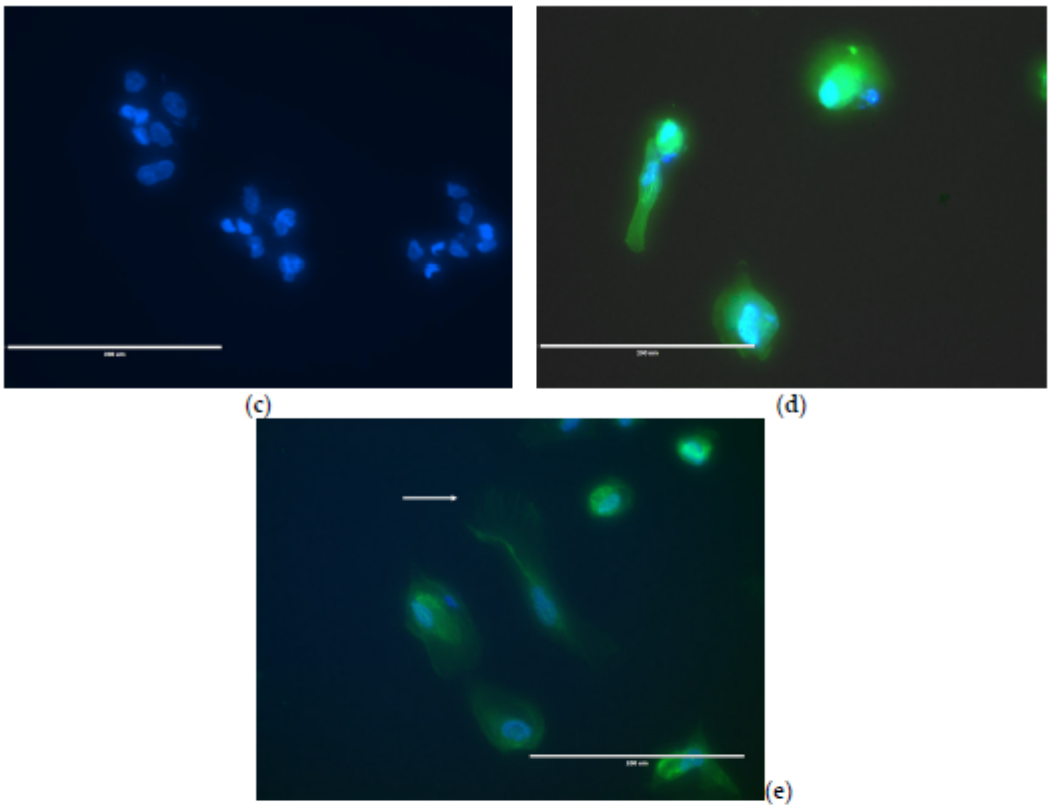

Figure S1. Differentiation of hPC was confirmed by immunofluorescence of synaptopodin, podocin, and nephrin. (**a**) Control without primary antibody revealed no unspecific binding of secondary antibody donkey anti-mouse IgG Alexa Fluor Plus 594, overlay with DAPI indicated nuclei. Scale bar 250 µm; (**b**) Synaptopodin (red) was expressed by differentiated hPC. Nuclei staining was performed with DAPI. Scale bar 100 µm; (**c**) Control without primary antibody revealed no unspecific binding of secondary antibody goat anti-rabbit Alexa Fluor Plus 488, overlay with DAPI indicated nuclei. Scale bar 200 µm; (**d**) Podocin (green) and (**e**) nephrin (green) were expressed by differentiated hPC. Foot processes are visible in (**e**) indicated by white arrow. Scale bars 200 µm.

S 2. Additional Characterization of hPC

Cellular appearance differed between differentiated hPC exhibiting an arborized shape (Figure S2a), and proliferating, undifferentiated hPC that showed typical "cobblestone" pattern (Figure S2b). This appearance was also described before [1]. Furthermore, synaptopodin (*SYNPO*) gene expression (forward primer (5′-3′) – gaggacctagcagacgttgg, reverse primer (5′-3′) – tctgagtacccctccatgct) was shown on differentiated hPC, while undifferentiated hPC did not express *SYNPO* mRNA (Figure S2c). Additionally, nephrin and podocin protein were detected by western blot using rabbit anti-nephrin antibody (cat. no. PA5-72826, Thermo Scientific) and rabbit anti-podocin antibody (cat. no. P0372, Sigma), both diluted 1:500 and incubated at 4 °C overnight as primary antibodies and horseradish peroxidase conjugated goat anti-rabbit (cat. no. sc-2004, Santa Cruz Biotechnology) as secondary antibody. Nephrin and podocin were expressed on differentiated and proliferating podocytes, albeit the undifferentiated hPC exhibited weaker expression of both (Figure S2d, e).

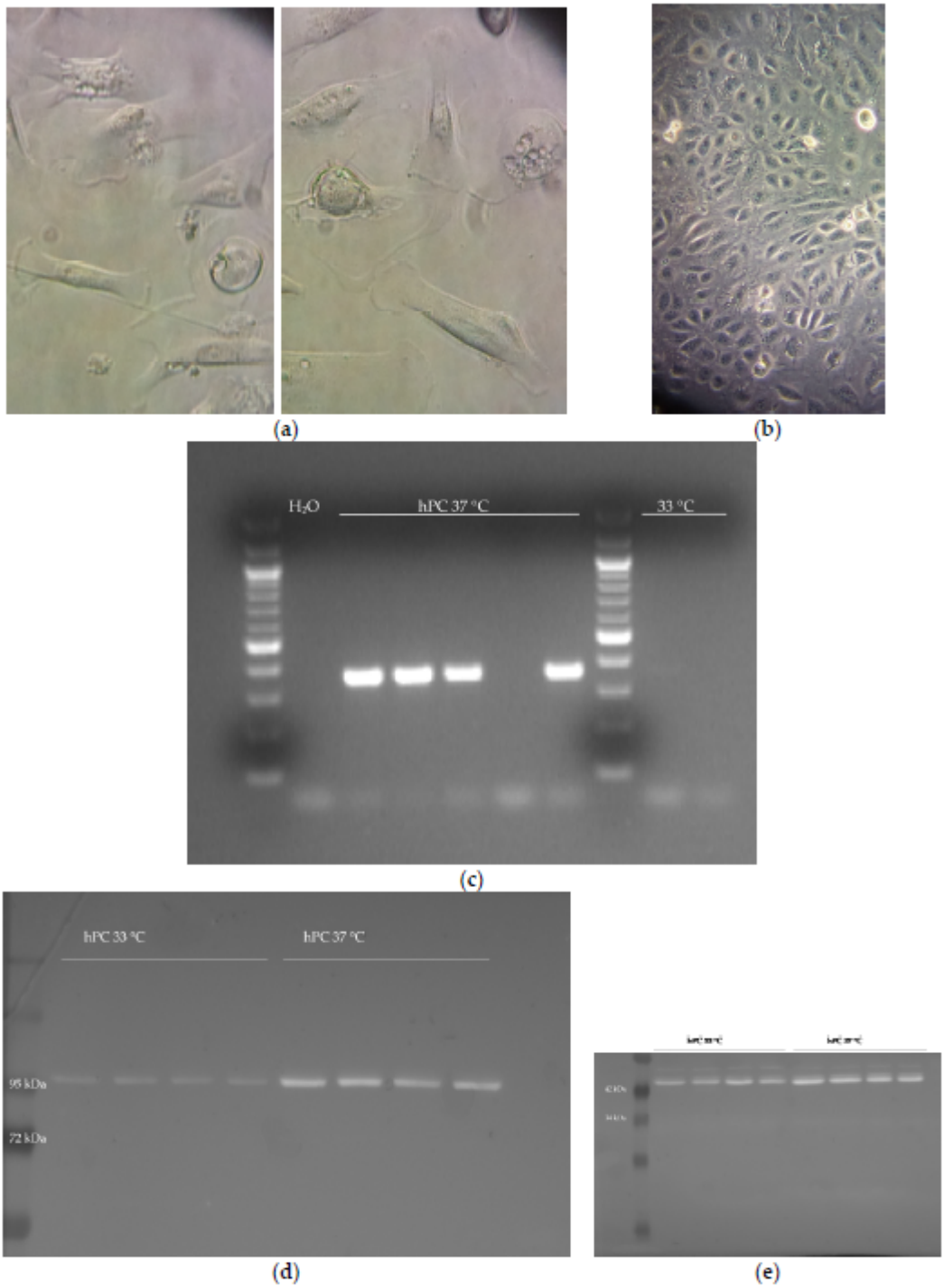

Figure S2. Characterization of differentiated and undifferentiated hPC. Light microscopy revealed an arborized shape of differentiated hPC at 37 °C (**a**), and a cobblestone pattern of undifferentiated hPC at 33 °C (**b**); (**c**) PCR revealed *SYNPO* gene expression in differentiated hPC ("hPC 37 °C") and no expression in undifferentiated hPC ("33 °C"); (**d**) nephrin and podocin (**e**) protein were detected by western blot in undifferentiated ("hPC 33 °C") and differentiated ("hPC 37 °C") hPC.

S 3. Expression of EP in hPC

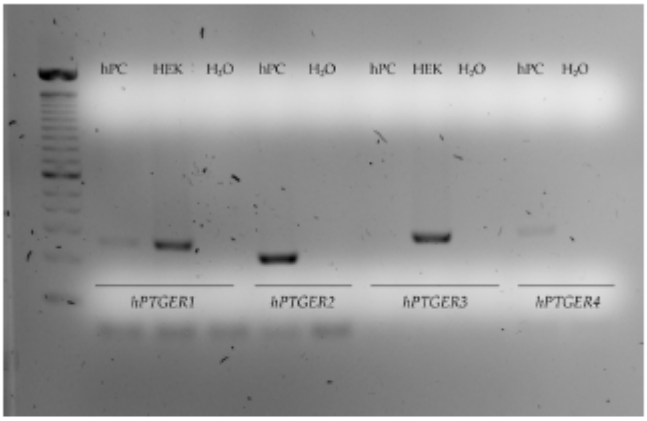

Figure S3. Characterization of hPC for EP receptor expression. *PTGER1* (EP1), *PTGER2* (EP2), and *PTGER4* (EP4) mRNA is present in differentiated hPC. HEK293 (HEK) served as a positive control where indicated.

S 4. COX2 expression in hPC after co-incubation with PGE2 1 µM and EP2 antagonist 1 µM

In a pilot test, we analyzed whether the selective EP2 antagonist PF-04418948 (1 µM) could abolish the effects of 1 µM PGE_2 on *COX2* mRNA expression. Stimulation of hPC with PGE_2 1 µM for 2 h revealed an increase in *COX2* mRNA (Figure S4). Upon PGE_2 stimulation, co-incubation with 1 µM of the selective EP2 antagonist PF-04418948 did not inhibit the PGE_2-mediated increase in *COX2* mRNA (Figure S4).

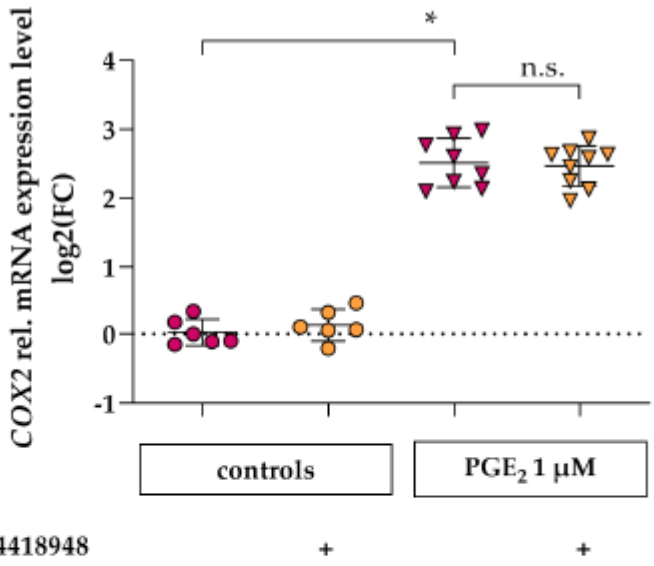

Figure S4. EP2 antagonist does not inhibit PGE_2 mediated *COX2* upregulation when applied with the same concentration as PGE_2. *COX2* mRNA-levels following PGE_2 stimulation with 1 µM for 2 h without concomitant EP2 antagonist (pink triangles) compared to controls without PGE_2 (pink circles), after co-incubation with 1 µM EP2 antagonist (PF-04418948, orange triangles) compared to controls without PGE_2 (orange circles). Each datapoint represents a single sample and plotted as mean ± SD (horizontal lines) per treatment group. Each treatment group consisted of n=6–9 replicates analyzed in a single experiment. Statistics: *, $p<0.01$; n.s., not significant, assessed by two-tailed Student's t-test.

S 5. LC/ESI-MS/MS for Analysis of Prostaglandins

Table S1. Multiple Reaction Monitoring in negative mode for LC/ESI-MS/MS.

Compound Name	Precursor Ion	Product Ion	Mass Res	CE (V)	Ret Time (min)
Tetranor PGFM	329	249	Unit	26	3
Tetranor PGFM	329	239	Unit	25	3
Tetranor PGFM	329	149	Unit	31	3
Tetranor PGFM	329	129	Unit	33	3
6-keto-PGF1a	369.2	245	Wide	28	4.61
6-keto-PGF1a	369.2	207	Wide	22	4.61
6-keto-PGF1a	369.2	163	Wide	29	4.61
TXB2-1	369.2	195.1	Wide	12	7.04
TXB2-1	369.2	169.1	Wide	14	7.04
11ß-PGF2a	353.2	273.2	Wide	22	7.3
11ß-PGF2a	353.2	193.1	Wide	26	7.3
11ß-PGF2a	353.2	291.2	Wide	21	7.3
PGF2a	353.2	291	Wide	23	8.84
PGF2a	353.2	273	Wide	22	8.84
PGF2a	353.2	193	Wide	28	8.84
PGF2a	353.2	165	Wide	27	8.84
PGE2-D4	355.2	275.2	Wide	18	9.84
PGE2	351.2	315.2	Wide	10	9.94
PGE2	351.2	271.2	Wide	18	9.94
PGE2	351.2	189.1	Wide	20	9.94
PGF2a-15-keto	351.2	315	Wide	11	10.64
PGF2a-15-keto	351.2	191	Wide	28	10.64
PGD2	351.2	315.2	Wide	11	11.3
PGD2	351.2	271.2	Wide	18	11.3
PGD2	351.2	233.2	Wide	10	11.3
PGD2	351.2	189.1	Wide	20	11.3
PGE2-15-keto	349.2	287.2	Wide	14	11.8
PGE2-15-keto	349.2	235.2	Wide	14	11.8
PGE2-15-keto	349.2	113.1	Wide	19	11.8
PGF2a-13,14dihydro-15keto	353.2	291	Wide	22	13.7
PGF2a-13,14dihydro-15keto	353.2	183	Wide	29	13.7
PGF2a-13,14dihydro-15keto	353.2	113	Wide	29	13.7
PGE2-13,14-dihydro-15-keto	351.2	315.2	Wide	20	14.4
PGE2-13,14-dihydro-15-keto	351.2	235.2	Wide	22	14.4
PGE2-13,14-dihydro-15-keto	351.2	175.2	Wide	22	14.4
PGE2-13,14-dihydro-15-keto	351.2	113.1	Wide	28	14.4
PGD2-13,14-dihydro-15-keto	351.2	315.2	Wide	12	17.7
PGD2-13,14-dihydro-15-keto	351.2	207.1	Wide	20	17.7
PGD2-13,14-dihydro-15-keto	351.2	175.2	Wide	20	17.7
PGD2-13,14-dihydro-15-keto	351.2	163.1	Wide	26	17.7
PGJ2	333.2	271.2	Wide	16	20.75
PGJ2	333.2	233.1	Wide	9	20.75
PGJ2	333.2	189.1	Wide	17	20.75
PGJ2-delta12	333.2	271.2	Wide	16	21.1
PGJ2-delta12	333.2	233.1	Wide	9	21.1
PGJ2-delta12	333.2	189.1	Wide	17	21.1
PGJ2-15-deoxy-delta 12,14	315.2	271.2	Wide	12	26.2
PGJ2-15-deoxy-delta 12,14	315.2	243.2	Wide	20	26.2
PGJ2-15-deoxy-delta 12,14	315.2	217.1	Wide	18	26.2

Compound Name	Precursor Ion	Product Ion	Mass Res	CE (V)	Ret Time (min)
PGJ2-15-deoxy-delta 12,14	315.2	203.1	Wide	24	26.2
PGJ2-15-deoxy-delta 12,14	315.2	158.2	Wide	20	26.2

1. Saleem, M.A.; O'Hare, M.J.; Reiser, J.; Coward, R.J.; Inward, C.D.; Farren, T.; Xing, C.Y.; Ni, L.; Mathieson, P.W.; Mundel, P. A conditionally immortalized human podocyte cell line demonstrating nephrin and podocin expression. *Journal of the American Society of Nephrology : JASN* **2002**, *13*, 630-638.

Auszug aus der Journal Summary List Publikation 2

Journal Data Filtered By: **Selected JCR Year: 2019** Selected Editions: SCIE,SSCI
Selected Categories: **"PERIPHERAL VASCULAR DISEASE"** Selected Category Scheme: WoS
Gesamtanzahl: 65 Journale

Rank	Full Journal Title	Total Cites	Journal Impact Factor	Eigenfactor Score
1	CIRCULATION	158,218	23.603	0.205020
2	CIRCULATION RESEARCH	51,539	14.467	0.071470
3	ANGIOGENESIS	3,571	9.780	0.005480
4	HYPERTENSION	36,242	7.713	0.046840
5	Journal of Stroke	1,247	7.470	0.004240
6	STROKE	66,466	7.190	0.078010
7	ARTERIOSCLEROSIS THROMBOSIS AND VASCULAR BIOLOGY	32,385	6.604	0.032080
8	EUROPEAN JOURNAL OF VASCULAR AND ENDOVASCULAR SURGERY	9,932	5.328	0.013510
9	International Journal of Stroke	4,853	4.882	0.015560
10	Current Atherosclerosis Reports	2,586	4.608	0.004550
11	THROMBOSIS AND HAEMOSTASIS	15,589	4.379	0.020570
12	CURRENT OPINION IN LIPIDOLOGY	4,151	4.254	0.005450
13	JOURNAL OF HYPERTENSION	16,940	4.171	0.020170
14	JOURNAL OF THROMBOSIS AND HAEMOSTASIS	17,598	4.157	0.025190
15	ATHEROSCLEROSIS SUPPLEMENTS	767	3.968	0.001220
16	ATHEROSCLEROSIS	24,587	3.919	0.036590
17	Journal of Atherosclerosis and Thrombosis	3,426	3.876	0.005190
18	AMERICAN JOURNAL OF PHYSIOLOGY-HEART AND CIRCULATORY PHYSIOLOGY	26,114	3.864	0.020400

Druckexemplar der Publikation 2

Riemer TG, Villagomez Fuentes LE, Algharably EAE, Schäfer MS, Mangelsen E, Fürtig MA, Bittner N, Bär A, Zaidi Touis L, Wachtell K, Majic T, Dinges MJ, Kreutz R. Do β-Blockers Cause Depression?: Systematic Review and Meta-Analysis of Psychiatric Adverse Events During β-Blocker Therapy. Hypertension. 2021 May 5;77(5):1539-1548.

https://doi.org/10.1161/hypertensionaha.120.16590

https://doi.org/10.1161/hypertensionaha.120.16590

https://doi.org/10.1161/hypertensionaha.120.16590

https://doi.org/10.1161/hypertensionaha.120.16590

https://doi.org/10.1161/hypertensionaha.120.16590

https://doi.org/10.1161/hypertensionaha.120.16590

https://doi.org/10.1161/hypertensionaha.120.16590

https://doi.org/10.1161/hypertensionaha.120.16590

https://doi.org/10.1161/hypertensionaha.120.16590

https://doi.org/10.1161/hypertensionaha.120.16590

Lebenslauf

Mein Lebenslauf wird aus datenschutzrechtlichen Gründen in der elektronischen Version meiner Arbeit nicht veröffentlicht.

Mein Lebenslauf wird aus datenschutzrechtlichen Gründen in der elektronischen Version meiner Arbeit nicht veröffentlicht.

Komplette Publikationsliste

Original articles

- Kourpa A, Schulz A, **Mangelsen E**, Kaiser-Graf D, Koppers N, Stoll M, Rothe M, Bader M, Purfürst B, Kunz S, Gladytz T, Niendorf T, Bachmann S, Mutig K, Bolbrinker J, Panáková D, Kreutz R. Studies in Zebrafish and Rat Models Support Dual Blockade of EP2 and EP4 (Prostaglandin E_2 Receptors Type 2 and 4) for Renoprotection in Glomerular Hyperfiltration and Albuminuria. Hypertension. 2023 Apr;80(4):771-782. doi: 10.1161/HYPERTENSIONAHA.122.20392. Epub 2023 Jan 30. PMID: 36715011.
  Impact factor 2022: 9.897
- Kourpa A, Kaiser-Graf D, Sporbert A, Philippe A, Catar R, Rothe M, **Mangelsen E**, Schulz A, Bolbrinker J, Kreutz R, Panáková D. 15-keto-Prostaglandin E2 exhibits bioactive role by modulating glomerular cytoarchitecture through EP2/EP4 receptors. Life Sci. 2022 Dec 1;310:121114. doi: 10.1016/j.lfs.2022.121114. Epub 2022 Oct 20. PMID: 36273629.
  Impact Factor 2022: 6.780
- Riemer TG, Villagomez Fuentes LE, Algharably EAE, Schäfer MS, **Mangelsen E**, Fürtig MA, Bittner N, Bär A, Zaidi Touis L, Wachtell K, Majic T, Dinges MJ, Kreutz R. Do β-Blockers Cause Depression?: Systematic Review and Meta-Analysis of Psychiatric Adverse Events During β-Blocker Therapy. Hypertension. 2021 May 5;77(5):1539-1548. doi: 10.1161/HYPERTENSIONAHA.120.16590. Epub 2021 Mar 15. PMID: 33719510.
  Impact Factor 2020: 10.190
- **Mangelsen E**, Rothe M, Schulz A, Kourpa A, Panáková D, Kreutz R, Bolbrinker J. Concerted EP2 and EP4 Receptor Signaling Stimulates Autocrine Prostaglandin E2 Activation in Human Podocytes. Cells. 2020 May 19;9(5):1256. doi: 10.3390/cells9051256. PMID: 32438662; PMCID: PMC7290667.
  Impact Factor 2020: 6.600
- Kisser B, **Mangelsen E**, Wingolf C, Partecke LI, Heidecke CD, Tannergren C, Oswald S, Keiser M. The Ussing Chamber Assay to Study Drug Metabolism and

Transport in the Human Intestine. Curr Protoc Pharmacol. 2017 Jun 22;77:7.17.1-7.17.19. doi: 10.1002/cpph.22. PMID: 28640954.
Impact Factor 2017: 2.65

Conference presentations

Posters

- **Mangelsen E**, Böhme K, Karsten P, Plum C, Kreutz R, Bolbrinker J „Charakterisierung von Komponenten des Prostaglandin-Signalwegs in einer humanen Podozyten-Zelllinie“, e-Posterpräsentation auf dem 43. Wissenschaftlichen Kongress Deutsche Hochdruckliga e.V. DHL® Deutsche Gesellschaft für Prävention, Berlin, 21.–23.11.2019.
- **Mangelsen E**, Böhme K, Plum C, Karsten P, Schulz A, Kourpa A, Panáková D, Kreutz R, Bolbrinker J „Prostaglandin E2-Stimulation induziert den Transkriptionsfaktor NR4A1 in humanen Podozyten über EP2- und EP4-Rezeptoren“ Posterpräsentation auf der 11. Jahrestagung der Deutschen Gesellschaft für Nephrologie (DGfN), Berlin, 01.–04.10.2020.
- Keiser M, **Mangelsen E**, Petrikat T, Oswald S „Investigation of the intestinal absorption of beta-lactam antibiotics using a PEPT1/MRP3 double-transfected cell line and the Ussing chamber technique” Meeting Abstract 83rd Annual Meeting of the German Society for-Experimental and Clinical Pharmacology and Toxicology (DGPT) / 19th Annual Meeting of the Association of the Clinical Pharmacology Germany (VKliPha), Heidelberg, 06.-09.03.2017

Mini Orals

- **Mangelsen E**, Rothe M, Bolbrinker J, Kourpa A, Panáková D, Kreutz R, Schulz A “Lipidomic Analysis in a Non-Diabetic Rat Model with Hyperfiltration and Albuminuria Reveals Dynamic Changes in the Prostaglandin E2 Pathway during Onset of Albuminuria as a Potential Causative Mechanism” ERA-EDTA 2021: 58th Congress of the European Renal Association and European Dialysis Transplantation Association 05.–08.06.2021.

Danksagung

Mein Dank gilt zunächst Professor Dr. med. Reinhold Kreutz. Als Erstbetreuer hat er mich bei diesem spannenden Thema mit Rat und Tat begleitet. Frau Privatdozentin Dr. med. Juliane Bolbrinker danke ich für die sorgsame Zweitbetreuung. Mein Dank geht außerdem an Frau Dr. rer. medic. Angela Schulz für Ihre Unterstützung bei den Versuchstieren, sowie an Claudia Plum, Petra Karsten und Karen Böhme für Ihre professionelle Assistenz im Labor.

Meiner Familie und meinen Freunden danke ich für ihre geduldige Begleitung. Wir stehen auf den Schultern von Riesen – in Dankbarkeit und Demut denke ich auch an Wissenschaftler*innen und Autor*innen, an Lehrer*innen und Dozent*innen, die meinen Weg in die Wissenschaft geprägt haben. Jede Aufzählung wäre hier unvollständig.